TECHNISCHE UNIVERSITÄT MÜNCHEN
Institut für Virologie

The impact of protein instability on target antigen processing, presentation and immunogenicity in MVA vaccines

Lena Kreuzer

Vollständiger Abdruck der von der Fakultät für Medizin der Technischen Universität München zur Erlangung des akademischen Grades eines

Doktors der Medizin (Dr. med.)

genehmigten Dissertation.

Vorsitzender:

Univ. - Prof. Dr. E. J. Rummeny

Prüfer der Dissertation:

1. Univ. - Prof. Dr. I. Drexler

2. Univ. - Prof. Dr. D. Busch

Die Dissertation wurde am 22.04.2015 bei der Technischen Universität München eingereicht und durch die Fakultät für Medizin am 18.11.2015 angenommen.

Erklärung

Ich erkläre an Eides statt, dass ich die der Fakultät für Medizin der Technischen Universität München zur Promotionsprüfung vorgelegte Arbeit mit dem Titel:

The impact of protein instability on target antigen processing, presentation and immunogenicity in MVA vaccines

im Institut für Virologie unter der Anleitung und Betreuung durch Prof. Dr. med. I. Drexler ohne sonstige Hilfe erstellt und bei der Abfassung nur die gemäß § 6 Abs. 6 und 7 Satz 2 angegebenen Hilfsmittel benutzt habe.

Ich habe keine Organisation eingeschaltet, die gegen Entgelt Betreuerinnen und Betreuer für die Anfertigung von Dissertationen sucht, oder die mir obliegenden Pflichten hinsichtlich der Prüfungsleistungen für mich ganz oder teilweise erledigt.

Ich habe die Dissertation in dieser oder ähnlicher Form in keinem anderen Prüfungsverfahren als Prüfungsleistung vorgelegt.

Ich habe den angestrebten Doktorgrad noch nicht erworben und bin nicht in einem früheren Promotionsverfahren für den angestrebten Doktorgrad endgültig gescheitert.

Die öffentlich zugängliche Promotionsordnung der TUM ist mir bekannt, insbesondere habe ich die Bedeutung von § 28 (Nichtigkeit der Promotion) und § 29 (Entzug des Doktorgrades) zur Kenntnis genommen. Ich bin mir der Konsequenzen einer falschen Eidesstattlichen Erklärung bewusst.

Mit der Aufnahme meiner personenbezogenen Daten in die Alumni-Datei bei der TUM bin ich einverstanden.

München, den 11. April 2015

Lena Kreuzer

Contents

List of Abbreviations

APC	antigen-presenting cell
CD	cluster of differentiation
CTL	cytotoxic T-lymphocyte
CVA	chorioallantois vaccinia virus Ankara
DC	dendritic cell
DNA	deoxyribonucleic acid
ER	endoplasmatic reticulum
FACS	fluorescence activated cell sorter
FCS	foetal calf serum
FS/SS	forward/sideward scatter
HSP	heat shock protein
IFN	interferon
IL	interleukin
MHC	major histocompatibility complex
MOI	multiplicity of infection
MVA	modified vaccinia virus Ankara
MVA-ubiOVA	MVA-ubG76/ovaR1
MVA-TO	MVA-ubi/Tyr_Sig/Ova
MVA-TOT	MVA-ubi/Tyr_Sig/Ova/Tyr_TM
ODC	ornithine decarboxylase
ORF	open reading frame
ova	ovalbumin
(m)RNA	(messenger) ribonucleic acid
rpm	rounds per minute
RT	room temperature
TAA	tumor-associated antigen
TO	ubi/Tyr_Sig/Ova
TOT	ubi/Tyr_Sig/Ova/Tyr_TM
ubi	ubiquitin
UFD	ubiquitin-fusion degradation
VV	vaccinia virus

Zusammenfassung

Weltweit breiten sich infektiöse Erkrankungen wie das Acquired Immune Deficiency Syndrome (AIDS) durch das Humane Immundefizienz-Virus (HIV), die Malaria und Tuberkulose noch immer kontinuierlich aus und stellen dabei eine Herausforderung an die Wissenschaft bezüglich Therapiemöglichkeiten und Heilung dar. Die Vakzinierung als ein wirksames Mittel, um Krankheiten zu kontrollieren oder gar auszulöschen, stellt eine der vielversprechendsten Möglichkeiten dar, diese Krankheiten entweder präventiv oder im kurativen Ansatz zu therapieren. Einer der sichersten viralen Vektoren für den Einsatz als Impfstoff im Menschen, mit der Fähigkeit eine starke und langanhaltende Immunantwort zu induzieren, ist das hoch attenuierte und in seiner Vermehrungsfähigkeit stark eingeschränkte modifizierte Vaccinia Virus Ankara (MVA).
Gene, die für spezifische Antigene intrazellulärer Pathogene oder auch für Tumor-assoziierte Antigene (TAA) kodieren, können, mit Hilfe von Transferplasmiden, in den viralen Vektor integriert und durch Impfung dem menschlichen Immunsystem zugänglich gemacht werden. Dabei spielt insbesondere die Aktivierung zytotoxischer (CD8+) T-Zellen eine entscheidende Rolle. Diese besitzen die Fähigkeit, infizierte Zellen oder Tumorzellen gezielt anzugreifen und zu zerstören. Die effiziente Aktivierung der T-Zellen erfordert die Präsentation von antigenspezifischen Peptiden mit MHC (major histocompatibility complex)-Klasse I-Molekülen auf professionellen antigenpräsentierenden Zellen, zum Beispiel auf dendritischen Zellen (DCs).

Dabei kann zum einen die infizierte DC selbst das Antigen synthetisieren und präsentieren (direkte Präsentation), zum anderen kann sie extrazelluläres Antigen, welches in anderen infizierten Zellen generiert wurde, aufnehmen und den T-Zellen präsentieren (Kreuz-Präsentation). Welche Art der Antigenpräsentation wann stattfindet, ist nicht geklärt, jedoch scheint insbesondere die Stabilität eines Antigens bei der Zugänglichkeit eines Antigens zu den verschiedenen Präsentationswegen ein wichtiger Faktor zu sein. Man nimmt an, dass stabiles Antigen mit einer langen Halbwertszeit gut kreuzpräsentiert wird, während instabiles Antigen, welches schnell degradiert wird, dem endogenen Präsentationsweg besser zugänglich ist und damit eine effiziente direkte Präsentation zur Folge hat. Um eine starke T-zelluläre Immunantwort nach Vakzinierung mit MVA hervorzurufen, ist es deshalb entscheidend, die Bedeutung der verschiedenen Antigenpäsentationswege nach Primär- und Sekundärimmunisierung mit MVA zu evaluieren sowie die optimalen Eigenschaften eines pathogenen Antigens zu definieren.

In dieser Arbeit dient das Protein Ovalbumin als Modellantigen für ein intrazelluläres Antigen. Das Ovalbumin soll hierbei der schnellen Prozessierung innerhalb des Ubiquitin-abhängigen Degradationsweges zugänglich gemacht werden. Ziel dieser Arbeit ist es, den Einfluß des genetisch modifizierten Ovalbumins hinsichtlich seiner Stabilität, der Antigenpräsentation und Immunogenität nach MVA Immunisierung zu untersuchen und die optimalen Eigenschaften eines Antigens für die Primär- und Sekundärimmunisierung mit MVA besser zu verstehen.
Für die weitere Charakterisierung des Proteins Ovalbumin wurden Western Blot Analysen,

Immunperoxidase-Färbungen, radioaktive Pulse-Chase-Assays und durchflusszytometrische Untersuchungen durchgeführt.
Ein ubiquitiniertes und der N-end-rule folgend degradierbares Ovalbumin (ubiOVA) zeigte, im Vergleich zu nativem, stabilem Ovalbumin (ova), eine gering verbesserte Proteindegradation in der Western blot Analyse sowie ebenso eine leicht effizientere Antigenpräsentation des ovalbuminspezifischen Peptids SIINFEKL auf B16-F1 Zellen in der FACS Analyse. Ein an die ubiquitinierte Signalsequenz der Tyrosinase (melanomspezifisches Antigen) fusioniertes Ovalbumin (TO) sowie eines, welches zusätzlich C-terminal die Transmembrandomäne der Tyrosinase enthält (TOT), zeigten jedoch sowohl eine deutlich schnellere Proteindegradation in den Immunperoxidase Färbungen als auch eine verbesserte Antigenpräsentation des ovalbumin-spezifischen Peptids SIINFEKL. Somit wurde Ovalbumin durch alle drei getesteten Modifizierungen insgesamt schneller degradiert und SIINFEKL, insbesondere durch die TO- Modifizierung, deutlich effizienter auf der Zelloberfläche präsentiert.
In *in vivo* Experimenten wurden CD8+ T-Zellantworten auf vektorspezifische Peptide sowie das ovalbuminspezifische Peptid SIINFEKL untersucht. Dabei wurden C57BL/6 Mäuse mit den verschiedenen MVA-Konstrukten (MVA-ubiOVA, MVA-TO und MVA-TOT) geimpft und die spezifischen CD8+ T-Zellantworten mit denen von Mäusen verglichen, in denen ein stabiles Ovalbumin (MVA-ova) nach MVA Immunisierung exprimiert wird. Alle Konstrukte riefen nach Primärimpfung eine schwächere ovalbuminspezifische CD8+ T-Zellantwort hervor als MVA-ova.
Diese Ergebnisse zeigen, dass ein stabiles Antigen während der Primärimmunisierung mit MVA Vakzin vorteilhaft gegenüber schnell degradiertem Protein ist. Primärimmunisierung mit MVA-ova und Sekundärimmunisierung mit den modifizierten rekombinanten Vakzinen riefen höhere CTL-Antworten hervor als eine Sekundärimmunisierung mit MVA-ova. Insbesondere das MVA-TO als sekundäres Vakzin war in der Lage, deutlich höhere ovalbuminspezifische CD8+ T-Zellantworten hervorzurufen als MVA-ova. Somit zeigt sich hierbei ein Vorteil instabiler Antigene für die Sekundärimmunisierung mit MVA Vakzinen.
Da es das Ziel ist, die Vakzinierung mit MVA durch die Induktion einer stärkeren Immunantwort auf das entsprechende Antigen weiter zu verbessern, erbringt diese Arbeit richtungsweisende Ergebnisse hinsichtlich der optimalen Antigenform sowie deren effizienterer Verwendung in der Primär- oder Sekundärimmunisierung in MVA Vakzinen. Die hierin gewonnenen Ergebnisse tragen so dazu bei, neue Richtlinien für die Immunisierung mit MVA Vakzinen zu etablieren. Die in dieser Arbeit aufgeführten Modifikationen eines Antigens können mit weiteren Impfstrategien, z.B. DNA Immunisierung oder B8R-knock out Viren, in vivo getestet werden und so vielleicht in Zukunft, nicht nur im Mausmodell, sondern auch im Menschen, zu einer stärkeren antigenspezifischen Immunantwort nach Immunisierung mit MVA beitragen.

Summary

Infectious diseases like HIV, malaria and tuberculosis are continously spreading and still pose a challenge for scientists regarding therapeutic intervention and healing. Vaccination as a proven tool for controlling and even eradicating diseases comprises a promising approach to address disease control either in a therapeutical or preventive setting. The highly attenuated and replication-deficient modified vaccinia virus Ankara (MVA) thereby constitutes one of the most promising viral vectors featuring a well established clinical safety profile and the ability to elicit a strong and long-lasting immune response.
Genes encoding for antigens of intracellular pathogens but also tumor-associated antigens (TAAs) can be subcloned in the viral vector via transfer plasmids and then, by vaccination, made accessible to the human immune system. In particular, the elicitation of specific (CD8+) T-cells are of critical relevance as they have the ability to specifically target and fight intracellular pathogens and tumor cells. The efficient activation of T-cells thereby requires the presentation of antigenic peptides in a MHC class I-restricted manner on professional antigen presenting cells, such as dendritic cells (DCs).

Dendritic cells can either present antigenic peptides derived from proteins synthesized in the infected DC itself (direct presentation) or from exogenously acquired antigen synthesized by other infected cells (cross-presentation). For the access of antigen to these two different antigen-presentation pathways metabolic stability of an antigen seems to be of critical relevance. Stable antigen is thought to be the optimal antigen formulation for cross-presentation whereas rapidly degraded antigen should be superior in endogenous presentation and, thereby, in direct priming. For the elicitation of a strong, long-lasting T-cellular immune response in immunization with MVA it is essential to enlighten the relevance of each antigen presentation pathway in primary and secondary immunization and to define antigenic features for the optimal immunization strategy.
In this study, ovalbumin was used as a model antigen. The ovalbumin protein shall be targeted for rapid intracellular processing by distinct modifications known to be associated with protein degradation. The aim of this study was to investigate the impact of ovalbumin modifications on ovalbumin stability, antigen presentation and immunogenicity in MVA immunization. Ovalbumin expression and stability was assessed by means of Western blot analysis, immunoperoxidase staining, radioactive pulse chase assays and flow cytometry.
An ubiquitinated ovalbumin (ubiOVA) targeted for rapid proteasomal processing as an N-end-rule substrate could slightly reduce the stability of ovalbumin as seen in Western blot analysis and caused an increase in presentation of ovalbumin-specific peptide SIINFEKL after infection of B16-F1 cells when compared to native ovalbumin (ova). When ovalbumin was fused to the ubiquitinated signal sequence of tyrosinase (a melanoma-associated antigen) (TO) and, in a second construct, was C-terminally linked to its transmembrane domain (TOT), a significantly enhanced degradation of ovalbumin was seen in immunoperoxidase staining. Especially the TO- modification of ovalbumin, however, was able to increase peptide presentation in DC2.4 cells as detected by FACS analysis. Hence, all three tested modifications of ovalbumin led to an increased instability of the protein with an

improved presentation of antigenic peptides.

In *in vivo* experiments, vector-specific as well as ovalbumin-specific CD8+ T-cell responses were assessed. C57BL/6 mice were immunized with different ovalbumin expression constructs (MVA-ubiOVA, MVA-TO and MVA-TOT) and specific CD8+ T-cell responses were compared with those of MVA-ova immunized mice (stable ovalbumin was expressed). Ubiquitinated ovalbumin expression constructs were able to elicit ovalbumin-specific CD8+ T-cell responses after priming which were lower compared to MVA-ova immunization. These results support the hypothesis that stable antigen is advantageous to rapidly degradable antigen during primary immunization with MVA. After primary immunization with MVA-ova and secondary immunization with ubiquitinated ovalbumin expression constructs stronger CTL responses were detected compared to a homologous prime/boost immunization with MVA-ova. This clearly demonstrates the advantage of rapidly degradable antigen in secondary immunization with MVA.

As it is of critical relevance to further identify strategies to enhance antigen-specific immune response in MVA immunization, this work contributes to define the optimal form of antigen and its need for application during prime or boost in MVA vaccines. Hence, information gathered from this study account for the establishment of new guidelines in MVA immunization strategies. Modifications of the target antigens used in this study might further be evaluated with other immunization strategies and could even be conducive to induce a strong, long-lasting and antigen-specific immune response after MVA immunization in humans.

1 Introduction

1.1 MVA as a potent and safe new generation vaccine

First attempts to develop immunization strategies against infectious diseases like smallpox started in the 10th or 11th century in Central Asia. Intranasaly applied variola scabs were used to immunize against smallpox, perhaps based on observations that prior smallpox protected against subsequent exposure [42, 109]. The term 'vaccination', however, was introduced in europe 1796 by Edward Jenner who discovered that cowpox, a mild illness in humans, induced protection against smallpox. Since then, immunization strategies and vaccine development have made incredible progress. Finally, even eradication of smallpox could be announced in the twentieth century [42]. The World Health Organization's (WHO) Expanded Programme on Immunization, starting in 1974, led to the availability of vaccines against measles, polio, diphtheria, tetanus, pertussis and tuberculosis in almost all developing and industrial countries. However, there are still many diseases reaching pandemic proportions representing a global developmental and public health threat. The rising numbers of HIV infection (since the start of the epidemic 60 million people around the world, more than 14,000 new infections every day [159]) as well as progredient spreading of malaria infection underline the indispensable and urgent need for new effective vaccines against infectious diseases. Apart from infectious diseases, cancer can be adressed by vaccination, too. Hence, as a major cause of death in industrialized and developing countries cancer together with infectious diseases are in the spotlight of vaccine research.

Inducing cellular immune response is essential to target infectious diseases

Worldwide an estimated 10.9 million people die as a result of infectious and parasitic diseases per year. Among them human immunodeficiency virus (HIV) (2,6 mio. new infections 2009 [160]), tuberculosis (2,6 mio./2008 [160]) and malaria (225 mio. cases in 2009 [157]) head the tables of morbidity and mortality [161]. Since the 1980's, more than twenty new pathogens with outstanding importance have been identified (e.g. Helicobacter pylori, HIV, Clamydia pneumoniae, Hepatitis C Virus)[79].
Some diseases like Acquired Immune Deficiency Syndrome (AIDS), malaria, tuberculosis and chronic hepatitis confront researchers in vaccine development with new challenges. Historically most vaccines against intracellular pathogens were whole live attenuated or inactivated microorganisms working by the elicitation of long-living plasma cells that produce antibodies to neutralize the toxin or to block the spread of the infectious agent.
Cellular immunity and the induction of a long-lasting memory immune response are of key importance for protection against most intracellular pathogens such as viruses, some bacteria and many parasites [117, 43]. In a vaccine setting, the induction of potent and

specific cytotoxic T-lymphocytes (CTL) which have the ability to recognize and eliminate infected cells before new virions are produced might lead to rapid clearance and prevention of clinical manifestations. Therefore, new vehicles, immunization adjuvants and protocols to increase CTL responses to distinct pathogens either in a therapeutic setting or as prophylactic application are under investigation.

Inducing cellular immunity is essential to target human cancer

In industrialized nations cancer is one of the three leading causes of death and is likely to become the most common fatal disease in future [69]. Approaches for tumor vaccination date back to the 1890's when the surgeon William B. Coley successfully treated patients with sarcoma using bacterial toxins. In 1909, Paul Ehrlich immunized animals with tumor cells on the premise that tumors occur at a high frequency in humans but are kept under control by the immune system [30].

Therapeutic vaccination against human cancer requires the destruction of all malignant cells without inflicting serious damage on the patient. The discovery that CTLs are a critical mediator of tumor immunity constitute the basis of current experimental approaches to cancer immunotherapy. Tumor associated antigens (TAAs) which are selectively or preferentially expressed by transformed cells can be recognized by CTLs, making vaccines based on TAAs the ideal approach to T-cell mediated immunotherapy [69]. Several investigations aim to combine the TAA with the appropriate route for delivering the antigen to the immune system.
The TAA can, for instance, be derived from antigens which are strictly tumor-specific and the result of point mutations or gene rearrangements (e.g. caspase 8 expressed by squamous cell carcinoma or cyclin-dependent kinase 4 expressed by melanoma). They can be expressed in particular types of tissue (e.g tyrosinase expressed by melanoma), or they can be derived from proteins encoded by viral oncogenes like human papilloma virus type 16 proteins E6 and E7 which are expressed in cervical carcinoma.

Challenging requirements for a vector vaccine

There are, of course, many requirements for a vector vaccine developed for human use:

(i) the ideal vehicle should be safe and cause no severe side effects upon application
(ii) it should enable the efficient synthesis of antigen and presentation of peptides
(iii) it should ideally activate both, the cellular and the humoral immune response
(iv) the application should lead to an effective protection against the illness resulting from the exposure to live pathogen
(v) as a practical consideration it should meet criteria that enable its fabrication.

Many vaccines have a good potential to elicit strong CTL responses. Attenuated virus and bacteria (live attenuated vaccines), replication-competent and replication-defective recombinant virus or bacteria (live vectored vaccines) and deoxyribonucleic acid (DNA) vaccines

(see below). Each of them has different features (dose requirements, boosting strategies, adjuvant needs) as well as different safety issues and a different potential for being hampered by pre-existing immunity [116].

Strategies for vaccination against intracellular pathogens

Multiple vaccine concepts and vaccination strategies were developed for immunization against cancer and intracellular microbial pathogens associated with infectious diseases. Those of main interest include vaccination with DNA plasmids, peptide-based vaccines, vaccines based on dendritic cells and vaccination with recombinant viruses.
The relatively recent observation on DNA as a delivery moiety for foreign gene products has revealed to be successful in murine models. The DNA is tailored to encode for an antigen of interest and subsequently injected in the muscle to confer systemic immunity. It was demonstrated to be able to elicit both arms of immunity, the cellular as well as the humural, in rodents and non-human primates. Once injected, cells transfected with DNA present the antigen to T-cells through MHC class I pathways.
Notably, the administration within human systems achieved little success and strategies to improve its poor immunogenicity like the use of adjuvants or different vaccination regimens (prime/boost modalities) are under investigation. [82]
Peptide-based vaccines used for the elicitation of specific T-cell responses have shown conflicting results so far. Only in some selected examples single epitopes administered with a variety of adjuvants have shown to be effective in animal models [126]. In most cases, however, vaccination with peptides showed limited therapeutic efficacy and under certain circumstances vaccination with peptides has even induced epitope-specific tolerization rather than activation. The reasons for the limited success in clinical studies which were mainly performed with melanoma-specific peptides MART-1, gp100, MAGE-3.A1 or tyrosinase in metastatic melanoma patients are not yet well understood. Weak immunogenic peptides, vaccination schedule, lack of CD4+ T-cell activation, the host's immune cell dysfunction or escape mechanisms of the tumor might all be possible explanations. [106]
Since dendritic cells (DCs) play a central role in the induction of antigen-specific T-cell responses, their use for active immunotherapy is of considerable interest. The DC can be pulsed with tumor antigens *ex vivo* and subsequently be injected subcutaneously or even directly in the lymph nodes. A number of important developmental issues like the ideal source and type of DC, the form of antigen and method of charging the DC, additional maturation signals and the route and timing of immunization are topical questions. For instance, several strategies have been performed to load the DC with tumor antigens including peptides, proteins, tumor cell lysates or tumor-derived RNA. Other strategies include DCs that were transfected with viral vectors expressing TAAs or the fusion of DCs with whole tumor cells. A number of studies in animal models have shown that DCs exposed to TAAs *in vitro* and administered to the animal can induce protection against tumor growth and confer CTL responses [87, 22]. Clinical responses such as stability of disease and tumor regression have been reported in some patients, particularly with melanoma,

myeloma and prostate cancer but have always been low.
Cancer vaccination strategies also include tumor cell based vaccines. The patient's autologous tumor cells are genetically modified to express cytokine genes or co-stimulatory molecules in order to enhance immunogenicity to the tumor. One important cytokine is the granulocyte macrophage colony-stimulating factor (GM-CSF) which is known to contribute to maturation of DCs and thus to enhance antigen presentation *in vivo*. This rather labour-intensive, slow and logistically difficult vaccination strategy has already shown some success in phase I/II clinical trials in humans for vaccination against melanoma, renal carcinoma and prostate cancer. [30]
However, some of the most important recent tools to induce cellular immunity against infectious diseases or cancer are recombinant viruses. Strategies have been designed to use viruses as immunization vehicles to elicit antigen-specific immune responses. In these approaches genes encoding for a target antigen are inserted into a viral vector. These target genes depending on the desired immunity can either be TAAs or antigens characteristically expressed by intracellular pathogens, e.g. Gag, Env, Pol and the accessory protein Nef in HIV [48].
The two currently most popular replication-defective recombinant viral vectors are modified vaccinia virus Ankara (MVA) and the adenovirus 5 vector (Ad5). Adenoviral vectors are limited to relatively short vaccine inserts ($\leq$5 kb), nevertheless first studies in the 1980's using recombinant adenoviruses that were performed against measles or HIV [2, 25] and later against malaria [119] and herpes simplex virus (HSV) [90] showed that they are efficient in expressing recombinant products and revealed them as powerful tools for inducing cellular immunity.

Viral vectors developed with the aim to be used in humans must have an extreme safety profile. This becomes even more important when they are supposed to be used in patients with impaired immune defense as a consequence of their disease or immunosuppressive treatment, e.g. cancer or HIV patients. The most promising candidates are highly attenuated or non-replicative viruses obtained either by serial passages in cell culture or genetic manipulation.

Modified vaccinia virus Ankara (MVA)

Live replication-competent vaccinia virus (VV) which had been successfully used for the eradication of smallpox has become a comprehensively investigated object of vaccine research. VV is a member of the *Orthopoxvirus* genus of the *Poxviridae* and possesses a large double-stranded DNA genome of approximately 200 kb. Many genes that contribute to virus replication are encoded by the central region of the genome, among them 90 genes are conserved in all sequenced poxviruses. These genes, which are not essential for virus replication but affect virus virulence and host range, are located towards each end. [98]
Under selective pressure viruses have developed mechanisms of evading or impeding host immune responses. Immune evasion genes, for example, can directly target host re-

sponses based on cytokine and chemokine function. Their products include homologues of interleukin-1β and α/β-interferon receptors, complement control proteins and serine protease inhibitors. The B8R gene, for example, encodes for a secreted protein with sequence similarity to the extracellular domain of the interferon-γ receptor. Host interferon-γ binds to the viral receptor homologue instead of the cell surface receptors and leads to neutralization of antiviral activities of interferon in the host‘s immune response. Nevertheless, the use of VV as recombinant vaccine against infectious diseases or cancer has been highly attractive and has already been evaluated in multiple clinical trials [74, 85, 9, 105, 12].

Albeit, its imperfect safety profile is a concern for general application. Severe side effects occuring during immunization with vaccinia viral vectors prompted the search for other, more attenuated and replication deficient viral vectors. This issue was addressed by Mayr et al. who developed the attenuated modified vaccinia virus Ankara (MVA) [89]. MVA is an artificial laboratory virus first generated in 1958. The Dermovaccinia virus strain chorioallantois vaccinia virus Ankara (CVA) was passaged over 570 times in primary cell culture until it suffered six major deletions of DNA including at least two host range genes [140]. The resulting MVA strain lost its broad cellular host range and thus the ability to productively grow in many cells of mammalian origin (including primary human cells). Only on primary chicken embryo fibroblasts (CEF) and baby hamster kidney cells (BHK) cells the virus strain is able to efficiently grow and replicate [34].

MVA which is used in this study is one of the most promising live viral vectors. It meets several criteria for an ideal vector system to target protein synthesis and vaccine development

(i) it has a large packing capacity for recombinant DNA
(ii) viral gene expression, early as well as late, are unimpaired and highly efficient [140]
(iii) there is no genomic integration or persistence in the host, reflecting its high safety profile
(iv) it shows high immunogenicity as vaccine, inducing cellular as well as humoral immune response
(v) the generation of the vector and vaccine is easy to perform. [36]

MVA has already been evaluated in many studies. It has been found to be immunogenic and protective when used as a candidate recombinant vaccine in animal models for viral or parasite infection [141, 62, 38, 125] or in a mouse-tumor cell challenge model [20]. Furthermore, in recent years there have been ongoing trials investigating its potential immunogenicity and safety as antigen delivery system in humans for vaccination against cancer [57, 118, 94, 3] or infectious disease [28, 37, 108, 51, 15].

Pre-existing immunity to MVA or VV, however, might affect immunogenicity of the target antigen delivered by an MVA vector vaccine within the scope of antivector immunity [36]. To address this issue several methods have been established. The application of DNA for priming before MVA boost immunization efficiently circumvents anti-vector immunity

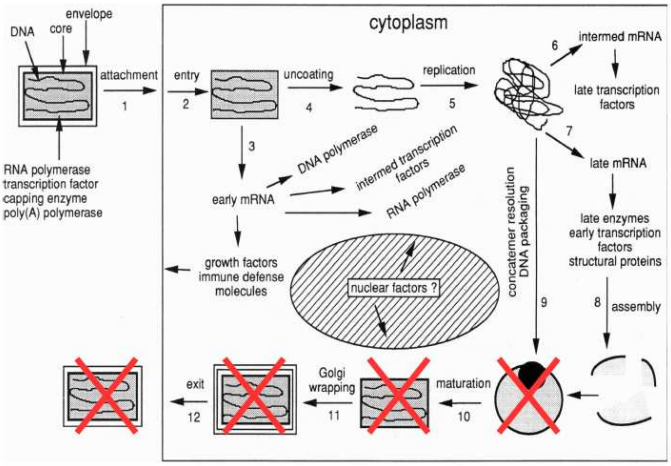

Figure 1.1: Abortive life cycle of replication-deficient MVA in non-permissive mammalian cells; modified from [97]

and has already been evaluated in clinical studies, e.g. with a pre-erythrocytic malaria antigen (TRAP) [162, 91]. In addition, the combination of different viral vectors, e. g. influenza [46], avipox [63, 5], Semliki Forest [55] or vesicular stomatitis virus [114] but also of non-viral vectors such as salmonella-based vaccines [40] or protein vaccines [39] in the combination with MVA expressing the same antigen are further approaches to enhance antigen-specific immune response.

1.2 Cellular immune response as a critical mediator to target intracellular pathogens

As a part of the adaptive immune response T-cells play a crucial role in defense and destruction of intracellular pathogens like parasites, bacterial pathogens and all viruses which replicate inside cells where they can not be detected by antibodies.
T-cells that have not yet encountered their antigen are known as naive T-cells. These naive T-cells recirculate between the bloodstreem and peripheral lymphoid tissue until they are activated into armed effector T-cells by direct interaction with cells presenting their specific antigen. The most important antigen-presenting cell is the highly specialized DC whose main function is to ingest and present antigen. DCs, macrophages and B-cells are known as professional antigen-presenting cells (pAPCs).
Once the DCs have encountered their antigen they migrate from the site of infection to the draining lymph nodes where they present the ingested and processed antigen to T-cells.

The activation of CD8+ T-cells

Pathogens once invaded in the host can be recognized through specialized surface receptors on cells of the innate immune system like macrophages and DCs. These surface receptors, also known as pattern-recognition receptors, are activated by a distinct set of molecular

patterns characteristic for pathogenic microorganisms. Their activation can either stimulate phagocytosis directly, by opsonization or it might induce the release of inflammatory mediators such as interferon(IFN)-α/β, tumor necrosis factor(TNF) and interleukin(IL)-2 by resident cells leading to further activation of innate immune responses and initiation of adaptive immunity.
Upon activation, APCs gain an increased capacity to migrate to lymphoid organs where they potentially activate naive T-cells. The activation of naive T-cells requires two signals. One signal functions through the antigen-specific T-cell receptor complex and the other signal is provided by the APC by means of costimulation. Costimulation describes the interaction between specialized molecules expressed on the surface of the T-cell and their counterparts on the APC. A very well defined costimulatory pathway is the interaction between cluster of differentiation(CD)28 expressed on the T-cell and B7-1 or B7-2 on the APC. Their interaction leads to enhanced IL-2 production. Costimulation can result in enhanced survival and increased proliferation but might also affect the quality of resulting T-cell response.
Under certain conditions, depending on the amount and type of pathogen, APCs do also require signals from CD4+ T-cells to 'help' activating CD8+ T-cell response. This help is provided by CD40L expressed on CD4+ T-cells interacting with CD40 on the APC which stimulates the latter to enhance expression of costimulatory ligands and secretion of cytokines as IL-12. In particular, both the CD4+ T-cell and the CD8+ T-cell need to recognize antigen on the same APC. Nevertheless, CD4+ T-cells may also directly activate CTLs by membrane bound ligands or cytokines. Once activated, the T-cell response undergoes three different and characteristic phases. After priming T-cells proliferate and differentiate into effector cells with cytotoxic activity expressing high levels of IFN-γ. The second phase comprises the contraction phase wherat antigen-specific T-cells decrease to 5-10% of the initial peak response. During the last phase the remaining T-cell population forms the memory T-cell pool which stays present for a longer period of time and can mediate long-term protection. [123]

The main antigen-presenting pathways

Intracellular pathogens like viruses can take over the cell's biosynthetic mechanisms to produce their own proteins. These virus encoded proteins are synthesized in the cytosol where they can be degraded into peptide-fragments by the major proteolytic machinery, the proteasome *(see section 1.3)*. Released peptides are transported to the endoplasmic reticulum (ER) via the *transporters associated with antigen processing -1* and *-2* (TAP) where they are loaded onto major histocompatibility complex (MHC) class I molecules. The exact length of bound peptides is determined by the configuration of the antigen binding groove in the particular class I molecules. Kb molecules, for instance, bind peptides of eight residues whereas Db binds nine aminoacids [52]. These peptides that bind with high affinity can stabilize the MHC complex which then leaves the ER and trafficks to the cell surface to display the associated peptide to T-lymphocytes. CD8+ T-cells recognize peptides that are presented in the context of MHC class I molecules which are present

on virtually all nucleated cells. Upon activation these cells aim to destroy infected cells including the residing pathogens by induction of apoptosis through ligand-induced death receptor triggering or via the release of perforins and granzymes.

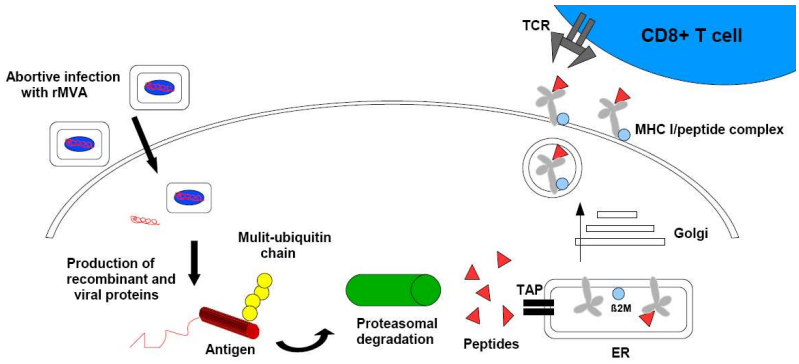

Figure 1.2: *Schematic map of ubiquitin-dependent antigen degradation and peptide presentation after infection with rMVA.*

Extracellular pathogens, however, like bacteria and their toxic products are internalized by phagocytosis, endocytosis or macropinocytosis into intracellular vesicles of cells. Proteins of these pathogens are degraded into peptides by proteases like Cathepsin S or L which are activated at low acidic pH. Having entered the endosomal pathway these peptides finally bind to a different class of MHC molecules, the MHC class II molecules, which are only expressed on pAPCs. The MHC-peptide complex is transported to the cell surface where the peptide can now be recognized by T helper cells (CD4+).
CD4+ T-cells are specialized in providing supporting signals to other cells like macrophages, B-cells or CD8+ T-cells via cytokine secretion or through direct cell-cell interaction. [123, 69]
Some pathogens like mycobacteria, the triggering agent of tuberculosis, or the protozoan parasite Leishmania, however, can invade antigen-presenting cells and flourish inside vesicular compartments where their proteins are not available for proteasomal degradation. Their pathogenic antigens are also presented through the endosomal pathway as described above.

Cross-presentation as an additional pathway to present MHC class I bound peptides

Bone marrow derived pAPCs possess a remarkable capacity to aquire and present antigen. They can internalize antigens from their extracellular environment and present them as MHC class I bound peptides to CTLs. This process has been termed 'cross-presentation' with the respective *in vivo* activation of T-cells referred to as 'cross-priming'. Since the discovery through Bevan et al. in the late 1970's [16] many studies have focussed on how the ability of pAPCs to present through both, the endogenous and the exogenous pathway, affects activation of CD8+ T-cells. That cross-presentation is actually efficient and important for priming CTLs has been shown for a subset of antigens [26], however, its *in vivo* relevance is still a point for controversial discussion [169].

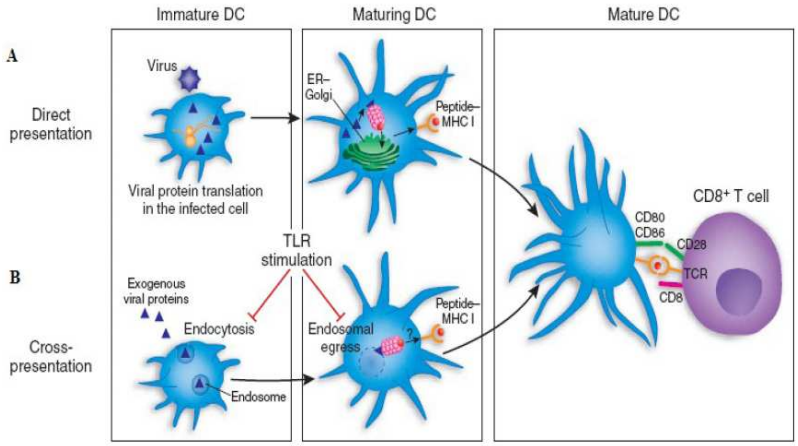

Figure 1.3: Schematic map of direct (A) and cross-presentation (B) pathways. [61]

The principal cells which were found to be capable for cross-presenting antigens *in vitro* were DCs and macrophages, although, under some circumstances, various other cells like B-cells [59, 145], neutrophils [111, 149] or endothelial cells [11] also have this capacity. Increasing evidence exists that DCs are the key cells needed to cross-prime CD8+ T-cells *in vivo* [132]. T-cells require their antigen from tissue derived DCs which transport the antigen to the draining lymph nodes and then transfer it to CD8α+ DCs for cross-presentation. Many forms of antigen, whole protein, heat shock protein (HSP)-peptide complexes and peptides can be cross-presented *in vitro* or when injected *in vivo* [132]. However, the form that is actually cross-presented under *in vivo* conditions is unknown. Albeit, many recent studies support the theory of whole proteins being the main source for cross-presentation [131]. In particular, long-lived forms of protein are supposed to be cross-presented much better than short-lived forms [155, 44].
The pathways by which cross-presentation takes place have been of considerable interest as they might help to determine the cross-presented form of antigen. One major mechanism is termed the 'phagosome-to-cytosol pathway' in which the antigen is internalized into phagosomes and transported to the cytosol where it is released into the classical endogenous pre-

sentation pathway. Another pathway constitutes the 'vacuolar pathway'. Here, peptides are generated within the classical MHC class II presentation pathway, proteasome- and TAP- independent but are instead loaded onto MHC class I molecules. A third pathway that might contribute to cross-presentation is the 'gap-junction pathway' by which APCs acquire peptide fragments generated by other cells through gap-junctions which are then transported via TAP to the ER. Some soluble proteins were found to be internalized by endosomes and then transported back to the cytosol for degradation by the 'ER-associated degradation' (ERAD) system. This pathway has been termed the 'endosome-to-ER pathway' but its importance is not yet clearly elucidated. [132]
Cross-presentation also represents a mechanism that could contribute to evolutionary fitness. By virtue, (i) some viruses may have evolved to avoid infecting APCs in order to evade immune surveillance, (ii) cross-presentation would enable the surveillance of tumors and (iii) is important for generating immunity to viruses that have restricted tissue-tropism [134] and (iv) it would serve as a mechanism for tolerizing CTLs to self antigens not synthesized by pAPCs (cross-tolerance). [26]

1.3 Increasing epitope expression contributes to improved vaccine efficacy

Cellular or viral proteins are sythesized in cellular ribosomes located in the cytosol. From this newly synthesized protein fraction about 40% are destroyed shortly after synthesis providing a pool of peptides that can potentially be presented to CTLs in a MHC class I restricted manner. Presumably, newly synthesized proteins are not the only source for antigenic peptides. An additional source for antigenic peptides might be 'defective ribosomal products'(DRiPs) which mainly consist of premature termination products and misfolded full-length forms that are directed to degradation by cytosolic proteases and are produced as a byproduct of normal protein synthesis [164].

In eucaryotic cells an energy dependent protease, the proteasome, is the principal mechanism that accounts for degradation of the majority of cellular short-lived proteins. The proteasome plays an essential role in generation of peptides from intracellular antigens which are presented to T-cells. Its major function is the selective and ATP-dependent degradation of cytosolic, nuclear and membrane bound proteins as well as the regulation of protein destruction in the cell. [77]
Its proteolytically active sites are located in a cylindrical enzymatic chamber, the 20S core, which has a 19S regulator complex at either end. This complex of one 20S and two 19S units forms the 26S proteasome.
The two 19S regulatory particles have two multi-subunit components, the 'base' and the 'lid'. The base, which binds to the 20S core, mainly consists of ATPases which contribute

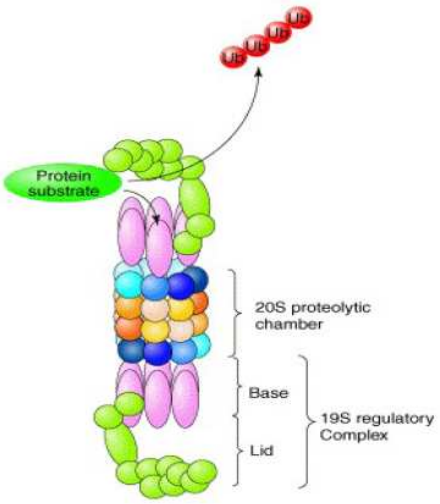

Figure 1.4: The proteasome [29]

to the recognition of potential degradation signals like polyubiquitin chains and help to unfold substrates and channel them into the core. The lid, however, contains 10-12 distinct proteins each present in equal numbers whose roles are less well understood [65]. The 20S core is composed of four heptameric rings with the two outer rings consisting of seven homologous α-subunits (α1-α7) that control the access to the catalytic chamber and interact with regulatory factors. The two inner rings contain the β-subunits which harbour the catalytically active-site threonines in the β1, β2 and β5 subunits. Each of the three β-subunits has a different preference for cleaving after acidic ('peptidyl glutamyl peptide hydrolyzing activity' or 'caspase-like'), basic ('trypsin-like') or hydrophobic ('chymotrypsin-like') residues. [76]

In particular, the proteasome generates peptides that range from two amino acids to at most 30 residues of which only about 30% are eight to nine residues or longer and thus can potentially serve as precursors for antigenic peptides [75]. Goldberg et al. stated, the proteasome must mainly be responsible for the removal of the C-terminal flanking residues of a peptide so that many generated peptides are still N-terminally extended and need to be trimmed by aminopeptidases in the cytosol or ER [52].
The degraded protein fragments then enter the MHC class I presentation pathway. Peptides are transported to the ER via the Tap1/Tap2 heterodimer where they associate with MHC class I molecules. The resulting complexes are transported to the cell surface where they can be recognized by CD8+ T-cells.

The quantity of MHC class I/peptide complexes presented to CD8+ T-cells is suggested to be one of the most critical factors regulating the strength of CTL response. APCs expressing more MHC class I molecules associated with the appropriate peptide potentially yield a more effective and vigorous CTL response to the relevant antigen [144, 54, 96]. Several lines of evidence have suggested that by targeting vaccine antigens for rapid intracellular degradation within the MHC class I presentation pathway, the more efficient degradation in the cytosol will yield increased amounts of peptide substrates available for presentation to cytotoxic T-cells [144, 4].
However, as explained above, the metabolic stability has been defined as one of the most critical factors for the availability and access of antigen in either of the two antigen-presenting pathways, direct and cross-presentation. Thus, for efficient priming of CTLs following immunization with MVA, target antigens require distinct features to be presented optimally by a particular pathway. But still very little is known about the contribution of the different antigen presentation pathways in immunization with MVA. Understanding which antigen-presenting pathways govern the induction of CTLs during priming and

boosting with MVA would enable the selection of efficient antigen formulations and thus would provide access to improved rational vaccine design [44].
As with MVA it is generally possible to stimulate CTLs through direct as well as through cross-priming. It has been shown that MVA is capable of infecting human and mouse dendritic cells leading to an efficient expression of viral and recombinant antigens [72, 44]. Late antigens, however, can not be synthesized in DCs and direct presentation to CTLs is abrogated due to an early block in viral life cycle [72, 24]. Nevertheless, MVA can induce CTLs recognizing late viral antigens indicating that these antigens might be cross-presented [32, 35]. Furthermore, mice immunized with TAP-deficient RMA-S-HHD cells infected with rMVA, yielded T-cell responses comparable to those induced be live vaccines with regard to size and immunodominance hierarchy of CTLs specific for viral and recombinant determinants, indicating that cross-presentation alone is sufficient to elicit strong CTL responses to MVA vaccines [44]. Consequently, cross-presentation is assumed to play a key role in the process of priming with MVA.
For secondary immunization, however, direct presentation is suggested to be of critical relevance. It was shown that the expansion of virus-specific CTLs in boosting is regulated by T-cell cross-competition favoring T-cells that are able to rapidly detect infected cells. Hence, the outcome of T-cell competition was heavily influenced by the timing of antigen presentation with peptides rapidly presented during viral life cycle advantageous to late peptide presentation [73].

In the present study, rMVA expressing differently modified ovalbumin gene products were constructed *(Fig. 1.6 B II, C II, C III)*. These modifications shall target the model protein ovalbumin for rapid intracellular processing by the proteasome making use of different strategies to enhance the protein‘s turn-over rate *(section 1.4)*.
Based on findings by Drexler et al. (unpublished) that an ovalbumin protein stably linked to ubiquitin *(Fig. 1.6 B I)* showed rather disappointing results regarding protein degradation and antigen presentation, an N-end rule targeted ubiquitin-ovalbumin fusion protein was constructed in this study *(Fig. 1.6 B II)*. Within this construct, ovalbumin was employed as a vaccine antigen and a recombinant MVA vector was constructed that expressed an ubiquitinated ovalbumin protein under the control of the VACV natural early/late promotor P7.5 (MVA-$P_{7.5}$-ubG76/ovaR1). The antigen shall be targeted for rapid proteasomal processing by modification of the N-terminal amino acid methionine (M) in ovalbumin to arginine (R) (ovalbumin R1) and N-terminal fusion to the C-terminal amino acid glycine of ubiquitin (ubiquitinG76) according to the N-end-rule *(Fig. 1.5)* [10, 151].

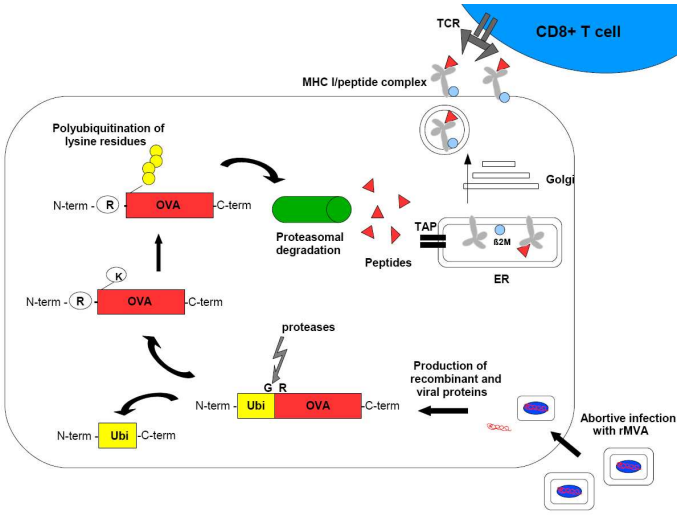

Figure 1.5: *Schematic map of synthesis and degradation of ovalbumin following the N-end rule after infection of the cell with MVA-ubiOVA.* After synthesis, the ubiquitin-ovalbumin fusion protein is split between the C-terminal amino acid glycine (G) of ubiquitin and the N-terminal amino acid arginine (R) of ovalbumin by cytosolic proteases. The primary destabilizing amino acid arginine at the N-terminal end of ovalbumin triggers polyubiquitination of lysine (K) residues in ovalbumin. These multi-ubiquitin chains target ovalbumin to the proteasome where it is degraded into peptide fragments which are then transported to the ER via the Tap1/Tap2 heterodimer. Loaded on MHC class I molecules peptides are finally presented to CTLs on the cell's surface.

The second part of in this study is based on findings that deubiquitination of an ubiquitin moiety is completely inhibited if the C-terminal glycine 76 of ubiquitin is mutated into alanine or valine in Saccharomyces cerevisiae [18] and remarkably, when fused to ß-Gal such as Ub^{V76}-V-ßgal, the protein is rapidly degraded within the ubiquitin fusion degradation (UFD)-pathway [70].
In our laboratory, the instability of a melanoma-specific antigen, tyrosinase, could markedly be increased by stable C-terminal fusion of ubiquitin (ubiquitinA76) to tyrosinase (tyrosinaseM1) resulting in a ubiquitinA76-tyrosinase fusion protein *(Fig. 1.6 C I)* [44]. The N-terminal region of this construct including the nonremovable ubiquitin moiety fused to the signal sequence of tyrosinase was suggested to constitute a general degradation signal applicable to other proteins such as ovalbumin. Hence, a recombinant MVA was constructed expressing the ubiquitinA76-tyrosinase (only signal sequence)-ovalbumin fusion construct *(Fig. 1.6 C II)*.
A third construct generated in this study and expressed by MVA was designed analogous to the latter but additionally had the transmembrane domain of tyrosinase at its C-terminal end given the hypothesis that expanded targeting to cellular compartments like the ER might further enhance MHC class I restricted peptide presentation to CTLs *(Fig. 1.6 C III)*.

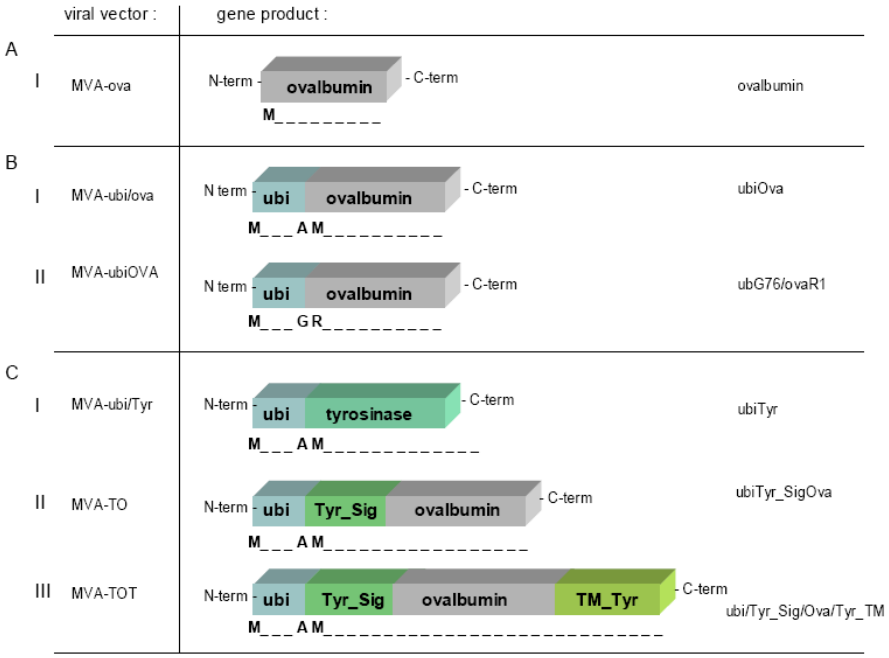

Figure 1.6: *Schematic diagram of gene products expressed by rMVAs with regard to this work.* The N-terminal amino acid components as well as the in frame transitions from ubiquitin to ovalbumin, tyrosinase or the tyrosinase signal peptide domain (Tyr_Sig) are indicated.

1.4 Diverse strategies to increase protein destruction

Cellular proteins in the cell are turned over at markedly different rates. The amount of intracellular protein degradation is a function of the cell's physiological state, continuously regulating the elimination of abnormal proteins, the maintenance of amino acid pools as well as the status of hormones, antigens and other effectors. Thus, metabolic stability or instability of proteins plays a central role in cellular mechanisms and life. The degradation is controlled differentially for individual proteins. Many pathways as well as enzymes contribute to the degradation of proteins. Among them, the ubiquitin-proteasome pathway has an indispensable role in protein degradation. The characteristics and signs, which might be specific sequences within a protein substrate, that influence the protein's rate of destruction and lead to its degradation are being elucidated, however, are not yet clearly defined.
By genetic manipulation, for instance replacement or addition of amino acid sequences representing 'degradation signals', it is possible to tag proteins to different degradation pathways and thereby enhance the rate of protein destruction.

Targeting proteins for rapid intracellular processing by the ubiquitin-proteasome pathway

The selective degradation of many short-lived or misfolded cellular proteins is carried out by the ubiquitin-proteasome pathway. Within this pathway, proteins destined for

degradation are covalently conjugated to a 76-amino acid residue protein termed ubiquitin. Ubiquitin-mediated protein degradation plays an important role in numerous basic biological processes including the selective and programmed degradation of cell-cycle regulatory proteins, tumor suppressors, protooncogenes and components of the signal transduction system. Furthermore, it is involved in transcriptional regulation, receptor down-regulation, endocytosis as well as in development and apoptosis.
The conjugation of an ubiquitin moiety to a protein substrate requires the sequential action of three different enzymes: E1, E2 and E3. In the first step, ubiquitin is activated in an ATP dependent process by binding to a cysteine residue of the activating enzyme E1, forming an ubiquitin adenylate. The activated ubiquitin is then transferred to an active site cysteine residue of a ubiquitin-carrier protein, E2. Finally, the ubiquitin protein ligase E3 catalizes the conjugation of the C-terminus of ubiquitin to an ϵ-amino group of the protein's lysine residues leading to an amide isopeptide linkage *(Fig. 1.7)*.

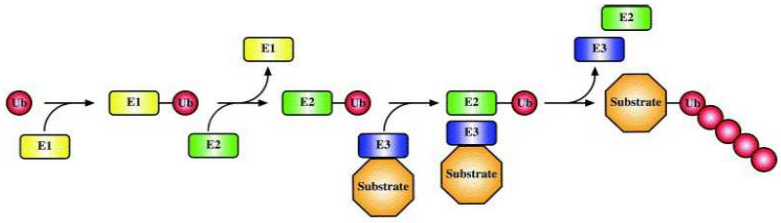

Figure 1.7: The process of ubiquitination [95].

This ubiquitination leads to the formation of a polyubiquitin chain in which the C-terminus of each ubiquitin is linked to a lysine residue (most commonly Lys48) of the previous ubiquitin moiety. Consisting of more than four ubiquitin molecules, the polyubiquitin chain is bound with high affinity from subunits of the 19S regulatory complex of the 26S proteasome. This association tags the protein ligated to the polyubiquitin chain into the core of the proteasome where it becomes degraded into peptide fragments in an ATP-dependent process. [60, 150]
Among signals inherent in primary protein structure which are responsible for protein ubiquitination and thus targeting for degradation, the best characterized is the N-end-rule system.
The N-end rule describes the relation between the half-life of a protein and its N-terminal residue.

N-terminal residue of ß-gal	In vivo half-life of ß-gal in S. cerevisiae
Arg	2 min
Lys	3 min
Phe	3 min
Leu	3 min
Trp	3 min
Tyr	10 min
His	3 min
Ile	30 min
Asp	3 min
Glu	30 min
Asn	3 min
Gln	10 min
Cys	>1200 min
Ala	>1200 min
Ser	>1200 min
Thr	>1200 min
Gly	>1200 min
Val	>1200 min
Pro	?
Met	>1200 min

Figure 1.8: Influence of the N-terminal residue of ß-gal on the protein's half-life in S. cerevisiae, modified from [151].

Bachmair et al. found strikingly different half-lives of ß-Galactosidase proteins *in vivo* depending on the nature of the amino acid at the N-terminus *(Fig. 1.8)* [10]. Hence, some amino acids confer increased half-life times to proteins when expressed at their N-terminus. Ferber and Chiechanover (1987) showed that for ubiquitin-dependent degradation of certain N-end rule substrates, the conjugation of arginine to their N-terminus is required, representing a primary destabilizing residue [151]. Specific lysine residues within the protein serve as the site for multi-ubiquitin chain attachment which is the required component for tagging the protein into the proteasomal core. The destabilizing N-terminal amino acid and a specific internal lysine residue represent the N-degron which are the two critical components of the N-end rule [151].

Alternative proteasome-dependent strategies in targeting proteins for rapid intracellular processing

Realini et al. proposed that specific stretches of alternating lysine (K) and glutamine (E) amino acids within a protein might promote expression of nearby sequences on MHC class I molecules [115]. These stretches were termed 'KEKE motifs' and were defined as greater than 12 amino acids in length, devoid of W, Y, F or P, more than 60% K and E/D and lacking five positive or negatively charged residues in a row.
Realini et al. based their hypothesis on the observation that the peptide SFFPEITHI, which originates from JAK 1 kinase and is found just four residues downstream from a strong 'KEKE motif', is presented 100 times more efficiently (10.000 copies per cell) than most other peptides presented on MHC class I molecules (10 to 100 copies per cell) [56].
'KEKE motifs' are suggested to target proteins to the proteasome through their ability to promote the association of proteins. Several proteins within the MHC class I presentation pathway contain 'KEKE motifs'. The proteasomal subunit C9, five subunits of the regulatory complex of the 26S proteasome as well as chaperonins hsp90 and hsp70, all those offering an optimal point of attack for KEKE mediated protein association [53]. In particular, integrating 'KEKE motifs' into proteins determined for efficient antigen presentation might provide an important possibility to target proteins for rapid proteasomal degradation.

Most of the proteins targeted for proteasomal degradation are marked by polyubiquitinylation. Some exceptions, however, are represented by a select group of labile proteins including ornithine decarboxylase (ODC), p21/Cip1, TCRα, IκBα, c-Jun, calmodulin and thymidylate synthase [65]. Among them, ODC offers the best understood case of ubiquitin-independent proteasomal degradation. ODC catalyzes the first step in the polyamine biosynthetic pathway providing the need for very high regulation as polyamines

are essential and ubiquitous in living cells but become toxic if present at excessive levels. In case of their accumulation, the production of a protein termed antizyme will be enhanced. Antizyme associates with ODC monomers and thereby prevents the association of two ODC molecules which are only enzymatically active as homodimers. Furthermore, it enhances the interaction of ODC with the proteasome leading to its processing and inactivation. Upon antizyme binding, ODC alters its conformation, exposing a C-terminal segment encompassing amino acids 423-461, which together with antizyme provides the 26S proteasome recognition signal [71, 80]. The attachment of these residues to other stable proteins as well as the attachment of whole ODC, however, can cause their instability [81, 86].

Proteasome independent protein degradation

Even though it is now broadly accepted that the proteasome is responsible for the generation of the majority of MHC class I ligands, there are many determinants whose generation from endogenous proteins is resistant to the effect of proteasome inhibition [7, 23, 84, 152]. In one case proteasome inhibitors do even enhance the generation of antigenic peptides [7]. Despite the fact that proteasome inhibitors induce stress proteins which might influence antigen presentation, and that a subset of proteasomes or activities present in proteasomes might be resistent to proteasome inhibitors, these results may indicate the presence of other cellular components that can compensate for the loss of proteasomal activity and may contribute to the pool of antigenic peptides. Furthermore, it was reported that proteasome inhibitors could completely abrogate the degradation of a protein (Ub-Arg-NP) by the proteasome without affecting protein-specific peptide generation [7].
One alternative protease for the generation of antigenic peptides might be provided by the tripeptidyl peptidase II. It was found that cells which adapted to growth in the presence of proteasome inhibitor NLVS (4-hxdroxy-5-iodo-3-nitrophenylacetyl-leu-leu-leucinal-vinyl sulfone) lacked functional proteasomes, but instead showed an increased amount of TPP II [49] and were sensitive to the TPP II inhibitor AAF-CMK [153].

1.5 Hen egg white ovalbumin- a model target protein

Ovalbumin is a glycoprotein with a molecular mass of 45 kDa composed of 386 amino acids. Physiologically it is found as the major protein in the 'white' of avian eggs representing up to 60-65% of the proteins (besides ovomucoid (protease inhibitor), ovotransferrin (iron-binding, bacteriostatic) and lysozyme (bactericide)) [67]. Since ovalbumin belongs to the serpin superfamily it has sequence similarities with many other proteins [67]. The serpin family consists of more than 300 homologous proteins with diverse functions, including the major serine protease inhibitors of human plasma which control enzymes of the coagulation, fibrinolytic, complement and kinin cascades as well as some proteins without any known inhibitory properties like ovalbumin [68]. One plausible factor which might contribute to the lack of inhibitory activity of ovalbumin is that usually serpins undergo a dramatic conformational change on interaction with an attacking protease that ovalbumin is not

able to go through [68]. Nevertheless, a putative reactive center can be determined in ovalbumin at residues 353-354 (Ala-Ser). With these residues inhibitory serpins tend to react with proteases as they mimic a good substrate and lead to cleavage with a subsequent conformational change (loop insertion) [68].

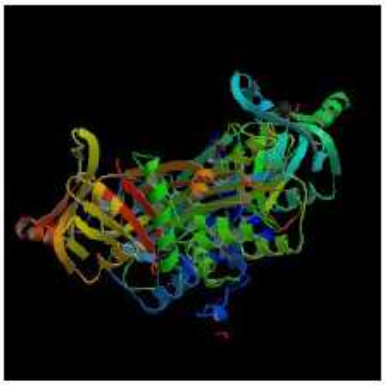

Figure 1.9: Molecular structure of ovalbumin.

The amino-acid sequence of ovalbumin was deduced from 1979 to 1981 [92, 100, 156] and revealed six cysteines with a single disulfide bond between Cys74 and Cys121. Although it is a secretory protein, its aminoterminus is acetylated and does not have a N-terminal leader sequence. Between residues 21 and 47 there was found an internal hydrophobic signal sequence which might be involved in transmembrane location [142]. For posttranslational modifications, it has two potential glycosylation sites at Asn293 and Asn317 recognized by glycosyltransferases and two phophorylation sites at serines 69 and 345.

Ovalbumin has been under scientific investigation since the late 19th century and was one of the first proteins to be isolated in purity. Its ready availability in large quantities has led to its wide-spread use as a standard preparation in studies of the structure and properties of proteins. Furthermore, it is under current investigation as an experimental model of allergy. However, still very little is known about its physiological function apart from its posssible role in transport and storage of metal ions [143] or the discovery that it might act as an amino-acid store for the growing embryo in egg-yolk [122]. There are certainly speculations that its serpin framework may have regulatory functions yet to be discovered.

Since its first isolation in the late 19th century, ovalbumin has been characterized in many studies. Soluble ovalbumin protein can be degraded into peptide fragments by the 20S proteasome [31] as well as the 26S proteasome [21] in the cytosol. In degrading ovalbumin the 26S proteasome makes 51 cuts [75] delivering one peptide, ovalbumin$_{257-264}$, termed SIINFEKL, which is presented on H-2K^b molecules on human and mouse cell lines [41]. However, only about 6% of degraded ovalbumin yield either a SIINFEKL or a SIINFEKL-containing peptide. Many of the peptides generated are N-terminally extended versions, accounting within the total yield of peptides for two or three fold more than SIINFEKL itself [52]. Those N-extended precursor-SIINFEKL peptides are finally trimmed by aminopeptidases in the cytosol or ER. One of such enzymes was identified as LAP (leucine aminopeptidase) [14] , a metalloprotease with broad substrate specifity and wide tissue distribution [52]. The generated peptide SIINFEKL is presented to CD8+ T-cells via the class I antigen-presenting pathway [121]. This particular peptide-MHC class I complex can directly be detected by a highly specific antibody, 25-D1.16 [110], which allows quantitation of TCR ligands on individual cells. Furthermore, polyclonal as well as monoclonal antibodies directed against specific domains of the protein exist.

As for deduction, ovalbumin constitutes a stable protein that can be degraded within the

ubiquitin-proteasome pathway and is a potent and immunogenic intracellular antigen for the stimulation of cytotoxic T-cells.

1.6 Aim of thesis

MVA constitutes one of the most promising viral vectors which is currently evaluated in multiple clinical trials. However, still very little is known about antigenic features required to elicit a strong, long-lasting T-cellular immune response. Within this study, ovalbumin will be used as a model antigen for an intracellular antigen. Different recombinant MVA vectors expressing genetic modifications of ovalbumin shall be constructed and characterized *in vitro* and *in vivo*. The protein shall be targeted for rapid proteasomal processing by distinct modifications known to be associated with protein degradation and the correlation of antigen stability with increased presentation of the ovalbumin-specific peptide SIINFEKL (OVA_{257}) on MHC class I molecules shall be investigated.

As metabolic stability is suggested to be of key importance for the access of antigen to either direct or cross-priming, *in vivo* experiments analyzing CTL response following immunization with MVA vectors expressing native versus rapidly degraded ovalbumin shall be performed to better understand the relevance of each antigen presentation pathway in primary and secondary immunization with MVA and to determine the optimal antigen formulation to be used in priming and boosting.

The first part of this study aimed to determine the optimal antigen-modification to increase the protein‘s instability and thus enhance ovalbumin-specific peptide presentation. For that purpose recombinant modified vaccinia virus Ankara (MVA) shall be constructed expressing modified ovalbumin gene products. MVA-ubiOVA thereby expresses an N-end-rule-targeted ovalbumin which shall be degradad within the ubiquitin-proteasome pathway. Two other rMVA (MVA-TO and MVA-TOT) shall be constructed using the stably ubiquitinated signal sequence of tyrosinase as a degradation signal fused to the N-terminal end of ovalbumin. One of these constructs (MVA-TOT) shall additionally contain the transmembrane domain of tyrosinase at its C-terminal end. These ovalbumin expression constructs shall be compared to MVA-ova expressing native ovalbumin.

i) After generation of rMVA it should primarily be elucidated whether the gene encoding for ovalbumin is integrated in the viral vector and if the system is able to efficiently express the recombinant antigen. For that purpose cells were infected or transfected with rMVA or plasmids, respectively, and Western blotting and immunoperoxidase staining will be performed using a rabbit polyclonal antibody to specifically detect ovalbumin protein.

ii) The effects of antigen modification on protein stability shall be evaluated using radioimmunoprecipitation assay. Degradation of the radioactively labeled and immunoprecipitated ovalbumin shall thereby be assessed by reduced radioactivity at later time points. Furthermore, in Western blotting and immunoperoxidase assays, protein stability and the contribution of proteasomal degradation in target protein processing shall be verified using chemical compounds like lactacystine and MG132 to block proteasomal activity.

iii) To assess the influence of antigen stability on peptide presentation, cells presenting SIINFEKL shall be quantified using flow cytometry. Furthermore, SIINFEKL concentration on a single cell level shall be determined by calculation of the mean fluorescence intensity (MFI).

A second part of this study aimed to determine the optimal antigen formulation suitable to elicit a strong, antigen-specific CD8+ T-cell response after primary and secondary immunization with rMVA.
Here, C57BL/6 shall be immunized with rMVA expressing different antigen formulations of the model protein ovalbumin. Priming shall be performed with 1×10^8 IE of rMVA expressing native ovalbumin in comparison with rMVA expressing modified ovalbumin. Mice shall be analyzed for their CTL response to SIINFEKL (OVA_{257}) and known MVA peptides $B8R_{20}$, $A3L_{270}$ and $K3L_6$ on day 8 post priming using intracellular cytokine staining for IFNγ (ICS). Boosting experiments shall be conducted using rMVA expressing native ovalbumin for priming and different rMVA for boosting on day 30. CTL response shall be assessed on day 6 post boost by ICS.

The present study aims to investigate the impact of ovalbumin modifications on protein stability and subsequent ovalbumin-specfic peptide presentation and aims to further determine optimal antigen formulations for primary and secondary immunization with the viral vector MVA to enhance antigen-specific CTL response.

2 Materials

2.1 Chemicals

Chemical	*Manufacturer*
Acrylamid/Bisacrylamid (30%)	National Diagnostics *(Atlanta, USA)*
Agarose	Gibco/BRL *(Eggenstein)*
Ammoniumchlorid	Sigma *(Munich)*
Ammoniumperoxodisulfat (APS)	Merck *(Darmstadt)*
ß-2-Mercaptoethanol	Sigma *(Munich)*
Bromphenol blue	Serva *(Heidelberg)*
Coomassie-Blue G250	Sigma *(Munich)*
D(+)-Glucose	Merck *(Darmstadt)*
DMSO	Merck *(Darmstadt)*
DTT	Serva *(Heidelberg)*
EDTA	Sigma *(Munich)*
Ethanol	Merck *(Darmstadt)*
Ethidiumbromide	Serva *(Heidelberg)*
Glycerol	Roth *(Karlsruhe)*
Hydrochloric acid 25% (HCl)	Fluka *(Buchs, Switzerland)*
Methanol	Merck *(Darmstadt)*
NP-40	Serva *(Heidelberg)*
o-Dianisidine	Sigma*(Munich)*
Paraformaldehyd (PFA)	Sigma *(Munichy)*
Ponceau S	Sigma *(Munich)*
Potassium chloride (KCl)	Merck*(Darmstadt)*
Reti-Phenol/Chloroform/Isoamylalcohol	Roth *(Karlsruhe)*
Sodium acetat	Fluka *(Buchs, Switzerland)*
Sodium azide	Sigma*(Munich)*
Sodium chloride (NaCl)	Fluka *(Buchs, Switzerland)*
Sodium Dodecyl Sulfate (SDS)	Fluka *(Buchs, Switzerland)*
Sodiumhydrogensulfate (Na2HSO4)	Fluka *(Buchs, Switzerland)*

Chemical	*Manufacturer*
Sucrose	Fluka *(Buchs, Switzerland)*
TEMED	Bio-Rad *(Munich)*
Triton X-100	Sigma *(Munich)*
Tris (Tris-Base;Tris-HCl)	Merck*(Darmstadt)*
Trypan blue	Biochrom KG *(Berlin)*
Trypsin	Biochrom KG *(Berlin)*
Tween 20	Sigma *(Munich)*

2.2 Radioactive chemicals

Radioactive chemicals	*Manufacturer*
Rainbow^{TM} [^{14}C]methylated protein molecular weight marker (14.3-220 kDa)	Amersham Biosiences *(Little Chalfont, UK)*
L[^{35}S] in vitro Cell Labelling Mix	Amersham Biosciences*(Little Chalfont, UK)*

2.3 Biochemicals

Biochemicals	*Manufacturer*
Bovine serum albumin (BSA)	Sigma *(Munich)*
Di-Sodiumchromat(Na251CrO4) in PBS	Hartmann-Analytic *(Braunschweig)*
Dulbecco's Modified Eagle Medium (DMEM)	Cambrex, BioWhittaker *(Verviers, Belgium)*
Ethidium monoazide bromide (EMA)	BD Pharmingen *(Hamburg)*
FBS (Fetal Bovine Serum)	Biochrom KG *(Berlin)*
GeneRuler^{TM} 1 kb DNA Ladder	Fermentas *(St. Leon-Rot)*
Interferonγ	Peprotech
Lactacystine (1mM Stock)	Sigma *(Munich)*
LPS	Sigma *(Munich, Germany)*
MG-132 (10mM Stock)	Sigma *(Munich)*
Na-pyruvate	Cambrex, BioWhittaker *(Verviers, Belgium)*
Pen-Strep (10.000 U penicillin/ml, 10 mg/ml Streptomycin)	Cambrex, BioWhittaker *(Verviers, Belgium)*
Phenylmethylsulfonyl fluoride (PMSF)	Sigma *(Munich)*
Prestained Protein Ladder Broad Range (6-175 kDa)	Amersham *(Little Chalfont, UK)*
Protein G-Plus Agarose	SC Biotechnology *(Santa Cruz, USA)*
Protein Kinase Inhibitor Cocktail (Mini-Complete)	Roche *(Mannheim)*
RPMI 1640	Biochrom KG *(Berlin)*
Trypsin/EDTA	Gibco BRL
Ultraglutamin (200 mM in 0.85% NaCl)	Cambrex, BioWhittaker *(Verviers, Belgium)*

2.4 Buffers

Buffer	*Manufacturer*
DNA sample	99.95 % Glycerol (v/v) 0.01 % NaP Buffer (v/v) 0.04 % Bromphenol blue (w/v)
FACS buffer pH 7.4	1 % BSA (w/v) 0.02% NaN_3 from 20% (w/v) stock diluted in PBS buffer
IPS Blocking Buffer	2% BSA diluted in PBS buffer
IPS Fixing Solution	50% acetone 50% methanol store at 4°C
Paraformaldehyde (PFA)	2% Paraformaldehyde (w/v) in PBS buffer
Phosphate-buffered saline (PBS) pH 7.4	0.14 M NaCl 2.7 mM KCl 3.2 mM Na_2HPO4 1.5 mM KH_2PO_4
Ponceau S solution	1% acetic acid 0.4% Ponceau S (w/v)
RIPA buffer pH 7.4	50 mM Tris-HCl 1% NP-40 (v/v) 0.25% Na-deoxycholate (w/v) 150 mM NaCl 1 mM EDTA Protease inhibitors were added directly before the assay: 1 mM PMSF 1 μg/ml Antipain 1 μg/ml Aprotinin 1 μg/ml Leupeptin
SDS-PAGE buffer pH 8.3 (10x)	25 mM Tris 192 mM Glycine 0.1% SDS (w/v)
SDS-PAGE fixing buffer	50% Methanol (v/v) 10% acetic acid (v/v) 40% H2O (v/v)

Buffer	*Manufacturer*
SDS-PAGE loading buffer pH 6.8 (2x)	50 mM Tris 2 % SDS (w/v) 0.04 % Bromphenol blue (w/v) 84 mM 2-Mercaptoethanol 20 % Glycerol (v/v)
Sucrose 36 % pH 9.0	36% sucrose (w/v) in 10 mM Tris
TAC (Erythrocytes lyses buffer)pH 7.2	0.15 M NH_4Cl 10 mM KHCO3 0.1 mM Na_2EDTA
TAE buffer pH 8.0	1 mM EDTA 20 mM sodium acetate
TBS (10x) pH 7.0	0.5 M Tris 2 M NaCl
TBS-T pH 7.0	TBS (10x) 0.1% Tween 20 diluted in MilliQ
TE buffer pH 8.0	10 mM Tris/HCl 0.1 mM EDTA
TEN buffer pH 7.4 (10x)	100 mM Tris 10 mM EDTA 1 M NaCl
Tris buffer pH 6.8 (1 M)	1 M Tris
Tris buffer pH 8.8 (1.5 M)	1.5 M Tris
Tris buffer pH 9.0 (1 mM)	1 mM Tris
Tris buffer pH 9.0 (10 mM)	10 mM Tris
WB-blocking buffer	1% bovine serum albumin (w/v) in 1x WB washing buffer
WB stripping buffer pH 6.8	100 mM 2-Mercaptoethanol 2 % SDS (w/v) 62.5 mM Tris/HCl
WB transfer buffer anode pH 8.3	25 mM Tris-Base 192 mM Glycin 20 % Methanol (v/v) diluted in MilliQ
WB transfer buffer cathode pH 8.3	0.5% SDS (w/v) in WB transfer buffer anode

Buffer	*Manufacturer*
WB-Tyr-lysis buffer pH 8.0	50 mM Tris/HCl 150 mM NaCl 0.02% NaN3 1% NP 40 diluted in 50 ml MilliQ(store at -20°C)
WB washing buffer pH 7.5 (10x)	50 mM Tris-Base 150 mM NaCl 0.05 % Tween 20

2.5 Enzymes

Enzyme	*Manufacturer*
Alcaline Phosphatase - Shrimp (SAP)	Roche *(Mannheim)*
Calf Intestine Phosphatase (CIAP)	Roche *(Mannheim)*
Klenow-Polymerase	Roche *(Mannheim)*
Proteinase K	Sigma *(Munich)*
Taq and Pwo DNA Polymerase	Roche *(Mannheim)*
Restriction enzymes	Roche *(Mannheim)*, NEB BioLabs *(Schwalbach)*
T4-DNA-Ligase	Roche *(Mannheim)*
Trypsin-EDTA (1x)	Invitrogen *(Karlsruhe)*

All enzymes were used with the buffers recommended and provided by the manufacturer.

2.6 Synthetic Oligonucleotides (Primer)

Primer	
NIH-GS83 5´- - - 3´	primer annealing with deletion III in MVA genome GAA TGC ACA TAC ATA AGT ACC GGC ATC TCT AGC AGT
IIIf1b 5´- - - 3´	primer annealing with deletion III in MVA genome CAC CAG CGT CTA CAT GAC GAG CTT CCG AGT TCC
K1Lint-1 5´- - - - 3´	primer annealing with the K1L gene sequence TGA TGA CAA GGG AAA CAC CGC
K1Lint-2 5´- - - - 3´	primer annealing with the K1L gene sequence GTC GAC GTC ATA TAG TCG AGC
pubi/ova1 (52685) 5´- - - - 3´	primer annealing with the N-terminal end of ubiquitin CAG ATC TTC GTG AAG ACC CTG

Primer	
pubi/ova3 (52687)	primer annealing with the N-terminal end of ovalbumin
5´- - - - 3´	GCT GAA GAG AGA TAC CCA ATC CTG
pubi/ova6 (52690)	primer annealing with the C-terminal end of ovalbumin
5´- - - - 3´	GGG GAA ACA CAT CTG CCA AAG AAG AG

2.7 Plasmids

Plasmid	
pIIIΔHRp7.5	Staib et al.
pIIIΔHRp7.5-ova	Drexler et al.
pIIIΔHRp7.5-ubG76/ovaR1 (ubiOVA)	Drexler et al.
pIIIΔHRp7.5-ubiTyr_SigOva (TO)	Drexler et al.
pIIIΔHRp7.5-ubiTyr_SigOva/TM_Tyr (TOT)	Drexler et al.

2.8 Antibodies

Specificity	*Conjug.*	*Source*
Rabbit polyclonal to Ovalbumin (1221)		Abcam *(London, UK)*
Anti-mouse IgG	PO	Dianova *(Hamburg)*
Anti-Mouse-CD16/CD32 (2.4G2)		BD PharMingen *(Hamburg)*
Peridinin chlorophyll protein-anti-CD4 (RM4-5)	PerCP	BD PharMingen *(Hamburg)*
Allophycoccyanin-anti-(Mouse)-CD62L (Mel-14)	APC	BD PharMingen *(Hamburg)*
Phycoerythrin-anti-Mouse-CD8a (53-6.7)	PE	BD PharMingen *(Hamburg)*
Anti-Mouse CD8a (53-6.7)	FITC	BD PharMingen *(Hamburg)*
Anti-Mouse IFN-y(XMG1.2)	FITC	BD PharMingen *(Hamburg)*
		BD PharMingen *(Hamburg)*
Anti-Rat IgG1 isotype control(R3-34)	FITC	

2.9 Synthetic Oligopeptides

Peptide	*MHC*	*aa Sequence*	*Origin*	*Reference*
Ova_{257}	H2-K^b	SIINFEKL	hen egg ovalbumin	Rotzschke et al. 1991
ß-Gal_{96}	H2-K^b	DAPIYTNV	ß-Galactosidase	Overwijk et al. 1997
$A3L_{270}$	H2-K^b	KSYNYMLL	122L-A3L	Moutaftsi et al. 2006
$K3L_{6}$	H2-D^b	YSLPNAGDVI	024L-K3L	Tscharke et al. 2005
$B8R_{20}$	H2-D^b	TSYKFESV	176R-B8R	Tscharke et al. 2005

2.10 Viruses

Virus	full name	reference
MVA-wt	MVA-II$_{new}$	provided by Drexler et al.
MVA-ova	MVA-P$_{7.5}$-ova	provided by Drexler et al.
MVA-ubiOVA	MVA-P$_{7.5}$-ubG76/ovaR1	generated within this study
MVA-TO	MVA-P$_{7.5}$-ubiTyr_SigOva	provided by Drexler et al.
MVA-TOT	MVA-P$_{7.5}$-ubiTyr_SigOva/TM_Tyr	generated within this study

2.11 Cell lines

Cells	*description*	*ATCC/ref.*
A375	Human malignant melanoma cells	CRL-1619
B16-F1	Murine melanoma cells (C57BL/6)	CRL-6323
BHK-21	Baby hamster kidney cells	CCL-10
CEF	Primary chicken embryo fibroblasts, freshly prepared	Mayr et al. 1974 [88]
CV-I	Normal African Green Monkey kidney fibroblasts	
DC2.4	Murine DCs	Kind gift from Dr. K.L. Rock
HeLa	Human cervix carcinoma cells	CCL-2
NIH-3T3	Murine fibroblasts	CRL 1658
RK-13	Rabbit kidney cells	CCL-37
RMA-HHD	Rauscher leukemia virus induced cells of C57BL/6 (H2b) origin	Kind gift from Dr. F. Lemmonier
B-LCL	Human HLA-A*0201 positive lymphoblastoid B cells	Kind gift from Dr. W. Kastenmueller

2.12 Cell culture media

Media	Composition
Basic Media	RPMI 1640 10%,8%,5%,2% FBS, heat inactivated 1% Pen-Strep
Only-Media	RPMI 1640
M2-Media	Basic Media 28 μl ß-Mercaptoethanol
RIPA-Starving Media	Dulbeccos Modified Eagle Medium 1% Pyruvat 1% Ultraglutamine

2.13 KITs

Product	*Manufacturer*
BD Cytofix/Cytoperm Plus Kit	BD Pharmingen *(Hamburg)*
FuGENE 6®	Roche *(Mannheim)*
Lipofectamin2000®	Invitrogen *(Karlsruhe)*
Lumi-Light®	Roche *(Mannheim)*
PCR Master Mix	Roche *(Mannheim)*

2.14 Consumables

Product	*Manufacturer*
3MM-Filter paper	Whatman *(Maidstone, UK)*
Cell culture flasks (T25, T75, T185, T225)	Greiner *(Nürtingen)*
	Corning *(New York, USA)*
	Nunc *(Wiesbaden)*
Cell culture plates 6-, 12-, 24-, 96-well	Corning *(New York, USA)*
Cell lifter	Corning *(New York, USA)*
Cell strainer 100 μm	BD Pharmingen *(Hamburg)*
FACS tubes	Bio-Rad *(Munich)*
Falcon tubes (15 ml, 50 ml; PS, PP)	BD Pharmingen *(Hamburg)*
GenePulser cuvettes	Bio-Rad *(Munich)*
Gloves	Kimberly-Clark *(Mainz)*
Hyperfilm^{TM} ECL	Amersham *(Little Chalfont, UK)*
Nitrocellulose membrane	Bio-Rad *(Munich)*
PCR reaction tubes	Eppendorf *(Hamburg)*
Petri dishes	Nunc *(Wiesbaden)*
Pipette tips (10 μl, 20 μl, 100 μl, 200 μl, 1000 μl)	Mol. Bioproducts *(San Diego, USA)*
Pipettes 'cellstar' (1-25 ml)	Corning *(New York, USA)*
Reaction tubes (0,5 ml, 1,5 ml, 2 ml)	Eppendorf *(Hamburg)*
Sterile filters (Minisart 0,2-0,45 μm)	Sartorius AG *(Göttingen)*
Syringes (5, 10, 20 ml)	BD Pharmingen *(Hamburg)*
Syringes (Omnifix-F 1 ml)	Braun *(Melsungen)*
Ultracentrifuge tubes (UltraClear)	Beckmann *(Munich)*

2.15 Laboratory Equipment

Equipment	Model/Type	Manufacturer
Block thermostat	BT 1302	HLC BioTech *(Bovenden)*
Centrifuge	Avanti J-25	Beckman *(Munich)*
	Megafuge 1.0R	Heraeus *(Hanau)*
	Biofuge fresco	Heraeus *(Hanau)*
	Biofuge pico	Heraeus *(Hanau)*
CO_2 Incubator	Function Line Hera Cell 150	Heraeus *(Hanau)*
	Cellstar	Nunc *(Wiesbaden)*
Contamination monitor	LB 122	Berthold *(Bad Wildbad)*
Cup sonicator	Sonopuls HD200	Bandelin *(Berlin)*
	TS73,	
	UW200	
Electro-blotting System	PantherTM SemiDry	Owl Scientific *(Portsmouth)*
Film processor	Curix 60	Agfa *(Köln)*
Flow cytometer	FACS Canto	BD Pharmingen *(Hamburg)*
Freezer (-20°C)	Excellence	Bauknecht *(Stuttgart)*
	Premium	Liebherr *(Ochsenhausen)*
Freezer (-80°C)	Hera freeze	Heraeus *(Hanau)*
	Ult 2090	Revco *(Asheville)*
Fridge (4°C)	UT6-K	Bauknecht *(Stuttgart)*
Gel Dryer	Model 583	Bio-Rad *(Munich)*
Haematocytometer	Neubauer counting chamber	Karl Hecht KG *(Sondheim)*
Horizontal Electrophoresis System	A1 Gator	Owl Scientific *(Portsmouth, USA)*
	A2 Gator	Owl Scientific *(Portsmouth, USA)*
Ice machine	AF 200	Scotsman *(Milan, Italy)*
Incubation shaker	Innova 4430	New Brunswick Scientific *(Nürtingen)*
Laminar flow	HERAsafe HS 12	Heraeus *(Hanau)*
Magnetic stirrer	Ikamag Reo	IKA Werke *(Staufen)*

Equipment	Model/Type	Manufacturer
Micropipette	Pipetman P10-1000	Gilson *(Middleton, USA)*
Microscope	Kolleg SHB 45	Eschenbach *(Nürnberg)*
	Axiovert 25	Carl Zeiss *(Oberkochen)*
Microwave	900W	Siemens (Munich)
Multi channel pipette	Transferpette-12 (20-200 μl)	Brand *(Wertheim)*
	Calibra 852	Socorex (Ecublens, Switzerland)
PCR Cycler	GeneAmpR PCR, System 2700	Applied Biosystems *(Foster City, USA)*
pH-Meter	InoLab pH Level 1	WTW GmbH *(Weilheim)*
Phosphor Imager	Molecular Imager PharosFX	Bio-Rad *(Munich)*
Phosphor Imager Screen	Imaging Screen-K	Bio-Rad *(Munich)*
Phosphor Screen Eraser	Screen Eraser-K	Bio-Rad *(Munich)*
Pipettor	easy jet	Eppendorf *(Hamburg)*
	pipetman	Gilson *(Middleton, USA)*
Power supply unit	Model 200 / 2.0	Bio-Rad *(Munich)*
	Power Pac	Biometra *(Goettingen)*
Rotor	Typ 19, SW28, SW 41	Beckmann *(Munich)*
Scale	SPO 51	Scaltec Instruments
	CP153	Sartorius *(Goettingen)*
Steam Sterilizer	Varioklav 500E	H+P *(Oberschleißheim)*
Thermomixer/ -block	Thermomixer 5436	Eppendorf *(Hamburg)*
	Comfort	Eppendorf *(Hamburg)*
Ultracentrifuge	Optima LE-8K	Beckmann *(Munich)*
Universal Hood	Gel Doc 2000	Bio-Rad *(Munich)*
UV Lamp	UVT 2035	Hero Lab *(Wiesloch)*
Vacuum aspirator	Unijet II	Uniequip *(Martinsried)*
Vacuum power heater	Univapo 100H	Uniequip *(Martinsried)*
Vertical Electrophoresis System	P9DS Emperor Penguin^{TM}	Owl Scientific *(Portsmouth, USA)*
Vortexer	VF2	IKA Werke *(Staufen)*
	Vortex Genie 2	Sci. Industries *(Bohemia, USA)*
Waterbath	U3	Julabo *(Seelbach)*

2.16 Mouse strains

All mice were derived from in-house breeding under specific pathagen-free conditions at the GSF animal facility in Neuherberg, Germany, following institutional guidelines.

Mice	*MHC haplotype*	*Source*
C57BL/6	H2-K^b	Charles River *(Sulzfeld)*

2.17 Software

Product	*Manufacturer*
FacsDIVA	Becton Dickinson *(Heidelberg)*
FlowJo 6.4.1	Tree Star *(Ashland, USA)*
GraphPadPrism 4	GraphPad Software *(San Diego, USA)*
Gimp 2.2.13	P. Mattis *(Berkeley, USA)*
LaTex	D.E. Knuth *(Stanfort, USA)*, L. Lamport *(Massachusetts, USA)*

3 Methods

3.1 Cell culture techniques

3.1.1 Cultivation of eucaryotic tissue cells

All cell culture experiments were conducted under sterile conditions. Adherent cells were grown in T185 cell culture flasks (185cm) *(Nunc)* at 37°C and a humidified (about 95% humidity) atmosphere with 5% CO_2 in a cell culture incubator. To keep cells in culture they were split 1:5 to 1:20 when a semiconfluent monolayer of 80-90% density has emerged. The growth medium was removed and after three times of washing with 10 ml cold PBS to remove the cell dedritus and FCS ingredients, cells were detached from the bottom of the flask by overlaying with 3 ml Trypsin-EDTA for 2-5 minutes and careful banging of the flasks. Subsequently, cells were resuspended in 7 ml of the adequate medium and the desired amount of cell suspension was subcultivated in a new cell culture flask with the appropriate amount (25-30 ml) of medium.
For further use, e.g. titration, transfection or analysis of gene expression, cells were plated out either on 6-, 12- or 96-well plates *(Corning Inc.)* in ratios from 1:5 to 1:20 (10-12 ml medium per plate) one or two days prior to use.

3.1.2 Cryo-conservation of eucaryotic cells

Cultured eucaryotic tissue cells were conserved and stored in liquid nitrogen (-196 °C) until they were needed for further experiments. While in their exponential growth phase, cells were harvested from T185 flasks by trypsination *(3.1.1)* and centrifuged for 5 minutes with 1400 rpm at 4°C. Pellets were gently resuspended in cold freezing-medium and finally transferred to sterile cryo-tubes *(Nunc)* as 1 ml alliquots. Before they were subjected to liquid nitrogen for long-time storage, cells were kept at -80°C for one night.

3.1.3 Restoring of cryo-conserved eucaryotic cells

To take cryo-conserved cells into culture again they were thawed in a 37°C water bath until they could easily be transferred into a 50 ml Falcon tube containing pre-cooled 40 ml cell-specific medium. To free the cell suspension from DMSO (of the freezing-medium), cells were washed once by centrifugation with 1400 rpm for 5 minutes at RT *(Megafuge 1.0R, Heraeus)*.
The cell pellet was resuspended in 10 ml of pre-warmed cell-specific culture medium and sowed in a T85 cell culture flask for further growth at 37°C and 5% CO_2 atmosphere. After two days, cultivation could be carried on in T185 flasks.

3.1.4 Determining the number of cells in a cell suspension

To determine the number of cells in a cell suspension, a Neubauer-hematocytometer was used. The Neubauer-chamber *(Fig. 3.1 B)* has nine big quadrats each having a size of 1 mm^2. With the height being 0.1 mm the defined volume of a big quadrat is 0.1 mm^3 (equivalent to 0.1 μl).

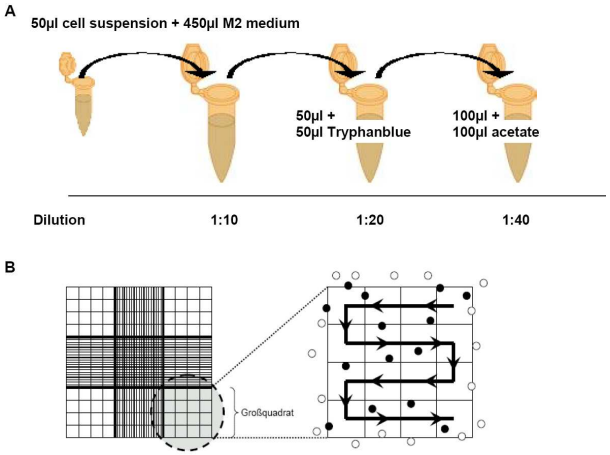

Figure 3.1: (A) Schema of one way to receive the needed dilution for determining the number of cells in a hematocytometer. (B) Schema of the Neubauer-hematocytometer quandrants with an optional way to count cells.

Cells of a cell suspension were centrifuged with 1400 rpm for 4 minutes at 4°C and the pellet was resuspended in 13 ml cell culture medium. Subsequently, 20 μl of the cell suspension were added to 80 μl of the azo-dye Trypan blue, resulting in a 1:5 dilution. Trypan blue owns the ability of staining only dead cells by penetrating their defective membranes.
Living, unstained cells were counted using a light microscope *(Biostar B5, Optech)* with 100-400 x magnifying lenses. Up to three big quadrants, each consisting of 16 small square boxes, were counted and the mean was calculated. To receive the number of cells per ml included in the cell suspension the calculated mean needed to be multiplied with the dilution factor, i.e. 0.2, and the chamber factor 10^4 to compensate for the 0.1 μl volume capacity of the chamber. To avoid counting cells several times they were counted following the schema of *Fig. 3.1 B*.

3.2 Techniques for molecular biology

3.2.1 Extraction of DNA from tissue culture cells infected with MVA

To assess specific parts of the viral genome cells were infected with rMVA (MOI=10) and harvested with a cell scraper 24 hours post infection. 1 ml of the cell suspension was centrifuged with 14.000 rpm for 5 minutes and the pellet was resuspended in 500 μl TE (1x) buffer. After freeze-thawing three times without additional sonification, the cell lysate was mixed with 50 μl TEN (10x), 22 μl proteinase K and 50 μl SDS(20%) and incubated at 56°C for 4 hours.

3.2.2 Purification of DNA by phenol-chloroform extraction and ethanol precipitation

Extracted DNA from cells infected with MVA needed to be purified of proteins, enzymes and other contaminating impurities. For that purpose, the DNA solution was mixed with an equal volume of phenol-chloroform by vortexing and centrifugation with 13.000 rpm for 5 minutes at RT. The resulted upper aqueous phase, containing the DNA, was removed

carefully and added into a fresh Eppendorf-tube. The latter steps were repeated up to three times to achieve a higher purification of DNA-solution. For precipitation and further concentration of DNA, 1/10 volume of sodium acetate (3M NaAc) and 2 volumes of ethanol abs. were added to the DNA-solution and incubated at -80°C for 30 minutes to aid precipitation. Subsequently, DNA solution was centrifuged with 13.000 rpm for 15 minutes at 4°C and the pellet was resuspended in 500 μl ethanol (70%). After an additional centrifugation step for 3 minutes at RT, the pellet was air-dried for 30 minutes and eluted in 50 μl TE buffer (1x).

3.2.3 Analytical horizontal gel electrophoresis

The horizontal agarose gel electrophoresis was used to verify the size of different PCR products. The agarose gel was prepared with a concentration of 0.8% to 1% agarose as recommended for DNA fragments of 0.5- 10 kb pairs.
Diluted in TAE buffer (1x), the agarose was heated-up until boiling for 1 minute and cooled down to 50°C. The fluorescent DNA-intercalating dye ethidium bromide (5 μg/100ml gel) was added for the following visualization of DNA.
A volume of 20 μl containing the aforementioned DNA solution and 20% DNA gel loading buffer were applied to the gel and electrophoresis was conducted with 85-90 V for up to one and a half hours. 6 μl of a premixed 1 kb DNA ladder *(Fermentas Gene Ruler 1kb DNA Ladder)* were used as mass standard.
The gel was removed from the chamber, analysed and photographed under UV-excitation (312 nm).

3.2.4 Polymerase Chain Reaction (PCR)

The method of polymerase chain reaction (PCR) was used to specifically amplify DNA fragments.
The method was invented by Kary Mullis in 1983 and carried the yield of the nobel prize in chemistry in 1993 which he shared with Michael Smith. As he already stated - "Beginning with a single molecule of the genetic material DNA, the PCR can generate 100 billion similar molecules in an afternoon. The reaction is easy to execute. It requires no more than a test tube, a few simple reagents, and a source of heat." - the handling has even become simplier today.
The PCR undergoes three main phases *(Table 3.1)*. At high temperatures the double stranded DNA is separated into two single strands by breaking apart the hydrogen bonds *(Denaturation)*. Lowering the temperature to approximately 5°C below the melting temperature of the used primers (45-60°C), the primers can now anneal to specific sites of DNA *(Annealing)*. A DNA-polymerase, e.g. Taq polymerase from the bacteria Thermus aquaticus, elongates the DNA strand to a double stranded DNA again *(Elongation)*.

For amplification of target genes in large quantities, a PCR Master Kit *(Roche, Mannheim)* was used following the manufacturer‘s instructions.

	Temperature	*Time*	*Cycles*
Initialization	94°C	2 min.	1x
Denaturation	94°C	30 s	
Hybridization	55°C	40 s	30x
Elongation	72°C	3 min	
Final Elongation	72°C	7 min	1x
Hold	4°C	∞	

Table 3.1: Table of PCR cycles.

3.2.5 Photometric analysis of nucleic acid concentrations

To determine the concentration of nucleic acids in a solution, the optical density (OD) was measured in a photometer at wavelength 260 nm. A H_20 filled tube served as reference. The OD_{260} of 1 thereby correlates with 50 μg/ml, respectively.

3.2.6 Transient transfection of eukaryotic cell lines

For transient transfection of eukaryotic cells with highly purified plasmid-DNA lipotransfection was used. Forming a DNA-cationic lipid complex, the DNA can permeabilize the cell membrane. Lipofectamin2000® or FuGENE 6® reagents were used following the manufacturer's instructions.
Before transfection, cells were infected with MVA-wt for one hour (MOI=10-20). The virus was added in 1 ml medium (10% FCS) per well and cells were incubated at 37°C and 5% CO_2 atmosphere. After incubation, the cells were washed once with RPMI Only medium purging them from FCS. The transfection solution was slowly trickled onto the cells before 1 ml RPMI Only medium was added. When indicated, cells were treated with 1- 5μl lactacystine and MG132.
After five hours of incubation at 37°C and 5% CO_2 atmosphere, one half of the medium was replaced by 0.5 ml RPMI containing 10% FCS. Finally, cells were incubated another nineteen hours before harvesting and further use.

3.3 Protein analysis

3.3.1 Immunoblotting (Western blot)

With the technique of immunoblotting the presence of a given protein in a cell lysate can be confirmed and additional data about its molecular mass and abundance can be obtained. The Western blot analysis consisted of three parts. Firstly, proteins solubilized in cell lysates were separated by their molecular mass using a SDS polyacrylamide gel. These seperated proteins were transferred to a nitrocellulose membrane where the protein could be detected using a specifically binding antibody and a labeled anti-immunoglobulin antibody.
Approximately 10^6 cells (e.g. BHK) were infected and harvested with a cell-scraper at

indicated time points. After centrifugation with 2000 rpm at 4°C for 5 minutes, the supernatant was removed and the pellet was resuspended in 80 μl Tyr-Lysis buffer. The lysate was freeze-thawed twice and another centrifugation step followed before the supernatant was transferred into a new Eppendorf tube for further use.

3.3.1.1 Analysis of proteins by denaturating SDS polyacrylamide gel electrophoresis

To separate proteins the lysates obtained as described in *3.3.1* were run on polyacrylamide gels. Polyacrylamide is a polymer that is made by crosslinking of acrylamide and N,N'-Methylenebisacrylamide through the detergents TEMED (N,N,N',N'-Tetramethylethylenediamine) and ammonium persulfate. Within this net small proteins are able to migrate fast whereas larger proteins migrate slower. Hence, sharp protein bands positioned depending on their molecular weight are obtained.
The amount of acrylamide in the gel depends on the proteins to be separated. A 10% acrylamide gel is provided for a molecular range from 16000 to 70000 bp and a 15% acrylamide gel for proteins from 12000 to 45000 bp.
The so called discontinuing SDS-PAGE is composed of a stacking gel (5%, pH 6.8) and a resolving gel (12%, pH 8.8). The stacking gel, in which the proteins are able to migrate much faster, shall focus the lysate to a sharp band. The resolving gel finally seperates them precisely.
During gel electrophoresis, binding of the strong ionic detergent sodium dodecyl sulfate (SDS) to the proteins causes their unfolding due to a abolition of hydrophobic interactions and leads to a negative charge of all proteins. Depending on the size of the SDS-polypeptide complex, the electrophoretic field can now drive protein migration through the gel to the anode.
The resolving gel was made as described in *Table 3.2* and was added to the gel chamber before it was immediately poured over with H_2O MilliQ and left for 1 hour at RT to polymerase. The water was poured away, the comb was placed at the top of the chamber and the stacking gel was added carefully avoiding foam formation. After 20 minutes the gel was placed in the SDS-PAGE gadget and poured over with SDS-running buffer. Before samples were applied into stacking gel pockets 5 x SDS-loading buffer was added and samples were heated up to 95°C for 5 minutes. The gel ran at 45-50 V over night until the bromophenol blue front reached the lower edge of the resolving gel.

Resolving Gel 12%	***50 ml***	***Stacking Gel 5%***	***20 ml***
H_2O MilliQ	16.5 ml	H_20 MilliQ	13.1 ml
Bis/acrylamide (30%)	20 ml	Bis/acrylamide (30%)	3.4 ml
Tris pH 8.8 (1.5 M)	12.5 ml	Tris pH 6.8 (1 M)	2.5 ml
SDS 10%	0.5 ml	SDS 10%	0.2 ml
APS 10%	0.5 ml	APS 10%	0.2 ml
TEMED	0.02 ml	TEMED	0.02 ml
		Ponceau S solution	0.5 ml

Table 3.2: Composition of gels used for SDS-PAGE.

3.3.1.2 Electroblotting of proteins by semi-dry technique

After proteins were separated by SDS-PAGE *(3.3.1.1)* they were transferred from the polyacrylamide gel to a nitrocellulose membrane via semi-dry blotting. The negatively charged proteins migrate from the gel to the membrane in direction of the anode where they bind via hydrophobic and electrostatic interactions.
The nitrocellulose membrane as well as eight pages of Whatman paper were cut to the size of the resolving gel and soaked with transfer buffer. The gel and the membrane were placed in the middle of the electro blotter each surrounded by 4 Whatman papers and the membrane being on the side of the anode *(Fig. 3.2)*. The transfer took place at 0.5 mA/cm^2 for 20 minutes and was confirmed by overlaying the membrane with Ponceau S solution for 10 minutes and washing with PBS.

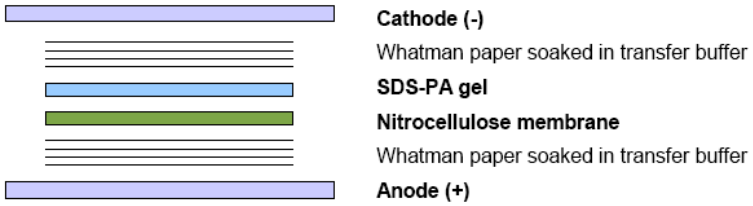

Figure 3.2: Schema for semi-dry blotting of proteins from the resolving gel to a nitrocellulose membrane.

3.3.1.3 Immunochemical detection of immobilized proteins

After protein transfer *(3.3.1.2)* the nitrocellulose membrane was blocked to prevent non-specific binding of antibodies at protein binding sites on the membrane. The membrane was incubated in TBS-T including 1% BSA for at least 1 hour at RT or over night at 4°C. In order to detect the protein of interest blotted on the membrane, incubation with the primary antibody diluted in the appropriate amount of Western blot blocking buffer followed. The rabbit polyclonal antibody against chicken ovalbumin (1:10.000) was incubated with the membrane for 1 hour at RT.
After washing the membrane three times with high volumes (about 200 ml) of TBS-T for 10 minutes on a rocker, the nitrocellulose membrane was incubated with the secondary antibody directed against the Fc-part of the primary antibody and conjugated with the detectable horseradish peroxidase (PO). The secondary antibody goat-PO anti rabbit was diluted as recommended (1:15.000) in Western blot blocking buffer and incubated with the membrane for 1 hour at RT. Excess antibodies were removed by three times of washing with 200 ml TBS-T.
For detection of antigen-antibody complexes on the membrane the Lumi-Light® Kit of Roche was used. About 50 μl/cm^2 of solutions 1 and 2 (1:1) were incubated with the membrane up to 10 minutes. The chemoluminescence reaction was detected using Hyperfilm^{TM} ECL X-ray films where the emission of photons (wavelength 425 nm) was visualized. The time of film exposure to the membrane varied from 1 second to 20 minutes.
Proteins were analysed for their correct sizes using a prestained protein marker as reference.

3.3.2 Radioimmunoprecipitation assay (RIPA)

Pulse-chase assays were performed to assess the stability of specific proteins synthesized in the cell. For that purpose, cells were infected with MVA and subsequently starved to decrease amino acid supply. The following incubation with the radiolabeled amino acid methionine, referred to as pulse period, yielded its integration into newly synthesized proteins. After immunoprecipitation, radioactivity was monitored and visualized by phosphor imager. Degradation of the antigenic protein could be detected as reduced radioactivity at later time-points.

3.3.2.1 Pulse-chase [^{35}S] labeling

About 1x10^6 cells (e.g. HeLa or LCL cells) grown in six-well plates were infected with rMVA or MVA-wt (MOI=20) and incubated for 5 hours at 37°C and 5% CO_2-atmosphere. Proteasome inhibitors lactacystine and MG132 (1-5 μl) could be added if indicated. After one step of washing with 1 ml methionine- and cysteine-free DMEM, cells were incubated with the starving medium for 25 minutes at 37°C. Again, cells were washed as described above. For 5 minutes, cells were labeled with 50 μCi (3.5 μg) [^{35}S]-methionine until solution was removed and cells were overlaid with 1 ml complete RPMI Only medium to stop the radiolabeling process.
Subsequently, cells were lysed with 200 μl Tyr-lysis buffer, scraped off and stored on dry ice until all time points were harvested. The lysates were freeze-thawed two times and centrifuged with 13.000 rpm for 3 minutes at 4°C. 150 μl of the supernatant were taken and mixed with 800 μl of freshly prepared RIPA-buffer containing protease inhibitors and 0.2 μg α-ovalbumin antibody when proceeded with immunoprecipitation *(3.3.3)*.
Samples were separated by SDS-PAGE as described in *3.3.1.1*. The rainbow [^{14}C] methylated protein molecular weight marker was used as a standard to identify the protein of interest. For fixation of protein bands, the gel was laid in a methanol (50%)-acetic acid (10%) solution for 20 minutes, cleared in Milli Q and laid between two cling films for drying in a vacuum dryer two hours at 80°C. Protein bands were finally analyzed by Phosphor Imager *(Bio Rad, Munich)* after 4 to 5 days of exposure to the screen *(Bio Rad, Munich)*.

3.3.3 Immunoprecipitation

Soluble proteins can be isolated from solution by binding through specific antibodies forming antigen-antibody complexes. These immunocomplexes can be extracted via binding to a solid support, e. g. the bacterial proteins protein A or protein G coupled to Agarose or Sepharose, and centrifugation.
For immunoprecipitation assays cell lysates were prepared as follows. About 1-3x10^6 cells were infected (MOI=10-20) with virus and after harvesting cells with a cell-scraper, the cell solution was centrifuged with 1500 rpm for 5 minutes and resuspended in 100 μl Lysis-buffer. Subsequently, cells were freeze-thawed twice and sonicated if not radiolabeled before.
Cells were centrifuged again with 13.000 rpm at 4°C for 10 minutes and the lysate was transferred to a new Eppendorf-tube. 900 μl of freshly prepared RIPA-buffer containing protease inhibitors and 0.2 μg of specific polyclonal antibody α ovalbumin was added and the solution was incubated for one hour at 4°C on a rocker.

Cautiously shaked protein G-Agarose (20 μl) was finally added to the samples before they were incubated at 4°C on a rocker over night. After three standardized steps of washing with RIPA-buffer, proteins could be separated and analyzed by SDS-PAGE *(3.3.1.1)*.

3.4 Immunohistochemical techniques

3.4.1 Immunoperoxidase staining

To detect ovalbumin in tissue culture, an immunohistochemical technique was used. Either BHK cells or CVI cells grown in six-well tissue culture plates were infected with MVA-wt and transfected with plasmids expressing modified ovalbumin. AraC (Cytosinarabinoside), which inhibits expression of late viral proteins, was optionally added 1:1000 for 30 minutes before infection.
After 24 hours of incubation at 37°C and 5% CO_2 atmosphere, the medium was removed and cells were fixed and permeabilized by overlaying with 1 ml fixing solution per well for 10 minutes at -20°C. This step helped to preserve ovalbumin in its native form allowing the first antibody to recognize its surface structure.
Fixing solution was removed and cells were washed twice with PBS. 2 ml blocking buffer were added to inhibit non-specific binding of the antibody before cells were incubated for 60 minutes at RT rocking slowly.
The blocking buffer was removed and cells were washed again before the first antibody (rabbit polyclonal to hen egg white ovalbumin) α ovalbumin was added in 1 ml diluted 1:1000 for another 60 minutes. The first antibody was removed and cells were washed three times thoroughly with 2 ml PBS per well for 5 minutes at RT rocking slowly to remove unbound antibody. The second antibody (α rabbit-PO) diluted 1:1000 in 2 ml per well was added and cells were incubated for 30-45 minutes at RT rocking slowly.
To proceed, a substrate solution was prepared by mixing 1 ml EtOH abs. with a flock of dianisidine in a 1.5 ml microcentrifuge tube by vortexing for 10 minutes. After centrifugation for 30 seconds with 1300 rpm at RT the supernatant was taken for further use.
200 μl of the saturated dianisidine solution were added to 9.8 ml PBS in a 15 ml conical Falcon tube and mixed by vortexing before it was filtered sterilely. After cells had been washed as described above 15 μl H_2O_2 were added to the final substrate solution by gently mixing before immediate use of 1 ml per well for peroxidase staining.
After 30 minutes of incubation a brown staining of cells could be detected under light microscope. When intensification of colouring came to an end substrate solution was replaced by 1 ml PBS.

3.5 Virological methods

3.5.1 Generation of recombinant MVA

For generation of recombinant MVA, the gene of interest needed to be subcloned into an MVA-transfer plasmid. From this plasmid, pIIIΔHR-$P_{7.5}$, the gene was transferred into major deletion site III of MVA via homologous recombination *(Fig. 3.3)*. After viral infection, genes of poxviruses are transcribed in the cytoplasm by the viral transcription

machinery. Expression of recombinant genes was therefore placed under control of the vaccinia virus promotor P7.5 which allows for early as well as for late gene expression.

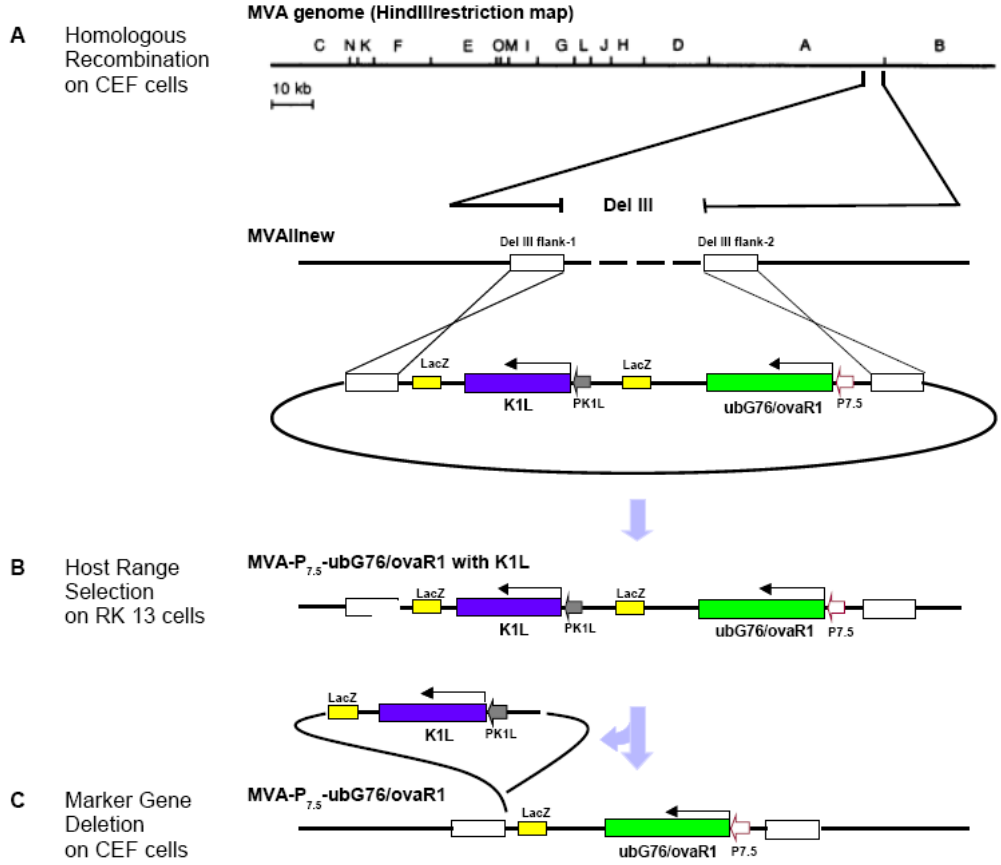

Figure 3.3: *Flow chart for the generation of recombinant MVA-$P_{7.5}$-ubG76/ovaR1.* (A) CEF cells were infected with MVA-wildtype and transfected with the vector plasmid carrying the gene ubG76/ovaR1, encoding for the ubiquitinated ovalbumin protein. The insertion cassette with ubG76/ovaR1 (under the vaccinia viral promoter $P_{7.5}$), the homologous LacZ sequences and the vaccinia virus host range gene K1L, was subcloned into the MVA genome due to analogous deletion site III-flanking sequences by homologous recombination. (B) By transient introduction of the K1L gene into the viral genome, the recombinant MVA, but not MVA-wildtype virus, acquired the ability to grow on RK13 cells. (C) Under non-selective growth conditions on CEF cells, K1L could be deleted from recombinant viral genomes by homologous recombination.

3.5.1.1 Stable transfection for the generation of recombinant MVA

CEF cells grown in six-well plates were infected with MVA-wt (MOI=0.05-0.1) and incubated for one hour at 37°C. The medium was removed and monolayers were washed once with 2 ml RPMI Only medium.
For transfection, Lipofectamin 2000^{TM} or FuGENE® reagents were used following the manufacturer's instructions. The transfection-solution was submitted directly onto the cell monolayer in drops before 1 ml of cell-specific medium was added. After five hours of incubation at 37°C, the medium was replaced by 2 ml of RPMI (10%) medium and cells were incubated for another fortythree hours. Cells were harvested with a cell scraper, resuspended and freeze-thawed three times at -80°C and a 37°C waterbath. Three times of sonification at maximum strength in icecold water followed before RK-13 cells grown in six-well plates were infected with a tenfold serial dilution (10^{-1} to 10^{-4}) of the harvested material. After two to five days viral foci were harvested ('picked') with a 10 μl pipette by aspiration and transferred to Eppendorf-tubes containing 500 μl RPMI 10% medium. The harvested viral plaques were prepared by freeze-thawing and sonification for further infection of RK-13 cells.

3.5.1.2 Isolation of recombinant MVA on RK-13 cells

Isolation and extraction of defined recombinant MVA requires the sorting of wildtype virus still present in cell lysates. For that reason, it was taken advantage of the disability of MVA to grow on RK-13 cells.
MVA has a characteristic host range. Lacking the gene for K1L, which is known to be a vaccinia virus host range gene, MVA does not have the ability to grow on RK-13 cells. Therefore, the gene was used as a selective growth marker. By transient introduction of the K1L gene into the viral genome via the vector plasmid, the virus acquires the ability to grow on RK-13 cells. Under these selective growth conditions only recombinant virus with the inserted k1L gene was able to grow and could efficiently be isolated on RK-13 cells *(Fig. 3.3 B)*. After three to six passages on RK-13 cells the absence of wildtype virus was confirmed by PCR analysis.

3.5.1.3 Generation of K1L-free recombinant MVA

To delete the host range marker gene K1L from recombinant viral genomes further passages on CEF cells were carried out. To grow on CEF cells, K1L is not required and is therefore eliminated under non-selective growth conditions. As K1L is flanked by two repetitive 216 bp sequences, the LacZ genes, the K1L expression cassette can easily be removed from the viral genome by homologous recombination [138].
CEF cells grown in 12-well plates were infected using tenfold serial dilutions (10^{-1} to 10^{-8}). Cells were harvested using a cell-scraper when viral foci could be detected.

3.5.2 Virus amplification

To amplify recombinant MVA on a large scale, CEF cell monolayers of 30-40 T225 tissue culture flasks were infected by overlaying with 5 ml virus suspension approximately corresponding to an MOI of 0.1 to 1 IU/cell. During virus adsorption for 1 hour at 37°C flasks were repeatedly shaked carefully to avoid drying of cells. About 30 ml virus growth

medium were added per flask which were further incubated for 2 days or until a cytopathic effect could be detected.
Cells were harvested by freeze-thawing once at -20°C. During the process of thawing, flasks were rocked boldly to support cell-dissolution from the flask's bottom with scraping ice slices. Harvested cell suspensions were transferred into 250 ml ultracentrifuge tubes and centrifuged with 17.000 rpm for 1.5 hours. The medium was discarded and pellets were resuspended and combined in 10 mM Tris pH 9.0 using approximately 1 ml per T225 culture flask. After freeze-thawing three times on dry ice and three times of thorough sonification on ice, virus material could be stored at -80°C as crude stock or admitted to further purification *(3.5.3)*.

3.5.3 Virus stock purification

For semipurification of crude stock preparations from cell debris and proteins, the virus stock was admitted to ultracentrifugation through a sucrose cushion.
The crude stock obtained as described in *3.5.2* was freeze-thawed three times and sonificated three times for one minute on ice. The dounce homogenizer, 80 ml 10mM Tris pH 9.0 and two 50 ml Falcon tubes were put on ice.
The crude stock was transferred to the cell douncer and the pistill was moved up and down 30 times. The suspension was allowed to cool down in between sets of strokes so that no heat could develop. The harvest was returned into the Falcon-tube and centrifuged with 4000 rpm for 5 minutes at 4°C before the supernatant was saved in a fresh 50 ml tube. The pellet was resuspended in 25 ml 10 mM Tris pH 9.0 and the suspension was admitted to the douncing procedure again. This process was repeated twice with the third supernatant being divided to Falcon one and two.
Ultracentrifuge tubes (SW 28) were prepared by filling half a volume with 36% sterile sucrose cushions (25 ml) and overlaying with equal volumes of virus suspension. The tubes were put into centrifuge buckets and tared to identical weight on a scale with 10 mM Tris pH 9.0. The ultracentrifugation was performed for 1.5 hours with 13.500 rpm and 4°C.
The supernatants were discarded and pelleted virus material was resuspended in 1 mM Tris pH 9.0. Approximately 1 ml Tris was used for ten T225 cell culture flasks of crude stock preparations.

3.5.4 Determining titers of virus stock preparation

To determine the titers of virus stock preparations subconfluent monolayers of CEF-cells grown in 96-well tissue culture plates were infected with different dilutions of recombinant MVA.
CEF cells were harvested from a T185 flask by trypsination and three times of washing with 10 ml PBS. When adherent cells came off, 7 ml RPMI (2%) medium were added. After resuspending, 1 ml was added to a final volume of 10 ml RPMI 2%. Out of this cell solution 100 μl were plated out on a flat bottomed 96-well plate for further use.
After freeze-thawing as described above, the MVA-virus stock preparation was primarily homogenized by sonification for 30 seconds in a cup sonicator at maximum strength and thorough vortexing. Subsequently, a 10-fold serial dilution ranging from 10^{-1} to 10^{-11} was prepared in RPMI-medium including 2% FCS. For infection, dilutions from 10^{-6} to 10^{-11} were taken. Using a total of 1,6 ml of each dilution 100 μl per well were added in replicates

of sixteen to the cell monolayers. One line was left uninfected to serve as negative control. After incubation at 37°C for three days to one week, plates were monitored under a microscope and all wells in which viral foci could be detected were counted.
For calculation of virus titers, the following formular was used:

$$Titer = 10a + 0,5 + (xa + 2/16) + (xa + 2/16) + (xa + 3/16)x10$$

3.5.5 Infection of tissue culture cells with MVA

Confluent monolayers of tissue cells cultured in 6-, 12-, 96- well plates were infected one day prior to further use or analysis of cells. Only 96-well plates were used immediately. The MOI (Multiplicity Of Infection) determined how many viral particles were submitted to infect one cell and thus was stated as infectious units (IU) per cell.
To calculate the amount of virus needed for infection, the virus titer was determined as described in *3.5.4*. The cell number as well as the desired MOI were needed. The MOI was calculated as follows:

MOI (IU/ml) × cell number (e.g. 1×10^6 in one 6 well)= X
X÷ virus titer(IU/ml) = ml of virus suspension needed

The virus suspension was thawed and homogenized by sonificating for 1 minute on ice in a cup sonicator *(Sonopuls HD200)* and additional vortexing to dissolve clusters of viral particles emerging at -80°C freezing. The growth medium of cells was discarded and the virus suspension diluted in the appropriate amount of medium was added. When indicated, 1-5 μl lactacystine and MG132 were added. Infected cells were incubated at 37°C and 5% CO_2- atmosphere until further use.

3.6 Immunological techniques

3.6.1 Immunization of mice

About 8 to 12 week old female C57BL/6 mice were used for immunization following different settings. Mice were either received from Charles River Laboratories or obtained from the institute's own breeding kept under pathogen-free conditions in the Institute's animal facilities. Dose requirements and inoculation routes are displayed in the following table:

Vaccine	*dose*	*diluted in:*	*application*
MVA-II$_{new}$	1x10^8	500μl PBS	intraperitoneally (i.p.)
MVA-ova	1x10^8	500μl PBS	intraperitoneally (i.p.)
MVA-ubiOVA	1x10^8	500μl PBS	intraperitoneally (i.p.)
MVA-TO	1x10^8	500μl PBS	intraperitoneally (i.p.)
MVA-TOT	1x10^8	500μl PBS	intraperitoneally (i.p.)

3.6.2 Isolation of murine splenocytes

The preparation of lymphocyte cultures was performed under semi-sterile conditions using sterile materials and solutions.
Mice were dispatched by cervical dislocation and subsequently disinfected and cleaned with ethanol (80%). The coat of the left abdominal region was removed with a 3 cm cut of a sterile scissor. The now visible peritoneum was opened with a 1-2 cm incision uncovering the spleen. The spleen was excised with tweezers, cleared of adhesive adipose tissue and immediatly transferred into 5 ml cold M2 medium (10% FCS).
To obtain single cells, the spleen together with the medium was transferred into a petri dish (⊘ 6 cm), squashed and triturated on a metalgrid with the punch of a 10 ml syringe until the spleen was completely dissolved in medium. The cell solution was returned to the Falcon-tube through a cell strainer and the metalgrid was washed once with 10 ml medium. Again, the remaining spleen tissue was triturated carefully and transferred to the Falcon-tube through the cell strainer.
The cell solution was centrifuged with 1500 rpm for 5 minutes at 4°C. Splenocytes were resuspended in 4 ml TAC erythrocyte lysis buffer and immediately incubated in a 37°C waterbath for exactly 2 minutes under continuous shaking. To stop lysis of erythrocytes, 40 ml cold M2 medium were added. Cells were put through a cell strainer again, centrifuged with 1500 rpm for 5 minutes and finally resuspended in 3 ml M2 medium.
Cells were counted using a Neubauer-hematocytometer as described in *3.1.4*. Approximately 60 to 140 million lymphocytes could be isolated from one spleen of a female C57BL/6 mouse.

3.6.3 Intracellular cytokine stain (ICS)

By means of the intracellular cytokine secretion assay, immunized mice were analyzed for their T-cell activation upon vaccination with recombinant MVA. Lymphocytes were analyzed for their surface markers and interferon-γ production by flow cytometry (FACS). After isolation of spleen cells as described in *3.6.2*, lymphocytes were stimulated *in vitro* with vaccinia viral and recombinant peptides in order to induce interferon-γ production due to specificity of T-cell receptors. Since interferon is a secretory protein, cells were additionally treated with brefeldin A to inhibit export of proteins from the endoplasmatic reticulum to the golgi apparatus. Hence, IFN-γ accumulates in the cell and can be detected by intracellular staining. After lymphocyte preparation and cell count as described in *3.6.2*, cells were syntonised to 2 x 10^7 cells per ml and transferred to a 96-well flat-bottom plate with one mouse representing one horizontal row.

3.6.3.1 Peptide stimulation

For peptide stimulation of lymphocytes about 4 x 10^6 freshly prepared spleen cells *(3.6.2)* were transferred in a 96-well flat-bottom plate. One mouse representing one horizontal row and the number of horizontal wells depending on the number of peptides. Additional wells prepared for each responder were used as control samples, isotype control and single stain controls. For each peptide a mastermix with 5 μl vortexed and sonicated peptide and 5 μl of brefeldin A in 1 ml M2 medium was prepared and resuspended. 50 μl of the mastermix were added to each well of one column stimulating T-cells of all mice. Cells of one additional row for the isotype control and 5 wells for single-color staining were

stimulated by addition of 1 μl aCD3e antibody. Two wells with cells stimulated with 4 μl aCD3e antibody were included as positive control with matched isotype control. Cells were incubated with the peptide for five hours at 37°C in a 5% CO_2-atmosphere and analyzed for their expression of cell surface markers and cytokine production as described in the following sections.

3.6.3.2 EMA-stain and Fc-blockage

Cells that were either harvested after infection, transfection or peptide stimulation were transferred to a 96-well V-bottom plate, centrifuged for 2 minutes with 1400 rpm and 4°C and were reunited in two horizontal rows in the middle of the plate in 200 μl FACS buffer by transferring the upper and the lower lines to the middle. All following incubations and pipetting steps were carried out on ice using pre-cooled solutions. After another centrifugation step, cells were resuspended in 100 μl FACS buffer containing 5 μg/ml anti-CD16/CD32 antibody and 1 μg/ml ethidium monoazide (EMA) and were incubated for 20 minutes on ice under bright lights. Afterwards, cells were washed three times by repeated centrifugation and resuspended in 180 μl FACS buffer per well.
The anti-CD16/CD32 antibody was used to saturate cellular Fc-receptors preventing unspecific binding of antibodies used later in this experiment. Ethidium monoazide (EMA) was used for live/dead discrimination. It is a positively charged molecule which is inoculated by cells with damaged membranes in a light-dependent process (dead cells) and can be photochemically and irreversibly crosslinked to nucleic acids. FACS-analysis then allows for specific detection of EMA stained cells by excitation with a 488 nm laser.

3.6.3.3 Staining of surface markers

For staining of extracellular surface markers Fc-blocked and EMA-treated cells *(3.6.3.2)* were resuspended in 50 μl FACS buffer containing PE-anti-CD8a [1:100], APC-anti-CD62L [1:200] and PerCP-anti-CD4 [1:200] antibodies and were incubated for 30 minutes in the dark. Cells prepared for single colour staining were resuspended in 50 μl FACS buffer containing 1 μl aCD4-PerCP, aCD8a-PE, aCD8a-FITC or aCD62L-APC antibody. One well was left unstained as negative control. After incubation, cells were washed 2.5 times by centrifugation and resuspension in 180 μl FACS buffer.
Single colour stained samples only needed extracellular staining and could therefore already be fixed by resuspension in 150 μl paraformaldehyde (PFA) solution (2%) and transferred into FACS-vials already containing 150 μl FACS buffer. When fixed in PFA, cells could be stored at 4°C in the dark for up to five days until FACS-analysis. If intracellular staining was required, cells were further treated as described in *3.6.3.4* and *3.6.3.5*.

Surface staining of SIINFEKL, which involved an unlabeled primary antibody (α SIINFEKL-K^b) diluted 1:5, was continued by incubation with a 1:250 dilution of a PE-labeled secondary goat anti-mouse antibody for 30 minutes in the dark, followed by washing as described above.

3.6.3.4 Permeabilization of cell membranes

For permeabilization, cells were incubated with 100 μl of BD Cytofix/Cytoperm for 15 minutes in the dark. 100 μl of BD Perm/Wash were added and cells were centrifuged with

1400 rpm for 2 minutes at 4°C. Cells were washed once by resuspending cell pellets in 150 μl BD Perm/Wash (1x) and subsequent centrifugation.

3.6.3.5 Intracellular cytokine staining

For intracellular staining of IFN-γ, 50 μl BD Perm/Wash buffer containing the anti-IFN-γ FITC-labeled antibody were added to permeabilized cells. Incubation was carried out for 30 minutes on ice in the dark. To determine the unspecific background of staining, samples preserved for isotype staining were incubated with a FITC-labeled IgG antibody (1:500) of the same isotype as the anti-IFN-γ antibody, but directed against an irrelevant epitope. After incubation with the antibodies cells were washed 2.5 times, fixed by resuspension in 125 μl paraformaldehyde (PFA) solution (2%) and transferred into FACS-vials already containing 125 μl FACS buffer. Cells could be stored at 4°C in the dark for up to five days until FACS-analysis when fixed in PFA. Stained cells were analyzed using the BD FACS Canto flow cytometer with FacsDIVA and FlowJo Software.

3.6.4 Fluorescence activated cell sorting (FACS)

Flow cytometry allows for analysis of single cells with a size between 0.5 μm and 40 μm diameter on the basis of light scattering, light excitation, and emission of fluorochrome molecules. By aspiration through a fine needle and hydrodynamic focusing, cells successively enter a detection channel where they pass through a set of laser beams. Analysis of cell size, granularity and protein expression is based on the forward light scatter (FSC), the sideward light scatter (SSC) and the emission of light by laser-activated fluorochromes, respectively. The usage of several lasers and different fluorochromes with distinct emission spectra allows for simultaneous analysis of a variety of different markers.
For analysis of cellular protein expression, primary antibodies conjugated with a fluorochrome or detection by a labeled, specific secondary antibody can be used. Analysis is possible for proteins expressed on the cell surface as well as for intracellular proteins after permeabilization and fixation of the cell. The optical readout from analyzed cells is converted into digital information in a detector system and can be visualized and analyzed using specific software such as FacsDIVA *(BD Biosciences)* or FlowJo *(TreeStar)*. Since emission spectra of some fluorochromes show partial overlaps, each experiment contains samples only stained with a single colour to define cells that are truly positive and to adjust instrument settings in order to subtract signal overlaps for each detection channel.
The following table shows used fluorescent dyes, their excitation and emission spectra as well as their excitation laser lines.

Fluorochrome	***Ex.-max. (nm)***	***Ex. Laser Line (nm)***	***Em.-max. (nm)***
Fluorescein isothiocyanate (FITC)	494	488	519
Allo-phycocyanine (APC)	650	595, 633, 635, 647	660
Peridinin- chlorophyll protein (PerCP)	482	488, 532	678
R-phycoerythrin (PE)	496, 546	488, 532	578

3.6.4.1 Gating strategies

To assess cell surface expression of SIINFEKL/H2-K^b complexes after infection with MVA and preparation of cells as described above, cells were gated using FacsDIVA and FLowJo 6.4.1 software as depicted in *Fig. 3.4*.

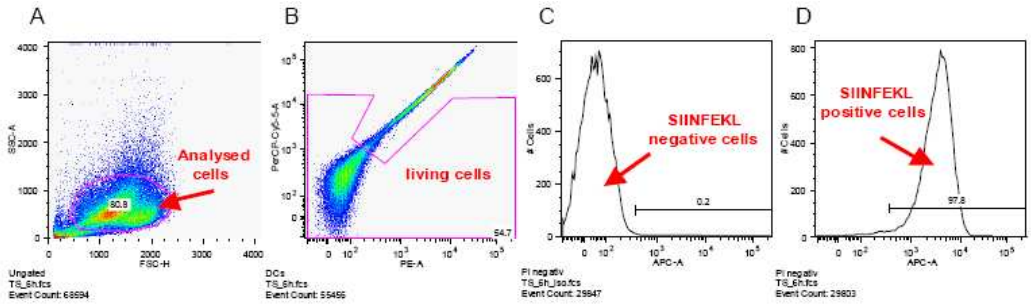

Figure 3.4: *Gating strategy employed for flow cytometric analysis of SIINFEKL surface expression.* (A) Gating of the main living cell population. (B) Discrimination between live and dead cells based on EMA staining. (C) Determination of a 'positive' gate which excluded all cells from negative control samples. (D) Determination of the positive cell population.

The gating strategy for flow cytometric analysis of intracellular cytokines after peptide stimulation of splenocytes *(3.6.3)* isolated from vaccinated C57BL/6 mice, is shown in *Fig. 3.5*.

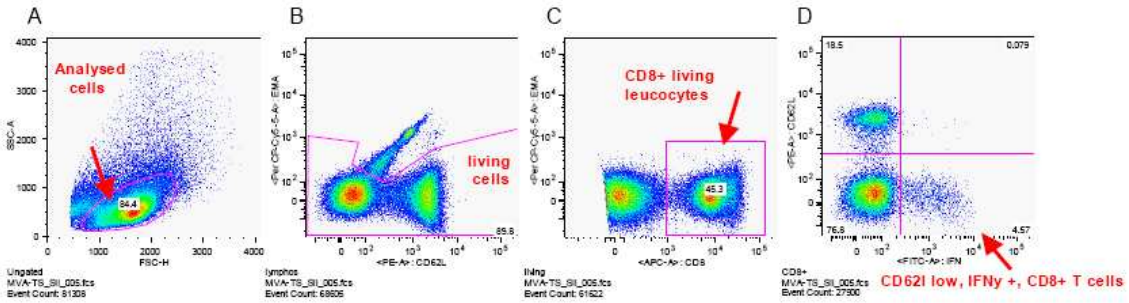

Figure 3.5: *Gating strategy for flow cytometric analysis of intracellular cytokine levels produced in response to peptide stimulation of splenocytes isolated from vaccinated C57BL/6 mice.* (A) major leucocyte population displayed in forward (FSC) and sideward (SSC) scatter. (B) Discrimination between live and dead cells, excluding the cells positive for EMA. (C) Gating of CD8+ living leucocytes. (D) Identification of IFN-γ positive or negative (X-axis), activated (CD62L low) or non-activated (CD62L high) CD8+ T-cells.

4 Results

4.1 Generation of MVA-ubiOVA, MVA-TOT and MVA-TO

Within this study two recombinant viruses (MVA-ubiOVA and MVA-TOT) were constructed and characterized *in vitro* and *in vivo*. A third virus included in this study (MVA-TO) was kindly provided by the laboratory of PD Dr. I. Drexler.

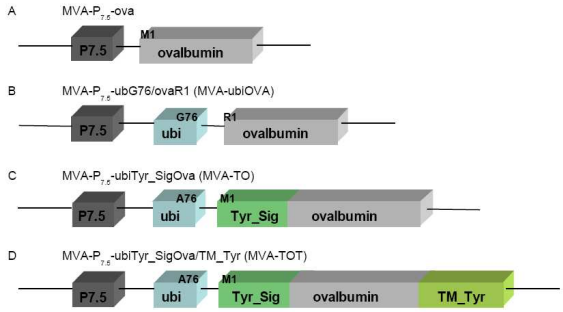

Figure 4.1: *Recombinant viral vectors MVA used within this study.* Two recombinant MVA expressing a modified ovalbumin gene were constructed for this study (MVA-ubiOVA (B) and MVA-TOT (D)). A third virus, MVA-TO (C), was provided by Drexler et al. .

MVA-ubiOVA *(Fig. 4.1 B)* encodes for an ovalbumin protein targeted for rapid proteasomal degradation making use of the N-end rule. Within that construct, the first amino acid of ovalbumin, methionine (M), is replaced by an arginine (R). After protein synthesis, the N-terminally fused ubiquitin is supposed to be split off by ubiquitin-hydrolases between the glycine 76 (G76) of ubiquitin and the arginine 1 (R1) of ovalbumin. The N-terminal amino acid arginine of ovalbumin, representing the primary destabilizing residue of the N-end rule, shall consecutively provide rapid degradation to the protein [10, 151].
The strategy to increase a protein's turnover rate underlying the construction of MVA-TO and MVA-TOT *(Fig. 4.1 C and D)* is based on findings that a stable N-terminal fusion of ubiquitin to a protein by converting glycine 76 of ubiquitine into an alanine 76 [18] can induce rapid proteasomal degradation within the UFD-pathway [70].

Within our laboratory, the instability of a melanoma-specific antigen, tyrosinase, could markedly be increased by stable N-terminal fusion of ubiquitin (A76) to tyrosinase (M1) [44]. The N-terminal region of this construct, including the nonremovable ubiquitin moiety fused to the signal sequence of tyrosinase, was suggested to constitute a general degradation signal applicable to other proteins such as ovalbumin. Hence, a recombinant MVA was constructed expressing a tyrosinase signal peptide-ovalbumin fusion protein stably linked to ubiquitin at its N-terminal end (MVA-TO) (Fig. 4.1 C).
MVA-TOT *(Fig. 4.1 D)* was designed analogous to MVA-TO but additionally included the transmembrane domain of tyrosinase at the C-terminal end of ovalbumin, hypothesizing

that this domain might play a key role in protein degradation by intensified targeting to cellular compartments or enhanced misfolding of the protein.

4.1.1 Generating MVA-ubiOVA

After a genetical and functional analysis of the transfer plasmid pIIIΔHRP$_{7.5}$-ubiOVA (pIII-ubiOVA), MVA-ubiOVA was generated as summarized in section *3.5.1*. To confirm the correct insertion of the transgene into deletion site III of the MVA genome PCR-analysis was conducted according to the following scheme *(Fig. 4.2)*.

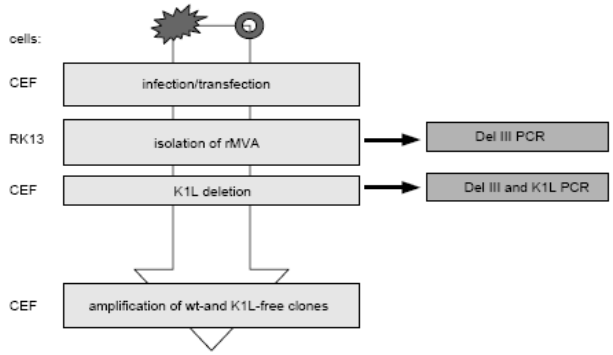

Figure 4.2: *Flow chart for MVA generation.* A first PCR of viral clones for deletion site III was performed after RK-13 cell passages. A second PCR for Del III and the K1L host range gene was conducted after further passages on CEF cells. Hence, a candidate clone for virus amplification and purification could be determined.

After passages on RK-13 cells the integrity of deletion site III was determined by PCR-analysis using primers NIH-GS83/IIIf-1B. As explicitly explained in *Fig. 4.6*, the expected sizes of gene fragments were as follows:

3800 bp	-	for the correct insertion of ubiOVA in MVA (MVA-ubiOVA + k1L)
2500 bp	-	for the correct insertion of ubiOVA in MVA (MVA-ubiOVA - k1L)
750 bp	-	for the 'empty' deletion site III of MVA-wt (MVA-wt
3800 bp	-	for the transfer plasmid pIII-ubiOVA (pIII-ubiOVA)
2250 bp	-	for the plasmid pIIIΔHR (LV)

As *Fig. 4.3* shows, deletion site III was detected as a 2500-3000 bp fragment in clones 1-4 and 7-21. A fragment corresponding to the size of MVA-wt (750bp) was detected in clones 5 and 6. Further passages were conducted on CEF cells using ubiOVA- positive rMVA clones as depicted in *Fig. 4.3*. Under these non-selective growth-conditions repetitive DNA sequences flanking K1L were responsible for removing the vaccinia virus host range gene from the viral genome by homologous recombination *(see Fig. 3.3)* [138].
In order to confirm the correct size of deletion site III and the absence of K1L another PCR with primers NIH-GS83/IIIf-1B and *K1L*int-1/*K1L*int-2 was conducted *(Fig. 4.4)*. Only clone 1, 12, 14, 17 and 21 could not be evaluated as rMVA with the correct insertion of ubiOVA and a size of 2500 bp. Furthermore, as depicted in *Fig. 4.4 B*, clones 5, 11, 14, 16, 17 and 19 were still tested positive for K1L. Consequently, a rMVA clone positive for the transgene but lacking K1L, as clone number 2, was used for further virus amplification.

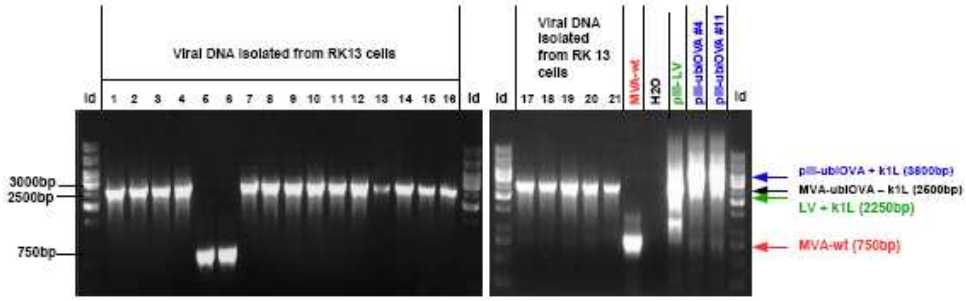

Figure 4.3: *PCR-analysis of viral DNA isolated from RK13 cells.* The correct insertion of the transgene ubiOVA into the MVA genome was confirmed using specific PCR-oligonucleotides for deletion site III (NIH-GS83/IIIf-1B). MVA-wt, H2O, pIIIΔHR-LV (pIII-LV) and two plasmids pIII-ubiOVA(#4 and#11) are shown as reference. A 1 kb DNA Ladder (ld) served as standard. Expected fragments are marked with an arrow according to their respective size.

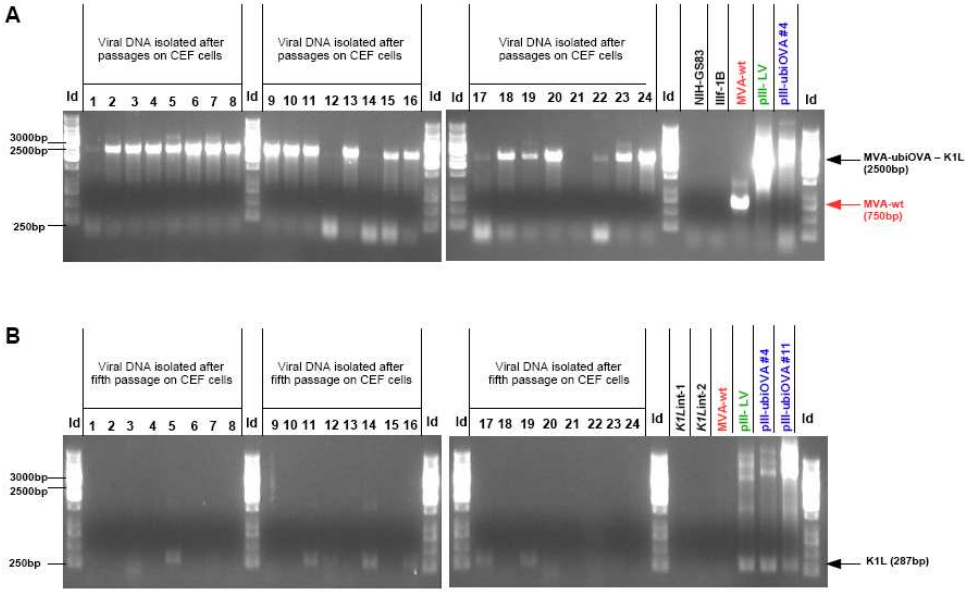

Figure 4.4: *PCR-analysis of rMVA isolated from CEF cells.* (A) The correct insertion of the transgene ubiOVA was confirmed with specific primers for deletion site III (NIH-GS83/IIIf-1B). (B) The deletion of the marker gene k1L was confirmed with specific primers *K1L*int-1/*K1L*int-2. In both figures (A, B), primers, MVA-wt, pIIIΔHRP$_{7.5}$ (pIII-LV) and pIII-ubiOVA are shown as reference. A 1 kb DNA Ladder (ld) served as standard. The arrow marks location of K1L-specific fragments within the gel.

4.1.1.1 PCR-analysis of final virus stock preparation of MVA-ubiOVA

To confirm the right insertion of the transgenes and the absence of wildtype virus in purified virus stock preparations PCR-analysis was conducted. The integrity of deletion site III was determined with primers NIH-GS83/IIIf-1B *(Fig. 4.5 A)*. The gene encoding for ovalbumin could be detected with primers pubi/ova 3 and pubi/ova 6 *(Fig. 4.5 B)*. To confirm the right size of ubiOVA primers pubi/ova 1 and pubi/ova 6 were used *(Fig. 4.5 C)*.

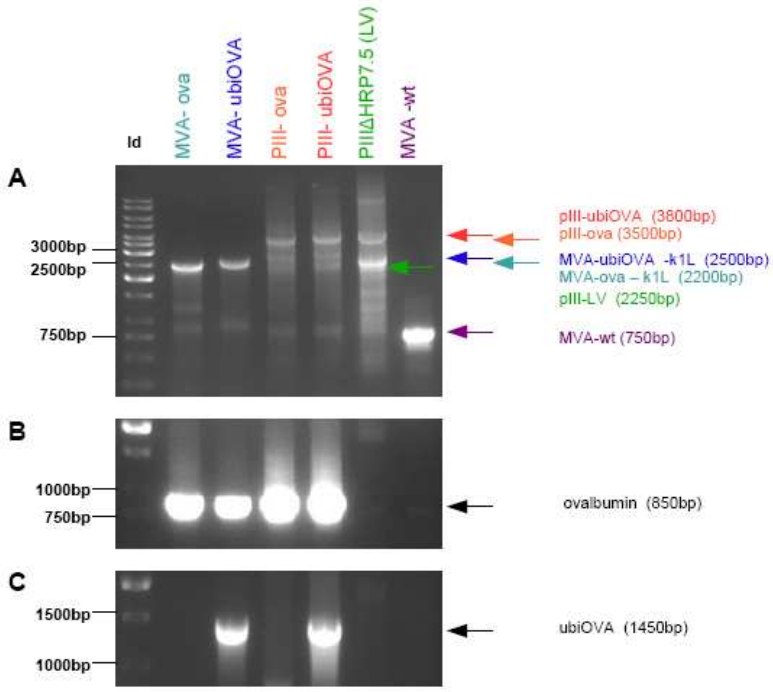

Figure 4.5: *PCR-analysis of purified rMVA.* Viral DNA isolated from CEF cells was amplified using primers for deletion III or the respective inserts. (A) The correct insertion of recombinant genes into deletion site III was determined using primers NIH-GS83/IIIf-1B. (B) The detection of the gene encoding for ovalbumin was performed with primers pubi/ova3 and pubi/ova6. (C) The ubiOVA fusion gene was specifically amplified with primers pubi/ova1 and pubi/ova6. A 1 kb DNA Ladder (ld) served as standard. Expected fragments are marked with an arrow according to their respective size.

The correct insertion of recombinant genes into deletion site III could be confirmed with primers NIH-GS83 and IIIf-1B *(Fig. 4.5 A)*. Furthermore, ovalbumin (850 bp) was detected in the right size after infection with MVA-ova or MVA-ubiOVA and after transfection with the plasmids pIII-ova and pIII-ubiOVA *(Fig. 4.5 B)*. The gene encoding for ubiOVA (1450bp) *(Fig. 4.5 C)* was detected after infection of CEF cells with MVA-ubiOVA or transfection with pIII-ubiOVA showing the correct insertion into the viral genome.

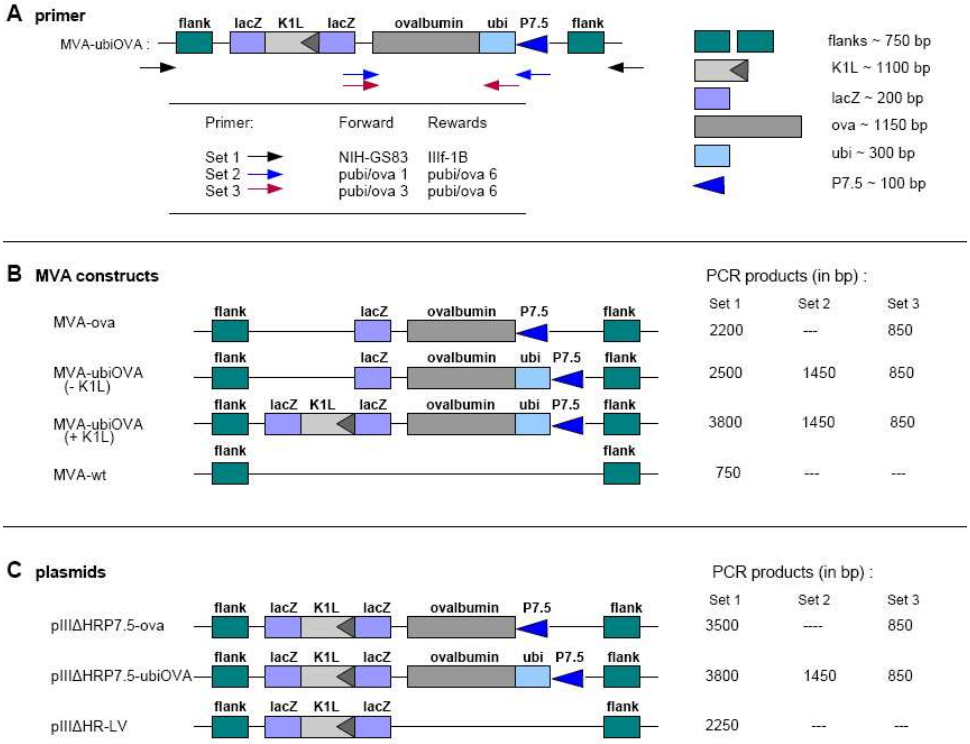

Figure 4.6: *(A) Primers (black, blue and red arrow) used for PCR-analysis and fragment sizes of MVA-ubiOVA, (B) recombinant viral vectors and (C) plasmids with their PCR products.*

4.1.2 Generating MVA-TOT

Analogous to section *4.1.1* MVA-TOT was generated and tested for the correct insertion of the transgene ubi/Tyr_Sig/Ova/Tyr_TM (TOT) by PCR following the flow chart of *Fig. 4.2*. The first PCR for deletion site III was performed after four passages on RK-13 cells and one passage on CEF cells. The expected size of gene fragments, explicitly described in *Fig. 4.10*, were as listed below:

3850 bp	-	for the correct insertion of the transgene TOT in MVA (MVA-TOT + k1L)
2550 bp	-	for the correct insertion of the transgene TOT in MVA (MVA-TOT - k1L)
3750 bp	-	for the correct insertion of the transgene TO in MVA (MVA-TO + k1L)
2450 bp	-	for the correct insertion of the transgene TO in MVA (MVA-TO - k1L)
750 bp	-	for the 'empty' deletion site III of MVA-wt (MVA-wt)
3850 bp	-	for the transfer plasmid pIII-TOT (pIII-TOT + k1L)
3750 bp	-	for the transfer plasmid pIII-TO (pIII-TO + k1L)
2250 bp	-	for the plasmid pIIIΔHRP$_{7.5}$ (pIII-LV)

Fig. 4.7 confirms the right insertion of the transgene TOT into the viral genome.

Some recombinant clones were taken for further passages on CEF cells. After five passages another PCR was conducted for deletion site III and K1L *(Fig. 4.8)*. As demonstrated in *Fig. 4.8 A* clones 1, 2, 9, 12, 13 and 16-20 could be evaluated as rMVA. Only one rMVA clone was tested negative for K1L *(Fig. 4.8 B clone 9)*. Hence, this clone was used for further amplification and final purification of the virus.

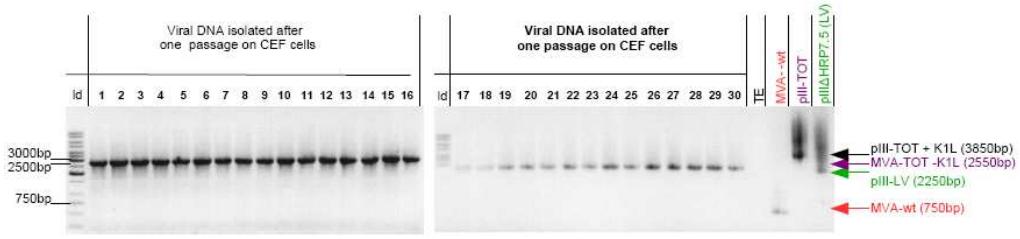

Figure 4.7: *PCR-analysis of rMVA isolated from CEF cells.* The correct insertion of the transgene ubi/Tyr_Sig/Ova/Tyr_TM (TOT) into the viral genome was confirmed by using specific primers for deletion site III (NIH-GS83/IIIf-1B). TE buffer, MVA-wt, pIIIΔHRP$_{7.5}$-TOT and pIIIΔHRP$_{7.5}$ (LV) are shown as reference. A 1 kb DNA Ladder (ld) served as standard. Expected fragments are marked with an arrow according to their respective size.

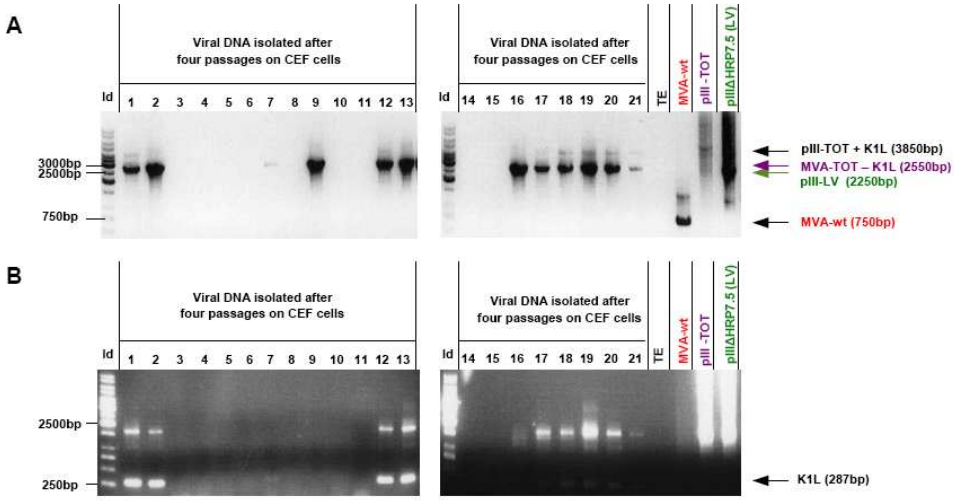

Figure 4.8: *PCR-analysis of rMVA isolated from CEF cells.* (A) The correct insertion of the transgene TOT was confirmed with specific primers for deletion site III (NIH-GS83/IIIf-1B). (B) Deletion of the marker gene K1L was confirmed with primers *K1L*int-1/*K1L*int-2. In both figures (A, B), TE buffer, MVA-wt, pIII-TOT, pIIIΔHRP$_{7.5}$ (LV) are shown as reference. A 1 kb DNA Ladder (ld) served as standard. Expected fragments are marked with an arrow according to their respective size.

4.1.2.1 PCR-analysis of final virus stock preparation of MVA-TO and MVA-TOT

The correct insertion of the transgene in final virus stock preparations of MVA-TO, MVA-TOT and MVA-ova was again confirmed by PCR-analysis *(Fig. 4.9)*.

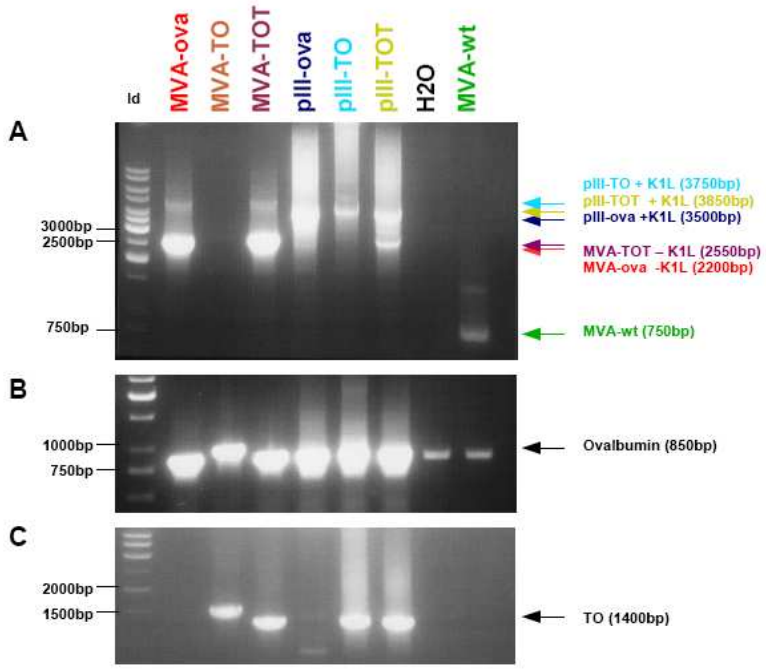

Figure 4.9: *PCR-analysis of purified rMVA.* Viral DNA isolated from CEF cells was amplified using different primers. (A) The integrity of deletion site III was determined using primers NIH-GS83/IIIf-1B. (B) The detection of the gene encoding for ovalbumin protein could be performed with primers pubi/ova3 and pubi/ova6. (C) The ubi/Tyr_Sig/Ova (TO) fusion gene was specifically amplified with primers pubi/ova1 and pubi/ova6. A 1 kb DNA Ladder (ld) served as standard. Expected fragments are marked with an arrow according to their respective size.

The correct insertion of the transgene TOT in deletion site III of the viral genome could be confirmed detecting a fragment with a corresponding size of 2550 bp. Deletion site III in MVA-ova was correctly assessed as a band with approximately 2200bp. Unfortunately no band was detected after infection with MVA-TO *(Fig. 4.9 A)*. With primers pubi/ova 3 and pubi/ova 6 a fragment of ovalbumin was detected with the correct size of approximately 850bp after infection with all recombinant viruses or transfection with the respective plasmids. With primers pubi/ova 1 and pubi/ova 6 a fragment including ubi/Tyr_Sig/Ova was detected at a size of approximately 1400bp. It could not be evaluated why the band detected with both primer pairs pubi/ova 1 and 6 and pubi/ova 3 and 6 after infection with MVA-TO was slightly larger compared to the other bands *(Fig. 4.9 B,C)*. To further assess the exact composition of MVA-TO, sequencing of the viral genome would be necessary.

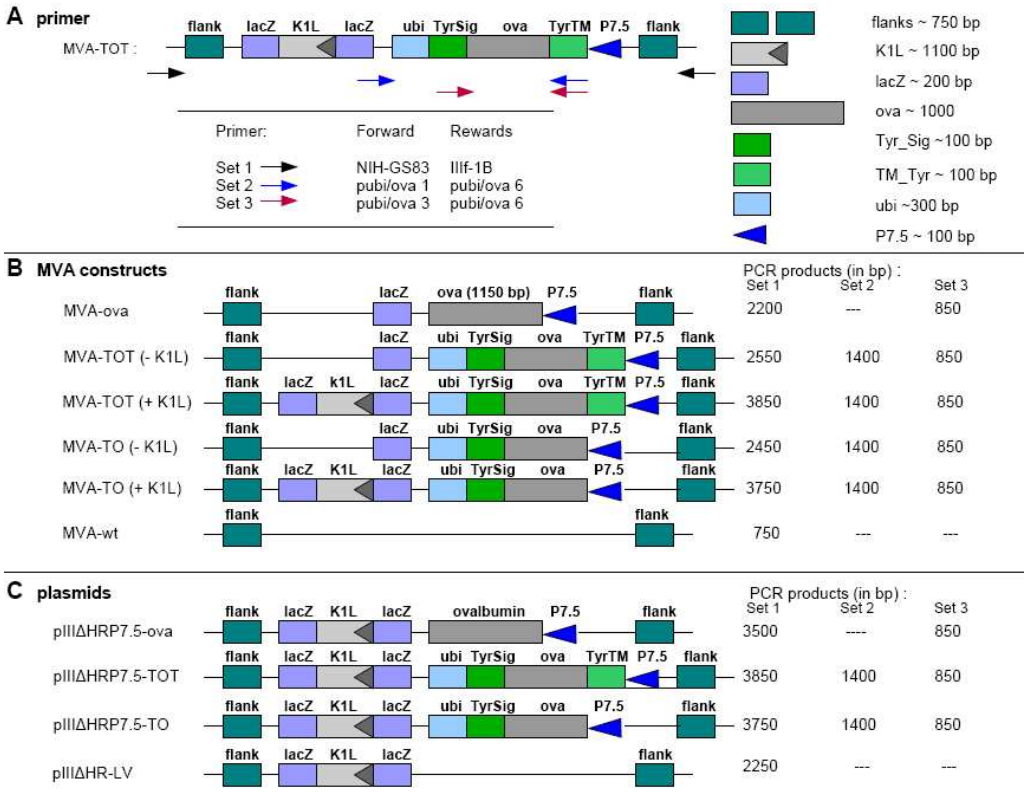

Figure 4.10: *(A) Primers used for PCR-analysis (Set 1 (black arrow): NIH-GS83, IIIf-1B, Set 2 (blue arrow): pubi/ova 1, pubi/ova 6, Set 3 (red arrow): pubi/ova 3, pubi/ova 6) and fragment sizes of MVA-TO and MVA-TOT on the right, (B) schematic of recombinant viral vectors and (C) plasmids with their PCR products on the right.*

4.2 Characterization of MVA-ubiOVA

4.2.1 Ovalbumin expression levels in cells transfected with ovalbumin expression constructs

Some experiments presented within this work were performed using plasmids expressing modified or native ovalbumin, as the final virus stock preparation of recombinant MVA was still in progress.

4.2.1.1 Analysis of protein levels by Western blot

Protein levels were comparatively analyzed by Western blot analysis after transfection of cells with plasmids pIII-ova and pIII-ubiOVA *(Fig 4.11)*. BHK cells were infected with MVA-wt, transfected as described in section *3.2.6* and harvested 13 hours post infection. pIIIΔHRP$_{7.5}$ (pIII-LV)-transfected cells, BHK cells and MVA-wt-infected cells are shown as reference. Immunoblotting was performed as described in *3.3.1* and ovalbumin protein was detected by the specific polyclonal antibody against ovalbumin. Some cells were treated with lactacystine to inhibit proteasomal activity (+LC).

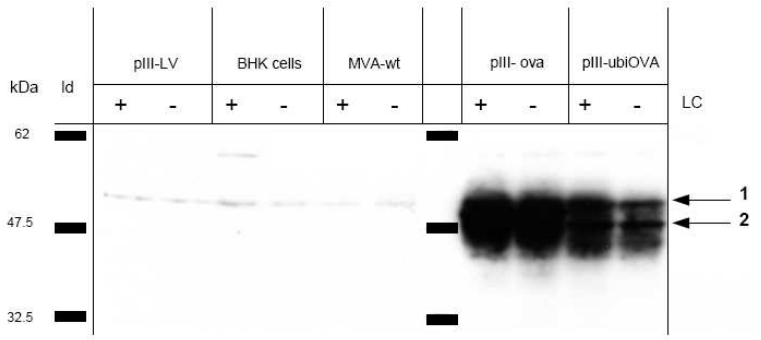

Figure 4.11: *Western blot analysis of ovalbumin synthesis in BHK cells.* Whole protein levels were assessed and compared after transfection with plasmids pIII-ova and pIII-ubiOVA. pIIIΔHRP$_{7.5}$-transfected cells (pIII-LV), BHK cells and MVA-wt-infected cells are shown as reference. Some cells were treated with lactacystine to inhibit proteasomal activity (+LC). A protein standard shows the molecular masses in kDa on the left (ld). Arrow 2 marks a protein band corresponding to the size of ovalbumin (45 kDa). Arrow 1 marks a protein slightly larger than ovalbumin, potentially representing a posttranslationally glycosylated form.

As expected, no ovalbumin-specific bands could be detected in pIIIΔHRP$_{7.5}$ (LV)- transfected, MVA-wt- or mock-infected cells. However, two bands could be ascertained after transfection of cells with pIII-ova and pIII-ubiOVA. One band was detected at a size of 45 kDa corresponding to the size of ovalbumin. The other protein-band appeared slightly larger than ovalbumin potentially representing a posttranslationally glycosylated form of the protein *(see Fig. 4.11, arrow 1)*. In cells transfected with pIII-ubiOVA, the ubiquitin moiety was cleaved by hydrolases and led to the appearance of a band corresponding to the size of the ovalbumin.
In the absence of proteasome inhibition there was less protein detectable in cells transfected with pIII-ubiOVA than in those transfected with pIII-ova. When proteasomal activity was abrogated in cells transfected with pIII-ubiOVA, however, a higher level of protein could

be detected. These findings led to the suggestion that ubiOVA is subject to a more rapid degradation than ovalbumin and renders the proteasome responsible for ubiOVA processing.

4.2.1.2 Results of immunoperoxidase staining

Intracellular ovalbumin synthesis was analyzed by immunoperoxidase staining in B16, BHK and CV-I cells twentyfour hours after transfection with ovalbumin expression constructs pIII-ova and pIII-ubiOVA. The protein was detected by a specific ovalbumin-binding primary antibody (rabbit polyclonal to hen egg white Ovalbumin) and a PO-labeled secondary antibody (α rabbit-PO).
The different cell lines showed varying numbers of ovalbumin positive cells presumably due to differences in their infectability and transfectability and their sensitivity to lactacystine treatment.

Figure 4.12: *Immunoperoxidase staining of ovalbumin in B16 cells.* Cells were infected with MVA-wt and transfected with ovalbumin expression constructs (pIII-ova, pIII-ubiOVA). Transfection with pIIIΔHRP$_{7.5}$ (pIII-LV) and infection of cells with MVA-wt are shown as negative control, infection with MVA-ova as positive control, respectively. A slightly more intense staining could be detected in cells transfected with pIII-ova indicating an increased protein accumulation when compared to cells transfected with pIII-ubiOVA.

Staining intensities of ovalbumin in B16 cells transfected with the two ovalbumin expression constructs pIII-ova and pIII-ubiOVA *(Fig. 4.12)* did not markedly differ, however, could be estimated as slightly more intense in those cells transfected with pIII-ova, indicating an increased protein accumulation when compared to pIII-ubiOVA transfected cells.
Intensity of the brown precipitation signal in cells transfected with pIII-ova was equally distributed and homologous whereas pIII-ubiOVA-transfected cells showed an accumulation of protein in cellular compartments and a weaker but homologous staining intensity in the cytosol.
As expected, pIIIΔHRP$_{7.5}$ (LV)-transfected cells and MVA-wt-infected cells showed no brown precipitation. In MVA-ova infected B16 cells, however, an intense staining was ascertained.

When immunoperoxidase staining was performed in BHK cells after transfection with pIII-ova and pIII-ubiOVA, the same staining intensity as in B16 cells could be detected on the single cell level. The efficiency of transfection, however, was higher than in B16 cells since more cells showed brown precipitates. In order to investigate the role of the proteasome in ovalbumin degradation BHK cells were treated with proteasome inhibitor lactacystine and MG132 *(+) (Fig. 4.13)*. The expected higher intensity of staining due to an accumulation of ovalbumin protein, however, was missing. There was, instead, a weaker

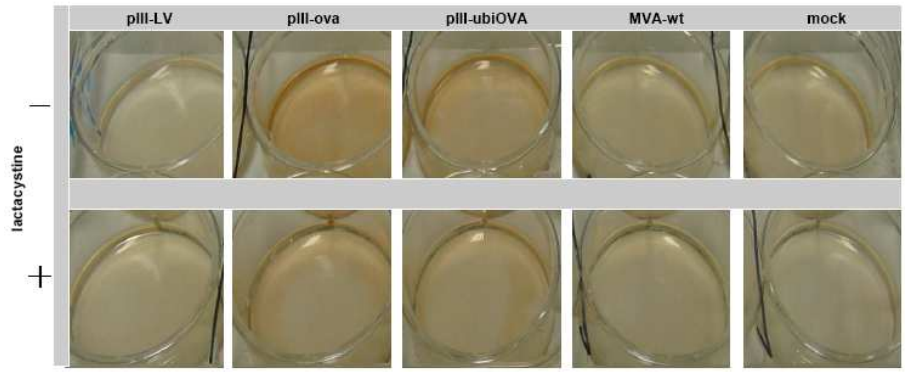

Figure 4.13: *Immunoperoxidase staining of ovalbumin in BHK cells.* Cells were infected with MVA-wt and transfected with ovalbumin expression constructs pIII-ova and pIII-ubiOVA. Transfection with pIIIΔHRP$_{7.5}$ (pIII-LV), infection with MVA-wt and BHK cells (mock) are shown as negative control. To inhibit proteasomal activity, lactacystine and MG132 were added to cells in the lower panel (+). Contrary to expectations, there was a weaker staining intensity detected in cells treated with proteasome inhibitors.

staining visible in each cell. Furthermore, less cells showed brown precipitation and more cells had gone into apoptosis.

To test whether the interference of lactacystine and MG132 with late gene expression might cause the less intense staining of cells which were treated with proteasome inhibitors, immunoperoxidase staining of ovalbumin was performed in CV-I cells which were treated with ara-C (cytosine arabinoside). Due to a block of late gene expression in all cells the effect of proteasome inhibition shall only affect early proteins. CV-I cells were infected with MVA-wt and transfected with ovalbumin expression constructs pIII-ova and pIII-ubiOVA *(Fig. 4.14)*. All cells were treated with ara-C for 30 minutes before infection. The proteasome inhibitors lactacystine and MG132 were added to the cells (+) *(Fig. 4.14 B)*. And indeed, staining on the single cell level turned out to be slightly more intense in those cells with proteasome inhibition indicating an accumulation of ovalbumin protein due to a diminished degradation by the proteasome. The different colours of brown tinge in pIII-ova and pIII-ubiOVA transfected cells were assumedly caused by varying light exposure during photographing.

4.2.2 Assessment of ovalbumin stability and peptide presentation after infection of cells with MVA-ova or MVA-ubiOVA

4.2.2.1 Analysis of ovalbumin stability using radioimmunoprecipitation

The stability of ovalbumin protein expressed by MVA-ubiOVA in Hela cells was determined by means of a radioimmunoprecipitation assay as described in section *3.3.2*. The stability of ubiOVA was compared to the stability of native ovalbumin expressed by MVA-ova to point out the effect of ubiquitination. Cells were starved and subsequently pulsed with radioactive ^{35}S for 10 minutes before they were chased in FCS only medium. Cells were harvested at indicated time points and immunoprecipitated samples were analyzed for their radioactivity by Phosphor Imager *(Personal Molecular Imager FX, BioRad, Munich)* after

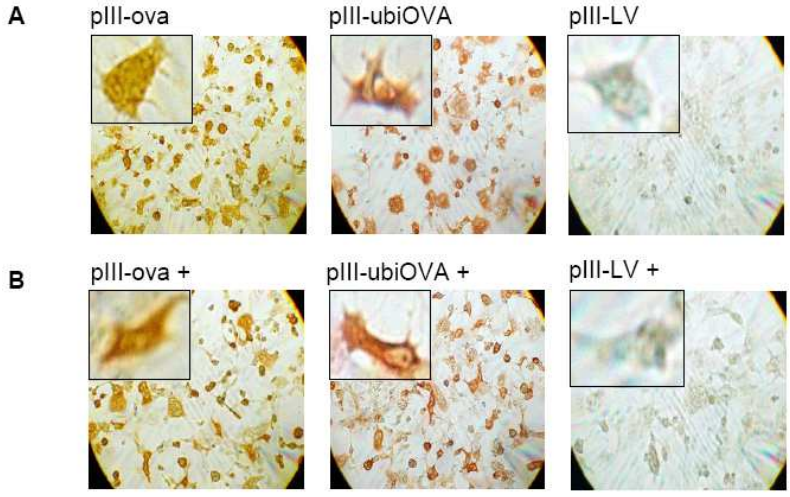

Figure 4.14: *Immunoperoxidase staining of ovalbumin in CV-I cells.* (A) CV-I cells were infected with MVA-wt and transfected with ovalbumin expression contructs pIII-ova and pIII-ubiOVA. Transfection with pIIIΔHRP$_{7.5}$ (pIII-LV) is shown as negative control. To block late gene expression cells were treated with ara-C for 30 minutes before infection (1:1000). (B) lactacystine and MG132 were added to inhibit proteasomal activity (+). Staining was slightly more intense in cells treated with proteasome inhibitors.

SDS-PAGE.
As depicted in *Fig. 4.15*, two bands were detected in cells infected with MVA-ova *(arrow 2 and 3)*. The lower band corresponded to a size of 45 kDa representing native ovalbumin whereas the source of the upper band remains ambiguous. It might on one side be a glycosylated form of the protein ovalbumin, which, however, is not detected after infection with MVA-ubiOVA, and thus rather unlikely. On the other side it might be an unspecific band which could also be seen in the radioimmunoprecipitation assay performed with MVA-TO and MVA-TOT *(see Fig. 4.25)*.

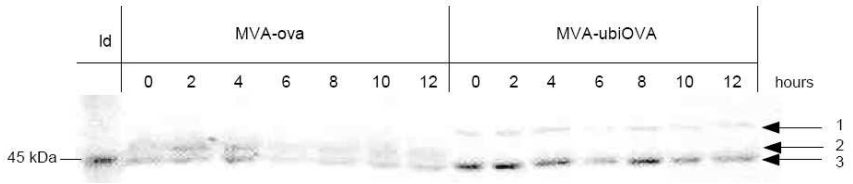

Figure 4.15: *Pulse-chase analysis and immunoprecipitation of ovalbumin.* Hela cells infected with MVA-ova or MVA-ubiOVA were pulse-labeled with ^{35}S-Met for 10 minutes and chased with an excess of unlabeled methionine for the indicated hours, followed by extraction, immunoprecipitation and electrophoretic analysis by SDS-PAGE. A Rainbow^{TM} [^{14}C]methylated protein molecular weight marker is shown as standard (ld). Arrow 1 marks a protein band corresponding to the size of ubiquitinated ovalbumin. Arrow 2 marks a protein band which might be a glcosylated form of ovalbumin or an unspecific band. Arrow 3 marks a protein band corresponding to the size of ovalbumin (45kDa).

After infection of cells with MVA-ubiOVA there was one band detectable migrating at the size of ovalbumin *(Fig. 4.15 arrow 3)* but also another band migrating at the size of ubiOVA which is 8 kDa larger than ovalbumin *(Fig. 4.15 arrow 1)*. These results might

indicate that not all ubiquitin moieties are split off of ovalbumin directly after protein synthesis.
After infection of cells with MVA-ova expressing native ovalbumin, the ovalbumin protein was detected for at least twelve hours after the pulse with a rather slow rate of degradation (confirmed by reproducible experiments). In cells infected with MVA-ubiOVA expressing ubiquitinated ovalbumin, ovalbumin could also be detected for twelve hours with no perceptible difference in degradation compared to native ovalbumin (confirmed by reproducible experiments).

4.2.2.2 FACS analysis of H2-K^b/SIINFEKL surface expression

Expression of H2-K^b/SIINFEKL complexes on B16-F1 cells was analyzed by flow cytometry to assess and compare the quantity of ovalbumin-specific degradation products. B16-F1 cells were infected with rMVA and harvested at indicated time points *(Fig. 4.16, 0-12 hours (X-axis))*. The proteasome inhibitors lactacystine and MG132 were additionally added if indicated (+LC). The presence of H2-K^b/SIINFEKL complexes was verified by staining with a specific mAb, 25D1.16. Cells that were already gone into apoptosis were excluded via staining with EMA.

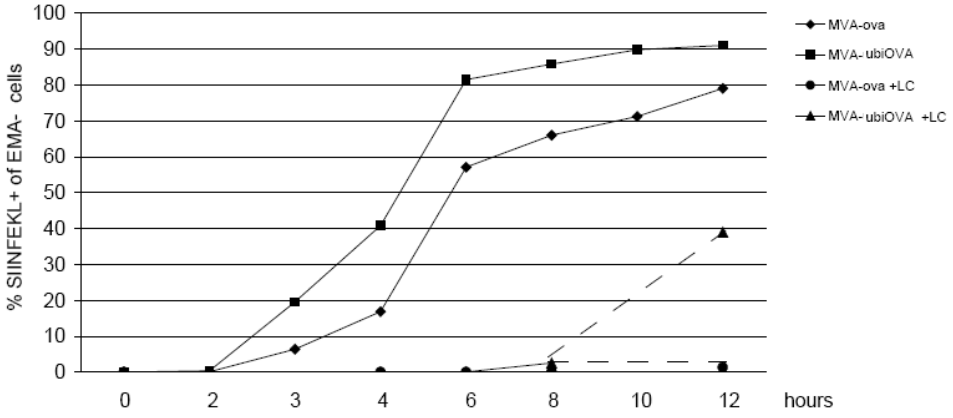

Figure 4.16: *Analysis of H2-K^b/SIINFEKL surface expression.* B16-F1 cells were infected with MVA-ova or MVA-ubiOVA and levels of H2-K^b/SIINFEKL complexes were determined by flow cytometry with 25D1.16 mAb at indicated time points (0-12 hours, X-axis). Some cells were treated with 1 μM lactacystine and 1 μM MG132 (+LC) to inhibit proteasomal activity.

The following table shows percentages of SIINFEKL+, EMA- cells after infection with MVA-ova or MVA-ubiOVA at indicated time points:

	0h	**2h**	**3h**	**4h**	**6h**	**8h**	**10h**	**12h**
MVA-ova	0,11	0,13	6,39	16,9	57,1	66	71,2	79
MVA-ova (+LC)				0.066	0.048	0.097		1.36
MVA-ubiOVA	0,06	0,4	19,6	40,8	81,5	85,8	89,8	91
MVA-ubiOVA (+LC)				0.074	0.067	2.58		39

As shown in *Fig. 4.16*, graphical analysis of B16-F1 cells positive for H2-K^b/SIINFEKL complexes (% of max) out of all analyzed living B16-F1 cells revealed an initiation of H2-K^b/SIINFEKL surface presentation two hours post infection with either of the two ovalbumin expression constructs. Already after three hours there were twice as many SIINFEKL-presenting cells after infection with MVA-ubiOVA when compared to cells infected with MVA-ova, indicating a much faster degradation of ubitinated ovalbumin. The expression of SIINFEKL on B16-F1 cells showed a parallel increase in MVA-ova- as well as in MVA-ubiOVA- infected cells until twelve hours post infection. The maximum of cells presenting SIINFEKL within the observed period of time was found after twelve hours. Ninety-one percent of cells infected with MVA-ubiOVA were positive for H2-K^b/SIINFEKL complexes as were seventy-nine percent of cells infected with MVA-ova.

Strikingly, when proteasome inhibitors were added, presentation of H2-K^b/SIINFEKL complexes was almost completely abrogated until eight hours post infection *(Fig. 4.16 +LC)*. After eight hours, cells infected with MVA-ubiOVA regained the capacity to present SIINFEKL, whereas in cells infected with MVA-ova no SIINFEKL presentation could be detected. A possible explanation might be that either the blocking of the proteasome in MVA-ubiOVA-infected cells was abolished or another mechanism of protein degradation started to mobilize.

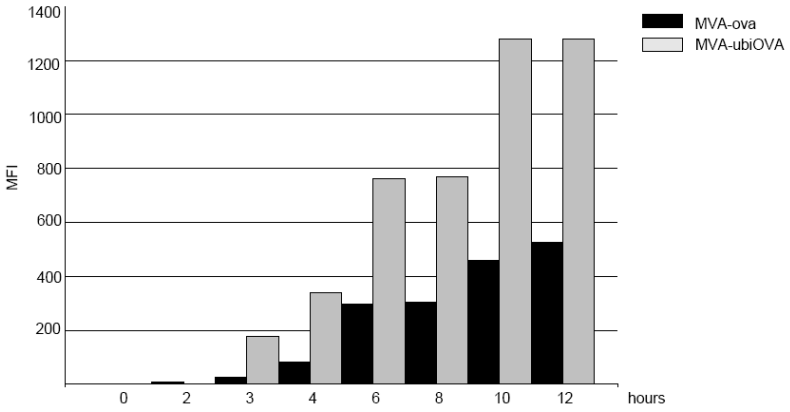

Figure 4.17: *Mean Fluorescence Intensity (MFI) of B16-F1 cells presenting H2-K^b/SIINFEKL complexes.* Cells were infected with MVA-ova or MVA-ubiOVA and were stained at indicated time points. H2-K^b/SIINFEKL presentation was analyzed by FACS. MFI is shown as an indicator for H2-K^b/SIINFEKL presentation on a single cell level.

B16-F1 cells (without proteasome inhibition) were analyzed for their mean fluorescence intensity (MFI) as a parameter to assess expression of H2-K^b/SIINFEKL complexes on a single cell level *(Fig. 4.17)*.

The mean fluorescence intensity (MFI) started to increase three hours post infection. Cells infected with rMVA expressing ubiOVA displayed a remarkably higher MFI already after four hours of infection indicating a much higher density of single H2-K^b/SIINFEKL complexes on MVA-ubiOVA-infected cells than on cells infected with MVA-ova.

4.2.3 Analysis of CD8+ T-cell mediated immunity following different vaccination schemes

In vivo vaccination experiments were comparatively performed using MVA-ova expressing full-length ovalbumin and MVA-ubiOVA expressing the ubiquitin-fusion construct. CD8+ T-cell responses to ovalbumin-specific peptide SIINFEKL (OVA_{257}) and to known MVA-specific peptides were determined using intracellular cytokine staining for IFNγ. The two rMVA were evaluated for their individual capacity to stimulate CD8+ T-cells after single immunization (priming) or after a heterologous prime-boost immunization.

4.2.3.1 Primary immunization with MVA-ubiOVA (compared to MVA-ova immunization)

C57BL/6 mice were immunized (1×10^8 IU in 500ml PBS) with MVA-ova (n=4) or MVA-ubiOVA (n=4) and analyzed for their CD8+ T-cell responses by ICS on day 8 post priming. As depicted in *Fig. 4.18* all mice immunized with ovalbumin expression constructs had SIINFEKL-specific CD8+ T-cells. Remarkably, mice immunized with MVA-ova had more SIINFEKL-specific CD8+ T-cells than those immunized with MVA-ubiOVA. The mean of SIINFEKL-specific CD62L-, IFNγ+ CD8+ T-cells of mice immunized with MVA-ova was 2.36% whereas the mean of CD62L-, IFNγ+ CD8+ T-cells of MVA-ubiOVA-immunized mice was 1.59% *(Fig. 4.18 B II)*. As demonstrated in *Fig. 4.18 B I* the difference was not significant with p=0.17. Vector-specific CTL responses were assessed by stimulation of isolated cells with vector-specific peptides $B8R_{20}$, $A3L_{270}$ and $K3L_6$. After stimulation with $B8R_{20}$ 12.9% B8R-specific CD8+ T-cells were detected in mice vaccinated with MVA-ubiOVA with no significant differences to mice immunized with MVA-ova.

4.2.3.2 Prime/Boost immunization with MVA-ova/MVA-ova and MVA-ova/MVA-ubiOVA

C57BL/6 mice were immunized with 1×10^8 IU MVA-ova i.p. (n=8) on day 0 and boosted with 1×10^8 IU i.p. of MVA-ova (n=4) or MVA-ubiOVA (n=4) on day 30 post prime. Specific CD8+ T-cell responses were analyzed on day 6 post boost by ICS *(Fig. 4.19)*.

Results of intracellular cytokine staining are graphed in *Fig. 4.20*. Stimulation with ß-Gal_{96} as well as samples stained with an IgG isotype antibody are shown as negative control. The CD8+ T-cell responses to MVA-specific peptides $B8R_{20}$, $A3L_{270}$ and $K3L_6$ reached up to 29.3% for the immunodominant peptide $B8R_{20}$ in MVA-ova-immunized mice, however, with no significant difference between the two prime/boost settings *(Fig. 4.20 B I)*.

Mice boosted with MVA-ubiOVA had more SIINFEKL-specific CD8+ T-cells (5.82%) than those mice boosted with MVA-ova (5.52%) *(Fig. 4.20 B II)*. Nevertheless, there was no significant difference detectable between the homologous and the heterologous prime/boost experiment with p=0.78 for the ovalbumin-specific peptide SIINFEKL *(Fig. 4.20 B I)*.

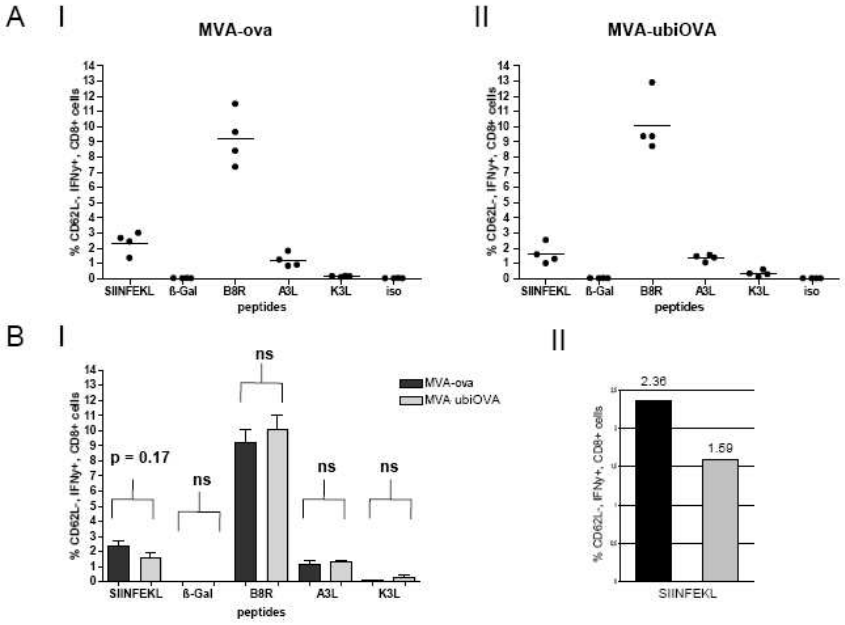

Figure 4.18: ***Primary response-*** *Antigen-specific CD8+ T-cells isolated on day 8 post immunization with MVA-ova or MVA-ubiOVA.* Frequencies of IFNγ-producing CD62L-, CD8+ T-cells specific for the ovalbumin epitope SIINFEKL and MVA epitopes $B8R_{20}$, $A3L_{270}$ and $K3L_6$ are shown. ß-Gal_{96} and isotype stained cells (iso) are shown as negative control. (A I) Specific CD8+ T-cell responses of four C57BL/6 mice immunized with MVA-ova. (A II) Specific CD8+ T-cell responses of four C57BL/6 mice immunized with MVA-ubiOVA. (B I) Mean frequencies of CD8+ T-cells specific for SIINFEKL, $B8R_{20}$, $A3L_{270}$, $K3L_6$ compared for both vaccines, MVA-ova and MVA-ubiOVA. There is no significant difference for the ovalbumin-specific peptide SIINFEKL (p=0.17) or MVA epitopes (ns=not significant). (B II) Mean frequency of SIINFEKL-specific CD8+ T-cells of mice immunized with MVA-ova (2.36%) compared to that of mice immunized with MVA-ubiOVA (1.59%).

Figure 4.19: *Vaccination schedule for a heterologous prime/boost setting.*

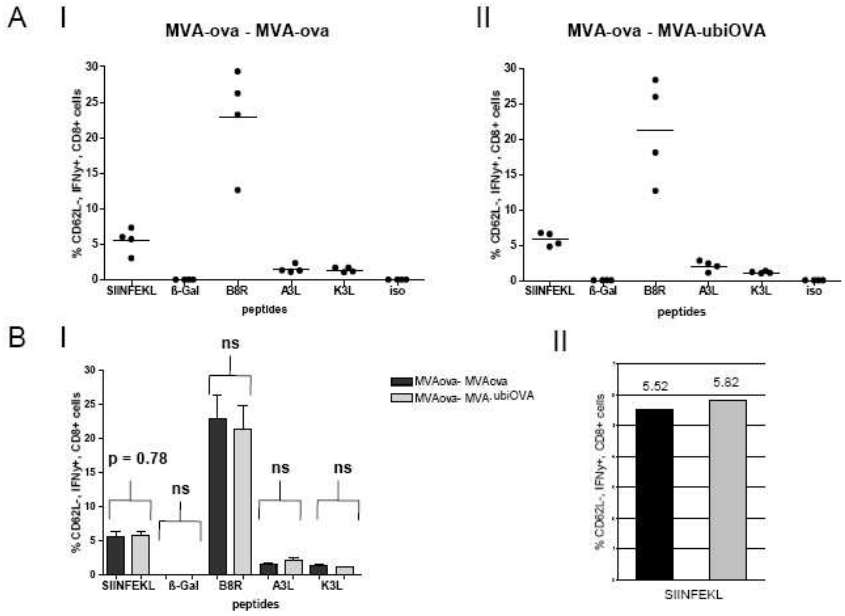

Figure 4.20: ***Secondary response-*** *Antigen-specific CD8+ T-cells of C57BL/6 mice primed with MVA-ova (n=8) and boosted with MVA-ova (n=4) or MVA-ubiOVA (n=4) isolated on day six post boost.* Frequencies of IFNγ-producing CD62L-, CD8+ T-cells specific for the ovalbumin epitope SIINFEKL and MVA epitopes $B8R_{20}$, $A3L_{270}$ and $K3L_6$ are shown. Samples stimulated with ß-Gal_{96} peptide and isotype stained cells are shown as negative control. (A I) Specific CD8+ T-cell responses of a homologous prime/boost setting with MVA-ova. (A II) Specific CD8+ T-cell responses of a heterologous prime/boost setting with MVA-ova and MVA-ubiOVA. (B I) Mean frequencies of CD8+ T-cells specific for SIINFEKL, $B8R_{20}$, $A3L_{270}$, $K3L_6$ compared for both prime/boost settings. There is no significant difference for the ovalbumin-specific peptide SIINFEKL (p=0.78) or MVA epitopes (ns=not significant). (B II) Mean frequency of SIINFEKL-specific CD8+ T-cells after the homologous prime/boost setting with MVA-ova (5.52%) compared to that of the heterologous prime/boost setting with MVA-ova and MVA-ubiOVA (5.82%).

4.3 Characterization of MVA-TO and MVA-TOT

4.3.1 Ovalbumin expression levels in cells transfected with ovalbumin expression constructs

4.3.1.1 Results of immunoperoxidase staining

Synthesis of ovalbumin after transfection with the two plasmids pIII-TO and pIII-TOT was analyzed in BHK and B16 cells. Presumably due to differences in infectability and transfectability and their sensitivity to lactacystine treatment the two cell lines showed varying numbers of ovalbumin positive cells as well as differences in staining intensity.

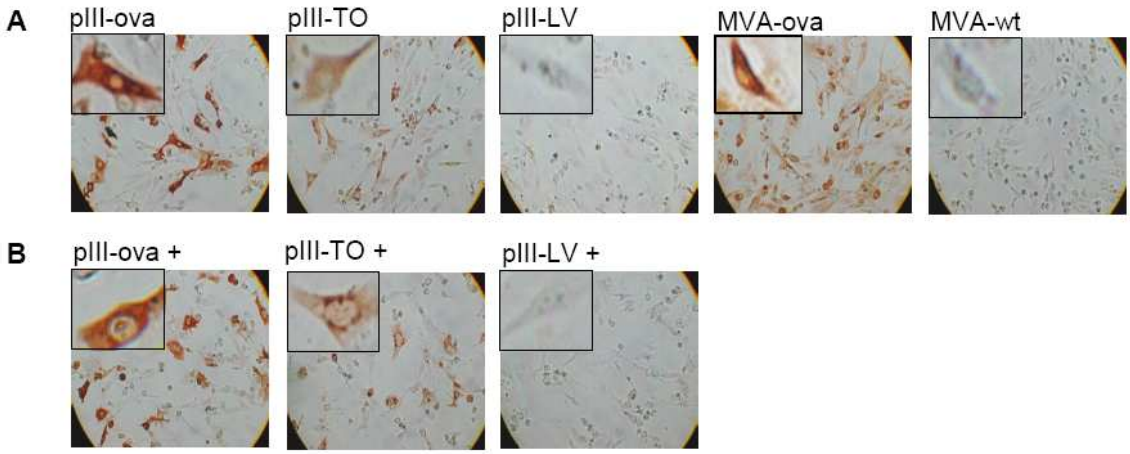

Figure 4.21: *Immunoperoxidase staining of ovalbumin in BHK cells.* (A) Cells were infected with MVA-wt and transfected with ovalbumin expression constructs pIII-ova or pIII-TO. Cells transfected with pIIIΔHR-$P_{7.5}$ (pIII-LV) and cells infected with MVA-wt are shown as negative control. Cells infected with MVA-ova are shown as positive control. (B) Lactacystine and MG132 were added to cells of the lower panel to inhibit proteasomal activity (+). There was a lower staining intensity detected in cells transfected with pIII-TO when compared to cells transfected with pIII-ova. Proteasome inhibition caused a protein accumulation.

Cells transfected with pIIIΔHR-$P_{7.5}$ (LV) and cells infected with MVA-wt showed no brown precipitation after immunoperoxidase staining (negative control). Cells infected with MVA-ova, however, as well as cells transfected with pIII-ova displayed a dark brown staining with no difference on the single cell level but a lower number of stained cells after transfection with pIII-ova *(Fig. 4.21 A)*. When proteasomal activity was abrogated in cells transfected with pIII-ova, staining intensity did not differ when compared to those cells without proteasome inhibition *(Fig. 4.21 B)*. Cells transfected with pIII-TO, however, displayed a significantly lower staining intensity than those cells transfected with pIII-ova *(Fig. 4.21 A)*. Moreover, cells treated with proteasome inhibitors showed an increased dark brown precipitate *(Fig. 4.21 B)*, indicating a rapid degradation of ovalbumin after transfection of cells with pIII-TO and a protein accumulation after proteasome inhibition.

In B16 cells pIII-ova showed similar staining patterns as in BHK cells *(Fig. 4.22)*. However, cells transfected with pIII-TOT and especially pIII-TO displayed only sparse brown precipitation. When proteasomal activity was abrogated in those cells, however, there was almost no significant difference in protein accumulation detectable making these results difficult to interpret. Either TO and TOT were subject to rapid degradation and

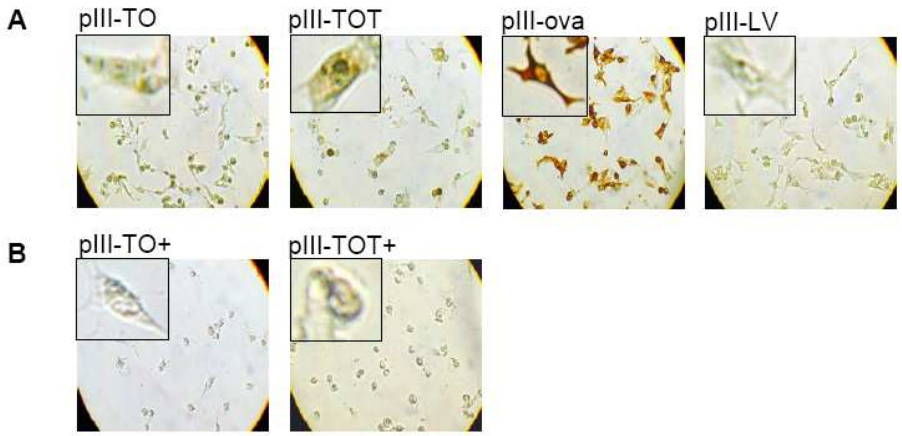

Figure 4.22: *Immunoperoxidase staining of ovalbumin in B16 cells.* (A) Cells were infected with MVA-wt and transfected with ovalbumin expression constructs pIII-ova, pIII-TO or pIII-TOT. Cells transfected with pIIIΔHR-$P_{7.5}$ (pIII-LV) are shown as negative control. (B) Lactacystine and MG132 were added to cells in the lower panel to inhibit proteasomal activity (+). A remarkably weaker staining intensity was detected in cells transfected with pIII-TO and pIII-TOT when compared to cells transfected with pIII-ova but no effect of proteasomal inhibition was ascertained.

inhibition of proteasomes was not sufficient or transfection with ovalbumin expression constructs went wrong.

4.3.2 Assessment of protein levels, ovalbumin stability and peptide presentation after infection of cells with MVA-ova, MVA-TO or MVA-TOT

4.3.2.1 Analysis of protein levels by Western blot

BHK cells were infected with MVA-TO or MVA-TOT and protein levels were quantified and compared to ovalbumin levels in cells infected with MVA-ova using Western blot analysis *(Fig. 4.23 and Fig. 4.24)*. Proteasome inhibitors lactacystine and MG132 were added to some cells to inhibit proteasomal activity (+LC). Cells infected with MVA-wt are shown as negative control *(wt)*. In all cells infected with MVA-ova two bands were detected. One band (45 kDa) corresponded to the size of ovalbumin *(blue arrow)* whereas the other band probably represents a glycosylated form of the protein *(red arrow)*. In cells infected with MVA-ova ovalbumin-specific protein levels seemed comparable and independent of proteasome inhibition declaring native ovalbumin a rather resistant protein. Remarkably, cells infected with MVA-TO displayed about five ovalbumin-specific bands detectable with the polyclonal antibody against ovalbumin *(Fig. 4.23)*. Bands 1 to 5 *(arrow 1-5)* probably represent different fragments of the fusion protein ubi/Tyr_Sig/Ova (TO) whereas band 6 is rather not specific. At least four forms *(Fig. 4.23, band 1, 2, 4, 5)* were dependent on proteasomal degradation since protein fragments seemed to accumulate when proteasome inhibitors were added. Band 5 seemed yet to be the only band that is only detectable with proteasome inhibition. This protein fragment is obviously subject to rapid degradation by the proteasome. In particular, the TO fusion protein constitutes a protein that is cleaved into noncontiguous fragments directly after synthesis or it might also be, due to its genetic constitution, a source for DRiPs *(see [164])*.

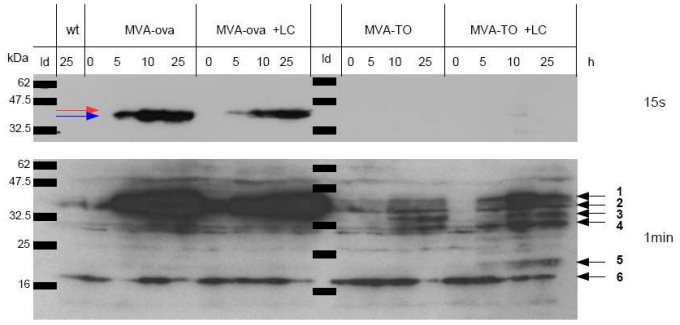

Figure 4.23: *Western blot analysis of ovalbumin synthesis.* BHK cells were infected with MVA-ova or MVA-TO (MOI=10) and harvested at indicated time points (0,5,10,25 h). Ovalbumin levels were assessed by the use of a rabbit polyclonal antibody against ovalbumin. Lactacystine and MG132 were added to some cells to block proteasomal degradation (+LC). Cells infected with MVA-wt are shown as negative control (wt). A protein standard shows the molecular masses in kDa on the left and in the middle (ld). Time of exposition of the film can be seen on the right side of the figure (15 s, 1 min). One band corresponds to the size of ovalbumin (blue arrow), another band probably represents a glycosylated form of the protein (red arrow). Arrow 1-5 mark different fragments of the fusion protein ubi/Tyr_Sig/Ova (TO) whereas band 6 is rather not specific.

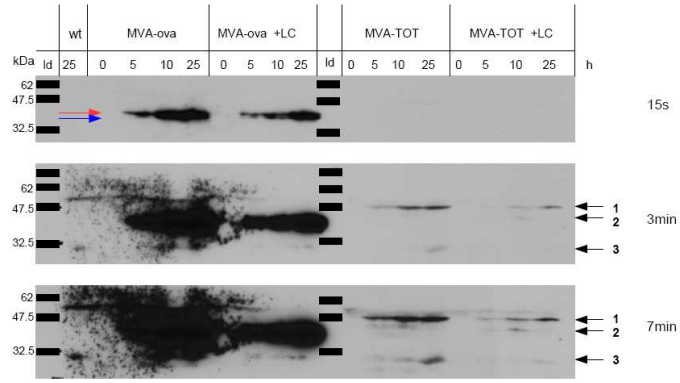

Figure 4.24: *Western blot analysis of ovalbumin synthesis.* BHK cells were infected with MVA-ova or MVA-TOT (MOI=10) and harvested at indicated time points (0,5,10,25 h). Ovalbumin levels were assessed by the use of a rabbit polyclonal antibody against ovalbumin. Lactacystine and MG132 were added to some cells to block proteasomal degradation (+LC). Cells infected with MVA-wt are shown as negative control (wt). A protein standard shows the molecular masses in kDa on the left and in the middle (ld). Time of exposition of the film can be seen on the right side of the figure (15 s, 3 min,7 min). One band corresponds to the size of ovalbumin (blue arrow), another band probably represents a glycosylated form of the protein (red arrow). Arrow 1-3 mark different fragments of the fusion protein ubi/Tyr_Sig/Ova/Tyr_TM (TOT).

Even though the protein structure of TO does not differ much from the protein structure of TOT, Western blot analysis varied strongly. In cells infected with MVA-TOT three bands could be detected *(Fig. 4.24)*. One band *(arrow 1)* appeared at a size of 48 kDa likely representing the ubiquitinated TOT-protein. Another band *(arrow 3)* was detected at 30 kDa almost only in cells with proteasomal activity. All of these protein fractions showed no cohesion with proteasomal degradation as there was no protein accumulation when proteasomal activity was blocked.

4.3.2.2 Analysis of ovalbumin stability using radioimmunoprecipitation

The stability of recombinant ovalbumin fusion proteins expressed by MVA-TO and MVA-TOT was analyzed in LCL cells *(Fig. 4.25)*. The stability of native ovalbumin expressed by MVA-ova was used as reference to perspicuously demonstrate the effect of protein modifications. A radioimmunoprecipitation assay was performed as described in section *3.3.2*. Cells were starved and pulsed with radioactive ^{35}S for 10 minutes before they were chased in FCS only medium. Cells were harvested at indicated time points and immunoprecipitated samples were analyzed for their radioactivity by Phosphor Imager *(Personal Molecular Imager FX, BioRad, Munich)* after SDS-PAGE.

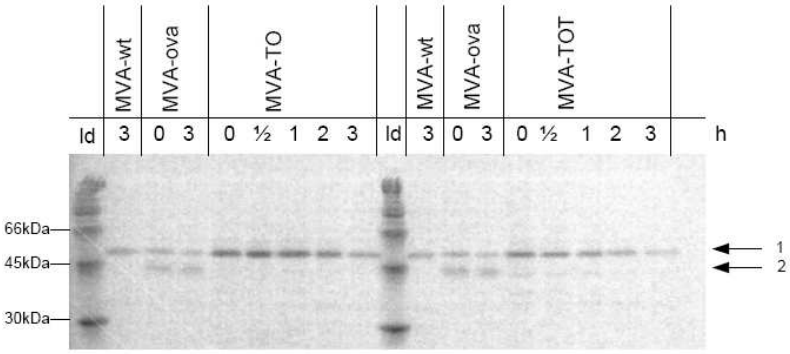

Figure 4.25: *Pulse-chase analysis and immunoprecipitation of ovalbumin.* LCL cells infected with MVA-ova, MVA-TO or MVA-TOT were pulse labeled with ^{35}S-Met for 10 minutes and chased with an excess of unlabeled methionine, followed by extraction, immunoprecipitation and electrophoretic analysis by SDS-PAGE. A Rainbow^{TM} [^{14}C]methylated protein molecular weight marker served as standard (ld). Arrow 1 marks a protein which can be detected after infection with ovalbumin expression constructs MVA-ova, MVA-TO and MVA-TOT, as well as after infection of cells with MVA-wt. Arrow 2 marks a protein band corresponding to the size of ovalbumin (45 kDa).

After infection of LCL cells with MVA-ova one band corresponding to the size of ovalbumin (45 kDa) was detected *(Fig. 4.25, arrow 2)*. This band was detected for at least three hours. Another band *(arrow 1)* was ascertained with a size between 45 kDa and 66 kDa after infection of cells with ovalbumin expression constructs MVA-ova, MVA-TO and MVA-TOT, as well as after infection of cells with MVA-wt *(wt)*, indicating that this band might rather be an unspecific or arteficial band. After infection with MVA-TO only band 1 *(arrow 1)* can be seen. In cells infected with MVA-TOT, however, there is an additional dim band *(arrow 2)* detectable at time points cero and a half. These results do as well indicate that modified ovalbumin proteins TO and TOT are rapidly degraded.

4.3.2.3 FACS analysis of H2-K^b/SIINFEKL surface expression

Assessment of H2-K^b/SIINFEKL surface expression was performed in DC2.4 cells infected with MVA-ova, MVA-TO and MVA-TOT *(Fig. 4.26)*. Cells were harvested at indicated time points (0, 2, 4, 6, 8 hours) and analyzed by flow cytometry as described in section *3.6.4*. MVA-ova-infected but isotype-stained cells were used as negative control *(MVA-ova_iso)*.

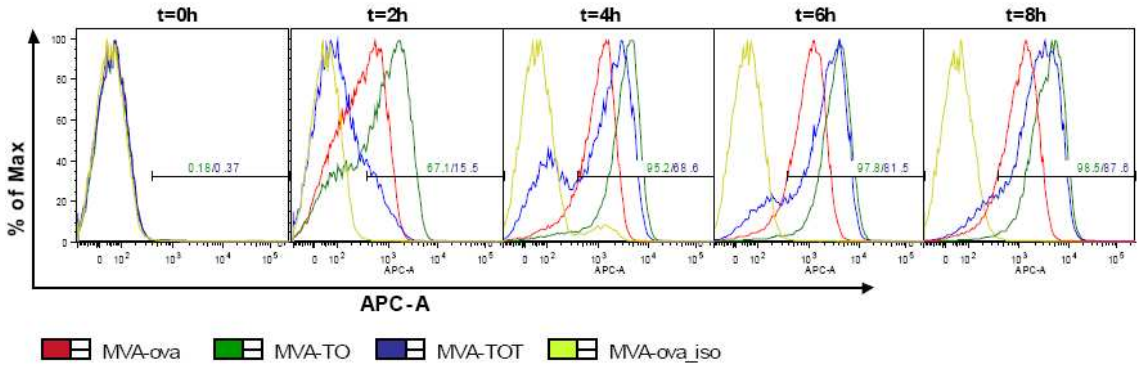

Figure 4.26: *Kinetic analysis of H2-K^b/SIINFEKL presentation.* Levels of H2-K^b/SIINFEKL surface presentation were assessed in DC2.4 cells after infection with MVA-ova (red), MVA-TO (green) or MVA-TOT (blue). Cells infected with MVA-ova but isotype stained (MVA-ova_iso) are shown as negative control (yellow). The graphic analysis for different time points is shown (t=0, 2, 4, 6, 8 hours). Numbers indicate cells positive for H2-K^b/SIINFEKL complexes (% of max) after infection with MVA-TO (green) or MVA-TOT (blue).

Graphic analysis of DC2.4 cells positive for H2-K^b/SIINFEKL complexes (% of max) out of all analyzed living DC2.4 cells revealed an initiation of H2-K^b/SIINFEKL surface presentation already two hours post infection for all ovalbumin expression constructs *(Fig. 4.27)*. Cells infected with MVA-TO reached a maximum of 98.5% cells positive for H2-K^b/SIINFEKL within the kinetic analysis of eight hours.

Cells infected with MVA-ova and MVA-TOT displayed the same amount of SIINFEKL-positive cells eight hours post infection (MVA-ova 87.5% and MVA-TOT 87.6%). The discrepancy between H2-K^b/SIINFEKL presentation in MVA-TO- and MVA-TOT- infected cells might be attributed to a SIINFEKL- negative population detected in cells infected with MVA-TOT which might be explained with varying infectivity.

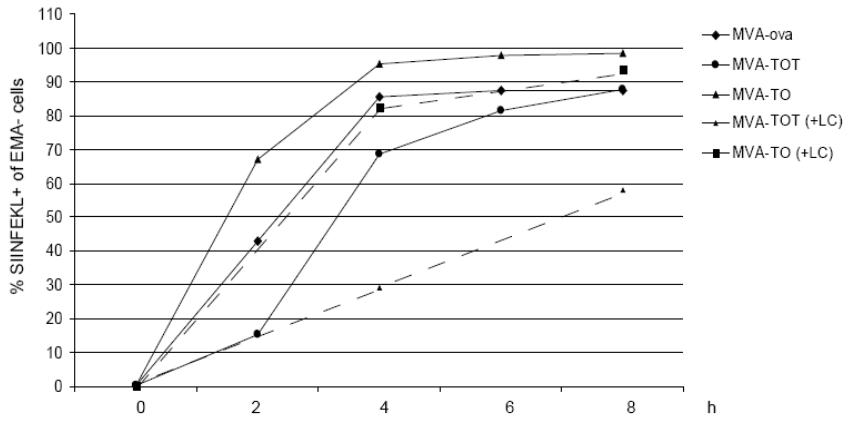

Figure 4.27: *Kinetic analysis of H2-K^b/SIINFEKL presentation.* DC2.4 cells were infected with MVA-ova (◇), MVA-TO (△) or MVA-TOT (•) and levels of H2-K^b/SIINFEKL complexes were determined by flow cytometry with the 25D1.16 mAb at indicated time points (X-axis, t= 0, 2, 4, 6, 8 hours). Lactacystine and MG132 were added to some cells (- - -) to block proteasomal activity (+LC).

In the following table percentages of H2-K^b/SIINFEKL-positive cells are listed for the different constructs at indicated time points:

	0h	**2h**	**4h**	**6h**	**8h**
MVA-ova	0.17	42.9	85.4	87.5	87.5
MVA-TO	0.18	67.1	95.2	97.8	98.5
MVA-TO (+LC)	0.26		82.3		93.7
MVA-TOT	0.37	15.5	68.6	81.5	87.6
MVA-TOT (+LC)	0.13		29.2		58.1

When cells were analyzed for their mean fluorescence intensity (MFI) as an indicator for H2-K^b/SIINFEKL presentation on a single cell level, infection with MVA-TO and MVA-TOT showed a remarkably increased presentation of SIINFEKL compared to cells infected with MVA-ova *(Fig. 4.28)*. Especially infection with MVA-TO could significantly enhance presentation of SIINFEKL on DC2.4 cells. The discrepancy between MVA-ova-infected cells in *Fig. 4.16* and *Fig. 4.27* might be attributed to different cell lines.

By inhibiting the proteasome in those cells infected with MVA-TO or MVA-TOT, expression of H2-K^b/SIINFEKL was reduced rather marginally *(Fig. 4.27 and Fig. 4.29)*. However, a slight reduction was ascertained especially in cells infected with MVA-TOT indicating a contribution of proteasomal degradation in TO- and TOT-protein destruction.

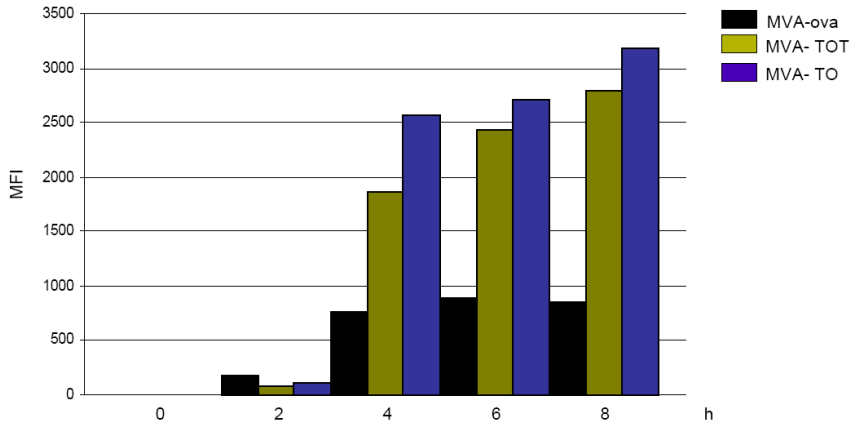

Figure 4.28: *Mean Fluorescence Intensity (MFI) of DC2.4 cells presenting H2-K^b/SIINFEKL complexes.* Cells were infected with MVA-ova (black), MVA-TO (blue) or MVA-TOT (green) and stained at indicated hours post infection (X-axis, t= 0, 2, 4, 6, 8 hours). H2-K^b/SIINFEKL presentation was analyzed by FACS. MFI of cells is shown as an indicator for H2-K^b/SIINFEKL complex density on a single cell level.

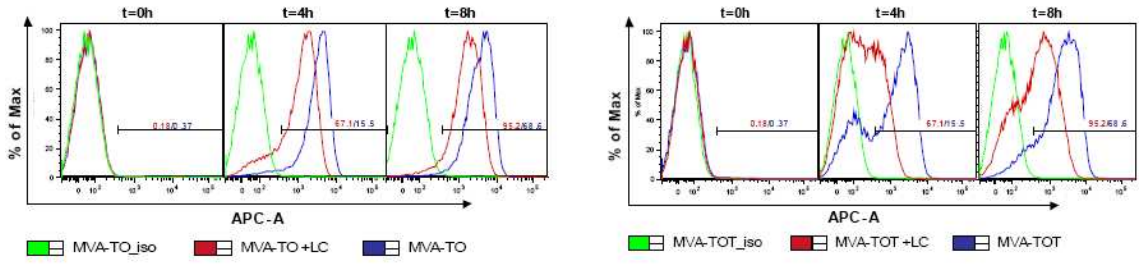

Figure 4.29: *Effect of proteasome inhibition on H2-K^b/SIINFEKL presentation after infection with MVA-TO or MVA-TOT.* DC2.4 cells were infected with MVA-TO (left panel) or MVA-TOT (right panel) and treated with proteasome inhibitors lactacystine and MG132 (+LC). Levels of H2-K^b/SIINFEKL complexes were determined by flow cytometry at indicated time points (t= 0, 4, 8 hours). Cells infected with MVA-TO or MVA-TOT but isotype-stained are shown as negative control (MVA-TO_iso, MVA-TOT_iso).

4.3.3 Analysis of CD8+ T-cell mediated immunity following different vaccination schemes

As described in section *3.6* immunization experiments were conducted with MVA-TO and MVA-TOT and specific CD8+ T-cell responses to ovalbumin-specific peptide SIINFEKL (OVA_{257}) and known MVA peptides $B8R_{20}$, $A3L_{270}$ and $K3L_6$ were characterized using intracellular cytokine staining for IFNγ. The two modified ovalbumin expression constructs MVA-TO and MVA-TOT were compared to MVA-ova. Gating strategies were applied as described in section *3.6.4.1.*

4.3.3.1 Primary immunization with MVA-TO and MVA-TOT (compared to MVA-ova immunization)

In two experimental settings C57BL/6 mice were immunized (1×10^8 IU in 500ml PBS) with MVA-ova (n=4 in *Fig. 4.30* A I, *Fig. 4.31* A I) and compared to MVA-TO immunization (n=4 in *Fig. 4.30* A II) or MVA-TOT (n=4 in *Fig. 4.31* A II) and analyzed for their CD8+ T-cell responses by ICS on day 8 post priming. One mouse primed with MVA-ova had to be excluded from the analysis due to a lack of any immune response *(Fig. 4.31 A I)*.

Mice immunized with MVA-ova had a SIINFEKL-specific CD8+ T-cell response ranging between 0.87% and 3.54% with a calculated mean of 1.99%. Mice immunized with MVA-TOT, however, only reached a mean of 1.57% SIINFEKL-specific CD8+ T-cells. Even though the difference between SIINFEKL-specific responses of MVA-ova- and MVA-TO-primed mice could not be evaluated as statistically significant (*Fig. 4.30 B I*, p=0.54), MVA-TO- primed mice displayed a perceivably lower response. CD8+ T-cell responses to MVA-specific peptides did not differ between mice immunized with either of the two viruses. The CD8+ T-cell response to $B8R_{20}$ thereby reached from 7.22% in mice immunized with MVA-TOT to 7.86% in those mice immunized with MVA-TO. The stronger CD8+ T-cell response to $B8R_{20}$ after immunization of mice with MVA-TO indicates that the enhanced SIINFEKL-specific T-cell response in mice immunized with MVA-ova can not be attributed to different amounts of virus during immunization.

In contrast to results obtained for MVA-ubiOVA and MVA-TO priming, immunization with MVA-TOT let to slightly more SIINFEKL-specific CD8+ T-cells than MVA-ova immunization. There was no statistical significance, however (*Fig. 4.31 B I*, p=0.79). The higher response of splenocytes isolated from MVA-TOT- vaccinated mice after SIINFEKL-stimulation was rather attributed to the conspicuously lower response in MVA-ova-immunized mice in comparison to other experiments *(Fig. 4.31 1.19% vs. Fig. 4.30 1.99%)*. This circumstance might be explained with exclusion of one mice lacking any immune response. As for repeated experimental immunizations with MVA-ova the average percentage of IFNγ- producing, CD62Llow, CD8+ T-cells after SIINFEKL-stimulation was ranging between 1.99% and 2.36%.

4.3.3.2 Prime/Boost immunization with MVA-ova/MVA-TO and MVA-ova/MVA-TOT

Again in two experimental settings C57BL/6 mice were immunized with 1×10^8 IU MVA-ova i.p. (*Fig. 4.33 and Fig. 4.34*: n=4 in A I and A II) on day 0 and boosted with 1×10^8 IU i.p. of MVA-ova (*Fig. 4.33 and Fig. 4.34*: n=4 in A I) compared to MVA-TO (n=4

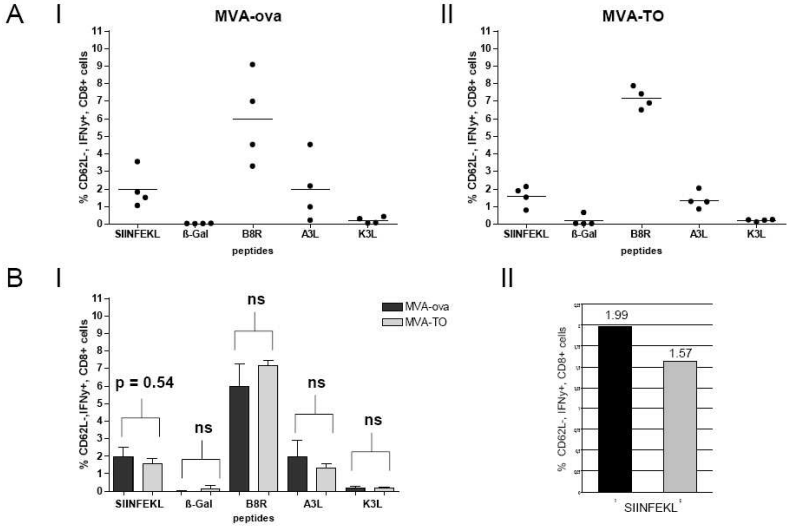

Figure 4.30: ***Primary response-*** *Antigen-specific CD8+ T-cell responses on day 8 post prime with MVA-ova or MVA-TO.* Frequencies of IFNγ-producing CD62L-, CD8+ T-cells specific for SIINFEKL or MVA epitopes $B8R_{20}$, $A3L_{270}$ and $K3L_6$ are shown. Cells stimulated with ß-Gal_{96} are shown as negative control. **Both figures** ***(4.30, 4.31)***: (A I) Specific CD8+ T-cell responses of four C57BL/6 mice immunized with MVA-ova or (A II) MVA-TO/MVA-TOT, respectively. (B I) Mean frequency of CD62L-, IFNγ+, CD8+ T-cells compared for both (A I and A II) experimental settings. The significance for different responses to SIINFEKL stimulation was evaluated as p=0.54 for MVA-ova versus MVA-TO priming and p=0.79 for MVA-ova versus MVA-TOT priming, respectively. There is no significant difference for MVA epitopes (ns=not significant). (B II) Mean of SIINFEKL-specific CD8+ T-cells of mice immunized with MVA-ova compared to that of mice immunized with MVA-TO/MVA-TOT.

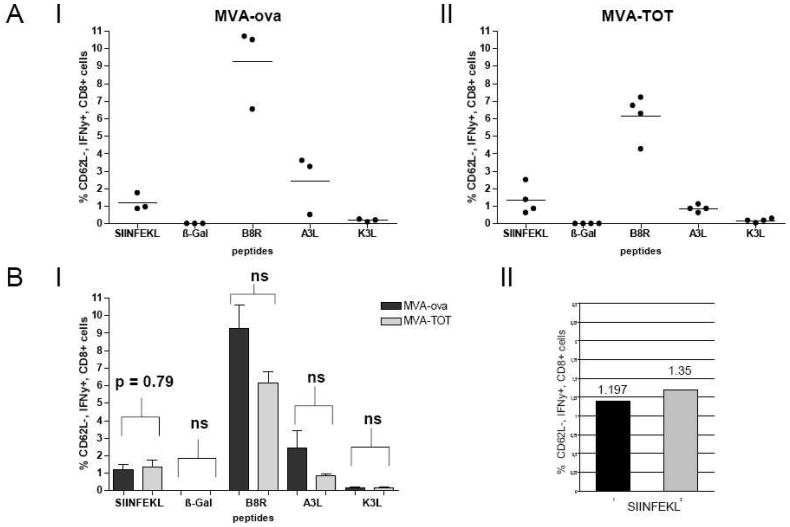

Figure 4.31: ***Primary response-*** *Antigen-specific CD8+ T-cell responses on day 8 post prime with MVA-ova or MVA-TOT. See also Fig. 4.30.*

in *Fig. 4.33* A II) or MVA-TOT (n=4 in *Fig. 4.34* A II) on day 30 post prime. Specific CD8+ T-cell responses were analyzed on day 6 post boost by ICS.

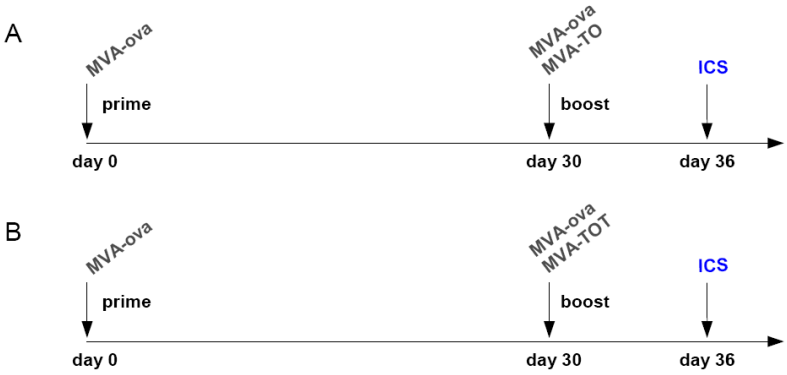

Figure 4.32: *Vaccination schedules for heterologous prime/boost settings.*

As demonstrated in *Fig. 4.33 B I*, a remarkable difference in the amount of SIINFEKL-specific IFNγ-producing, activated CD8+ T-cells was noted between the two experimental prime-boost settings. Mice boosted with MVA-TO had set up more SIINFEKL-specific CD8+ T-cells (average 7.39%) than mice boosted with MVA-ova (average 3.94%), albeit with no statistical significance (*Fig. 4.33 B I*, p=0.096).
As depicted in *Fig. 4.34* B I, priming with MVA-ova and boosting with MVA-TOT has also led to more SIINFEKL-specific CD8+ T-cells than the homologous priming and boosting with MVA-ova (p=0.72). MVA-ova boosting thereby reached 5.91% and MVA-TOT boosting 6.59% SIINFEKL-specific CD8+ T-cells .
The results obtained from the above mentioned experiments *(Fig. 4.33 and Fig. 4.34)* indicate that rapidly degraded protein is the optimal form of antigen to elicit a strong, specific CD8+ T-cell response in boosting with MVA.

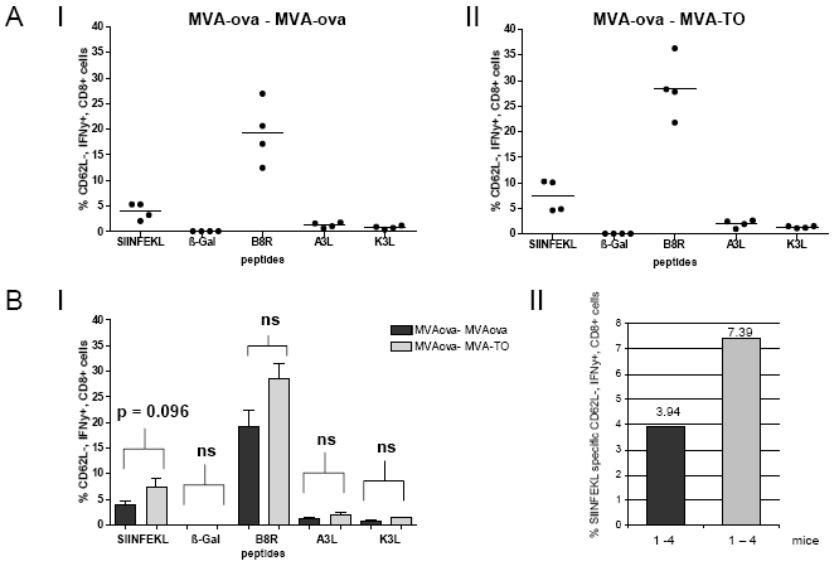

Figure 4.33: ***Secondary response***- *Antigen-specific CD8+ T-cells of C57BL/6 mice primed with MVA-ova and boosted with MVA-ova or MVA-TO isolated on day six post boost.* Frequencies of IFNγ-producing CD62L-, CD8+ T-cells specific for SIINFEKL or MVA epitopes $B8R_{20}$, $A3L_{270}$ and $K3L_6$ are shown. Samples stimulated with ß-Gal_{96} are shown as negative control. **Both figures** ***(4.33, 4.34)***: (A I) Specific CD8+ T-cell responses of a homologous prime/boost setting with MVA-ova compared to (A II) a heterologous setting with MVA-ova and MVA-TO/MVA-TOT, respectively. (B I) Mean frequency of CD62L-, IFNγ+, CD8+ T-cells compared for both (A I and A II) experimental settings. The significance for different responses to SIINFEKL-stimulation was evaluated for MVA-ova prime- MVA-ova boost versus MVA-ova prime- MVA-TO boost (p=0.096) and for MVA-ova prime- MVA-ova boost versus MVA-ova prime- MVA-TOT boost (p=0.72). (B II) Mean frequency of SIINFEKL-specific CD8+ T-cells of mice primed with MVA-ova and boosted with MVA-ova or MVA-TO/MVA-TOT.

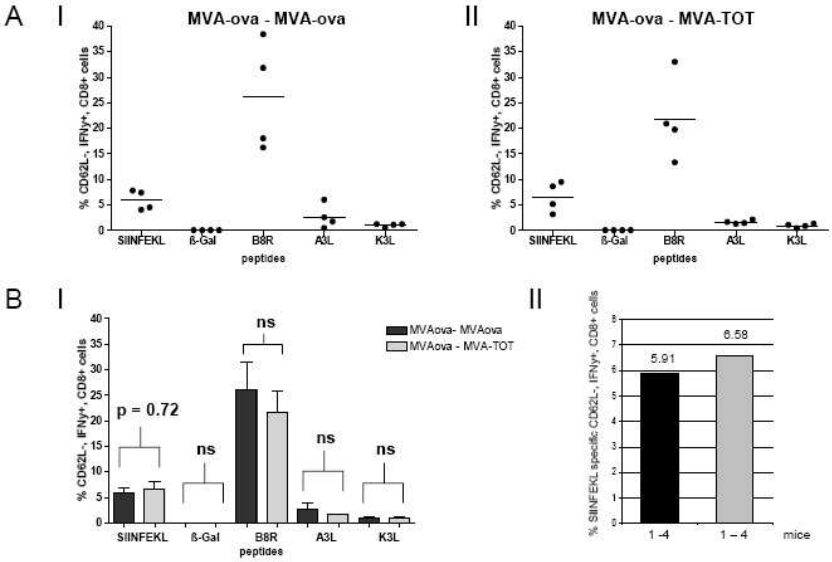

Figure 4.34: ***Secondary response***- *Antigen-specific CD8+ T-cells of C57BL/6 mice primed with MVA-ova and boosted with MVA-ova or MVA-TOT. See also Fig. 4.33.*

5 Discussion

Cytotoxic (CD8+) T-cells play a crucial role in resolving infections by intracellular pathogens such as viruses, bacteria and parasites [124, 78] as well as in mediating antitumor immunity [93, 120, 129, 50]. The identification of antigens selectively or preferentially expressed by intracellular pathogens or by transformed cells has led to the design of candidate vaccines against many infectious diseases or tumors aiming to elicit a strong antigen-specific CD8+ T-cell response. One of the most promising candidate vaccines is the recombinant viral vector system MVA. Due to a well established clinical safety profile and the ability to efficiently express recombinant genes [140] it has already been shown to stimulate immune responses against a large variety of different antigens with protective efficacy against viral infections, bacterial and parasitic diseases as well as tumors [20, 36, 91, 141]. One strategy to enhance CD8+ T-cell responses to specific pathogenic antigens is based on observations that targeting an antigen to undergo a more efficient processing by the MHC class I processing pathway will yield a more vigorous CD8+ CTL response against the respective antigen [144, 4]. In accordance with the findings of Tobery and Siliciano (1997) who had successfully targeted the nef protein for rapid cytoplasmatic degradation in a murine model, and Townsend et al. (1988) who had constructed a rapidly degraded ubiquitin-NP fusion protein, the present work aimed to determine the optimal antigen modification for rapid proteasomal degradation in the MVA vector system and wants to evaluate a strategy to enhance CTL responses by expressing unstable forms of the model antigen ovalbumin. The ovalbumin protein was employed as vaccine antigen and a recombinant MVA vector was created that expressed a ubiquitinated ovalbumin protein targeted for rapid proteasomal processing by modification of the N-terminal amino acid of ovalbumin into an arginine (R1), a primary destabilizing residue, and fusion to the C-terminal amino acid residue glycine of ubiquitin according to the N-end-rule [10, 151].

A second part within this study is based on findings that deubiquitination is completely inhibited if the C-terminal Gly^{76} of ubiqiutin is converted into an alanine or valine in Saccharomyces cerevisiae [18], moreover, when fused to ß-Gal such as Ub^{V76}-V-ßgal the protein is rapidly degraded within the UFD-pathway [70]. In our laboratory the instability of a melanoma-specific antigen, tyrosinase, could markedly be increased by N-terminal fusion of ubiquitin (A^{76}) to tyrosinase (M^{1}). Based on these findings, the N-terminal region

of this construct, including the nonremovable ubiquitin moiety fused to the signal sequence of tyrosinase, was suggested to constitute a general degradation signal applicable to other proteins such as ovalbumin. Hence, a recombinant MVA was constructed expressing a tyrosinase signal sequence-ovalbumin fusion construct stably linked to ubiquitin at its N-terminal end. A third construct expressed by MVA was designed analogous to the latter but additionally had the transmembrane domain of tyrosinase at its C-terminal end, given the hypothesis that expanded targeting to cellular compartments might further enhance MHC class I restricted peptide presentation to cytotoxic T-cells.

Evaluation of different strategies to enhance ovalbumin protein degradation

In Western blot analysis of infected BHK cells it was confirmed that ubiquitinated ovalbumin expressed by MVA-ubiOVA is migrating at the same size as native ovalbumin (45 kDa) expressed by MVA-ova showing the correct expression of ovalbumin and the complete removal of the ubiquitin moiety by cellular isopeptidases. Similar to results obtained with other proteins [10, 144, 147], Western blot analysis could confirm a notably, however sparsely, enhanced proteasomal degradation of ovalbumin due to an exposed N-terminal arginine according to the N-end-rule. There were notably lower protein levels detectable when proteasomes were fully active similar to what have been observed by Anderson et al. for an Ub-R-GFP fusion construct [4], indicating that a more rapid degradation is taking place. Nevertheless, ovalbumin could still be detected in the absence of proteasome inhibition in MVA-ubiOVA infected cells. Of note, different levels of protein were detected in MVA-ova- and MVA-ubiOVA-infected cells when proteasomal activity was abrogated. Whether this was due to differences in protein expression or due to other cellular mechanisms leading to enhanced degradation even in the presence of proteasome inhibitors is unclear. It has been suggested by Schwarz et al. (2000) that proteasome inhibition at lower concentrations of lactacystine (0.5-1 μM) might enable other proteases than the proteasome to produce antigenic peptides or their precursors [127].

Strikingly, a second and larger band was detected in all repeated experiments after infection with MVA-ova or MVA-ubiOVA indicating a persistant presence of a modified ovalbumin protein. The possibility that the larger band in MVA-ubiOVA-infected cells corresponded to an ubiquitinated form of ovalbumin due to an unsuccessful splitting of ubiOVA protein seemed unlikely since it was also present in MVA-ova- infected cells.

Ovalbumin is known to have a regular molecular weight of 45 kDa with two potential sites for glycosylation at asparagines 293 and 317 [68]. Examining the glycosylation of proteins

Sheares et al. (1985) could confirm the expression of glycosylated ovalbumin in a mouse L-cell/herpes simplex virus type 1 system by pulse-chase experiments [130]. Based on these findings it is likely that the second band, which was repeatedly confirmed in Western blot analysis, constitutes a glycosylated form of ovalbumin.

Further experiments using pIII-ubiOVA-transfected cells for immunoperoxidase staining failed to detect enhanced ovalbumin degradation, since there was no remarkable decrease in brown precipitation detectable in cells transfected with pIII-ubiOVA compared to cells transfected with pIII-ova which could be a marker for a rapid turnover of ovalbumin protein. Furthermore, there was no significant difference when proteasomes were inhibited in B16 cells. However, a reduced staining was confirmed in BHK cells when treated with lactacystine and MG132. This effect was attributed to the toxicity and ability of lactacystine to interfere with late viral gene expression in MVA-infected cells (Drexler et al., unpublished observation) and was addressed by initial treatment of CV-I cells with ara-C to block late gene expression and to rule out the adverse effects of proteasome inhibition. Staining on the single cell level then turned out to be slightly more intense in those cells with abrogated proteasomal activity, indicating a fractional accumulation of ovalbumin protein due to a diminished degradation by the proteasome.

To determine the stability of N-end rule targeted ubiOVA protein expressed by MVA-ubiOVA, pulse-chase experiments were conducted. In Hela cells infected with MVA-ubiOVA no enhanced degradation could be ascertained. In cells infected with MVA-ova, ovalbumin again appeared as two bands with one probably representing a glycosylated form of ovalbumin. The detected ovalbumin proteins were stable even 12 hours after the pulse confirming the stability of the native protein which has already been confirmed in our laboratory before. Shen & Rock (2003), however, had stably transfected DAP cells with a pcDNA3.1 expressing a full lenght ovalbumin (FL-OVA) and had found a half-life time of about 280 minutes.
The steady state levels of ovalbumin in cells expressing ubiOVA or native ovalbumin were different, with MVA-ova-infected cells displaying a visibly lower amount of ovalbumin protein already at 0 min chase- time. This difference was rather attrubuted to a difference in the amount of cells harvested after pulse-chase than to a difference in protein synthesis or degradation making the results of pulse-chase analysis of MVA-ubiOVA-infected cells compared to MVA-ova-infected cells difficult to interpret.
Intriguingly, in cells infected with rMVA expressing ubiOVA, a second protein band mi-

grating at the size of ubiquitinated ovalbumin was detected besides the expected ovalbumin protein migrating at 45 kDa which represents the deubiquitinated ovalbumin with an exposed N-terminal arginine according to the N-end rule. Obviously not all Ub-R-ova proteins synthesized within the translational machinery of the ribosomes were subsequently deubiquitinated by isopeptidases in the cytosol. Both protein signals, however, were detectable for 12 hours after the pulse, rather indicating no effect of N-end rule targeting on ovalbumin degradation. Whether the remaining stability of ovalbumin in MVA-ubiOVA infected cells can be attributed to different pulse-chase protocols in comparison to the latter can not be excluded since there were apparent differences. Infection time (2-8 hours), multiplicity of infection (MOI= 5-10) as well as the time of pulse labeling (5 to 60 minutes) varied profoundly. Tobery and Siliciano (1997) as well as Townsend et al. (1988) infected cells only for two hours compared to eight hours in this study but had a pulse period for 60 minutes, respectively.

As yet, only a sparsely enhanced degradation could be confirmed for ubiOVA in Western blot analysis. In flow cytometric analysis, however, presentation of the ovalbumin-specific peptide SIINFEKL bound to H2-K^b on B16-F1 cells was markedly increased when infected with MVA-ubiOVA in comparison to presentation of SIINFEKL/H2-K^b complexes on cells infected with MVA-ova expressing native ovalbumin. Furthermore, the density of SIINFEKL/H2-K^b complexes on the single cell level was higher in those cells infected with MVA-ubiOVA. These results were analogous to results obtained by Princiotta et al. (2003), who had found an enhanced presentation of the ovalbumin-specific peptide SIINFEKL on L-K^b cells after infection with a rVV expressing an N-terminally ubiquitinated influenza nucleoprotein (NP) fused with SIINFEKL and green fluorescent protein (GFP) at the COOH terminus (R-NP-GFP) compared to the presentation on cells infected with rVV-ova expressing native ovalbumin [112].

In Western blot analysis a slight accumulation of protein could be ascertained in those cells infected with MVA-ubiOVA after proteasomes were inhibited indicating that degradation of the protein ubiOVA is at least fractionally done by the proteasome. In immunoperoxidase staining experiments, however, no effect of lactacystine was detected after infection with MVA-ova or MVA-ubiOVA. Conversely, a markedly decreased presentation of SIINFEKL/H2-K^b complexes was seen after infection of B16-F1 cells with MVA-ubiOVA which were treated with proteasome inhibitors lactacystine and MG132 indicating that the proteasome is essential in generating the ovalbumin-specific peptide SIINFEKL which is bound to H2-K^b and presented to CD8+ T-cells.

Thus results of these experiments could demonstrate only a slightly enhanced degradation of ovalbumin expressed by MVA-ubiOVA in Western blot analysis and a slightly increased presentation of the ovalbumin-specific peptide SIINFEKL when compared to results obtained with MVA-ova.

Nevertheless, results of this study are in line, even though not as significant, with those obtained with other proteins such as HIV specific nef [144], influenza nucleoprotein (NP) [147], Green fluorescent protein (GFP) [58, 112] or ß-galactosidase [10] who could confirm increased instability of proteins upon N-end-rule targeting with M1R replacement in the protein as a critical component of the N-degron.

In addition to the strategy of N-end rule targeting, two other constructs were designed targeting ovalbumin for rapid degradation within the ubiquitin-fusion degradation pathway (UFD).

Kinetic Western blot analysis of UFD-targeted ovalbumin in MVA-TO- and MVA-TOT-infected BHK cells yielded surprisingly different results obviously depending on the signal sequence at the N-terminal end and the transmembrane domain of tyrosinase at the C-terminal end of ovalbumin. When cells were infected with MVA-ova, there were again two bands detectable with a polyclonal antibody against ovalbumin. One band with 45 kDa corresponded to the size of ovalbumin, a second band was slightly larger and might represent a glycosylated form of the protein. Addition of proteasomal inhibitors had no effect on protein accumulation.

When cells were infected with MVA-TO, however, five protein fragments could be detected with the same antibody. At least four forms were dependent on proteasomal degradation since there was an increase in protein levels in the presence of proteasome inhibitors. Only one fragment was not detectable when proteasomes were unimpaired and fully active, probably reflecting its rapid degradation within the proteasomal pathway. Nevertheless, it remains obscure which of the protein fragments finally included the ovalbumin-specific peptide SIINFEKL, which, as discussed later, is efficiently presented within the MHC class I pathway on cellular surfaces after infection of DC2.4 cells with MVA-TO. One possible explanation for the generation of these different protein fragments is provided by Yewdell et al. (1996) announcing that endogenous class I peptide ligands derive in part from defective forms of newly synthesized proteins (defective ribosomal products: DRiPs) which mainly consist of premature termination products and misfolded full-length forms of proteins (hypothesis of defective ribosomal products (TDH)) [164]. Furthermore, they assumed that DRiPs are degraded more rapidly than native proteins [163]. With regard

to results obtained by Western blot and flow cytometric analysis in this study, infection of cells with MVA-TO likely yielded in the generation of DRiPs of ubi/Tyr_Sig/Ova (TO) which caused increased presentation of SIINFEKL/MHC class I in comparison to infection with MVA-ova.
In Western blot analysis of cells infected with MVA-TOT, one band corresponding to ubi/Tyr_Sig/Ova/Tyr_TM (TOT) was detected at 48 kDa reflecting the correct expression of TOT and the stable conjunction of ubiquitin at its N-terminal end. This contradicts results obtained by Andersson et al. (2004) who had found the mutation of glycine to alanine (G76A) in ubiquitin failed to inhibit ubiquitin cleavage in mammalian cells for both GFP and ß-Gal [4].
In Western blot analysis, however, the ubiquitin moiety stably linked to the signal sequence of tyrosinase and the transmembrane domain at the C-terminal end did not induce rapid degradation of ovalbumin. The protein was detectable for at least 25 hours after infection with the protein levels rather decreased when proteasomes were inhibited. Whether these adverse effects can be attributed to the known cytotoxicity of lactacystine [127] remains ambiguous, since there seemed to be no influence of lactacystine toxicity in MVA-TO-infected BHK cells.

In further experiments characterizing MVA-TO an enhanced degradation of ovalbumin could be confirmed. Especially with immunoperoxidase staining a considerably lower amount of protein was detected in pIII-TO- transfected BHK or B16-F1 cells when compared to cells transfected with pIII-ova. Furthermore, a protein accumulation could be seen after treatment of cells with proteasome inhibitors. In pulse-chase experiments there was no band detected. Whether this was due to rapid degradation of the protein can not be determined.
After infection of cells with MVA-TOT, only a weak staining was noted on the single cell level after immunoperoxidase staining. However, an increased amount of protein level was detected at the site of cellular compartments, obviously attributable to the influence of the transmembrane domain of tyrosinase at the C-terminal end of ovalbumin. In pulse-chase experiments a dim band was detected at time point cero and a half indicating a rapid degradation of the protein.

To determine whether enhanced degradation of TO and TOT and the potentially increased availability of SIINFEKL would ultimately lead to an enhanced MHC class I loading and enhanced presentation of SIINFEKL/H2-K^b complexes on the cellular surface, B16-F1

cells were infected with MVA-TO and MVA-TOT and expression of SIINFEKL/H2-K^b complexes was assessed with the specific antibody 25-D1.16 [110] and analyzed by flow cytometry. As for the Ub-R-ova construct, presentation of SIINFEKL/H2-K^b complexes began two hours post infection with a maximum at eight hours post infection as the latest analyzed time point. The most effective presentation of SIINFEKL/H2-K^b complexes could be detected when B16-F1 cells were infected with MVA-TO, whereas the presentation of SIINFEKL in MVA-TOT-infected cells was even slightly less than in those infected with MVA-ova. Whether this can be attributed to a slower presentation of SIINFEKL can not be excluded since there was a group of cells which only slowly became SIINFEKL/H2-K^b presenting cells within eight hours. Comparing the amount of SIINFEKL on a single cell, the fusion protein TO targeted for the UFD-pathway could induce considerably higher quantities of SIINFEKL/H2-K^b complexes on a cell, leading to the suggestion that this construct will yield promising results in immunization experiments.

To further investigate the importance of the proteasome in the generation of the antigenic peptide SIINFEKL, proteasome inhibitors lactacystine and MG132 were added. The loss of proteasomal activity caused a decrease of H2-K^b/SIINFEKL presentation on both, MVA-TO and MVA-TOT infected cells, however, did not completely abrogate SIINFEKL presentation as in cells infected with MVA expressing the N-end-rule targeted Ub-R-ova. This varying effect of lactacystine has already been observed by Vanitsky et al. (1997) who had found the effects of proteasome inhibitors depending also on the type of antigen [152]. One explanation for this different effect of lactacystine could be that other proteases such as the tripeptidyl-peptidase II [45], furin [47] or thimet oligopeptidase [135] contribute to the production of MHC class I ligands when proteasomes are inhibited. TPP II is located in the cytosol and its regular candidate substrates are oligopeptides formed by the proteasome. It has been shown that some cells can adapt to conditions of proteasome inhibition through the induction of another high-molecular-weight-peptidase which has been identified as TPP II showing some endopeptidase activity [45, 49]. Nevertheless, the relative contribution of its activity in antigenic peptide generation when proteasomes are inhibited remains open and it can not be excluded that other proteases are able to substitute for proteasomal activity [146]. This hypothesis would also explain results obtained with Western blot analysis of MVA-TOT-infected cells *(Fig. 4.24)*. There was no effect of proteasomal inhibition even though there was a reduced presentation of H2-K^b/SIINFEKL detectable after proteasomal inhibition in flow cytometric analysis.

To summarize the *in vitro* results obtained in this study, only a slightly enhanced degradation could be demonstrated for the N-end rule targeted ovalbumin fusion construct ubiOVA in Western blot analysis, however, could significantly be seen for the UFD-targeted constructs TO and TOT in immunoperoxidase experiments. Moreover, two constructs (ubiOVA and TO) led to an increased presentation of SIINFEKL within the MHC class I pathway of B16 cells with a remarkable enhancement of H2-K^b/SIINFEKL on the single cell level. These results clearly indicate that targeting antigens for rapid proteasomal processing will yield improved presentation of antigenic peptides within the MHC class I antigen processing pathway, making especially the ubi/Tyr_Sig- sequence an interesting tool to be combined with other antigens to increase antigenic peptide presentation. Furthermore, differences in *in vivo* experiments conducted within this study with the different MVA vector constructs may be attributed to differences in antigen presentation.

Evaluation of MVA- and ovalbumin-specific CTL responses in different immunization settings

To investigate the consequences of a more rapid degradation of ovalbumin and the enhanced MHC class I restricted antigen presentation on CTL responses to the ovalbumin-specific peptide SIINFEKL, C57BL/6 mice were immunized with MVA-ubiOVA, MVA-TO and MVA-TOT. The results were compared to results of immunizations with MVA-ova expressing stable ovalbumin. Andersson & Barry (2004) had demonstrated that both, N-end rule targeted as well as UFD-targeted GFP, were rapidly degraded and were able to elicit a significantly higher percentage of CD8+ tetramer+ T-cells two weeks after DNA immunization of BALB/c mice [4]. Tobery & Siliciano (1997) found the beforementioned rapidly degraded Ub-R-nef protein to be the optimal construct to elicit an antigen-specific CTL response after immunization of BALB/c mice [144]. Both studies indicate that increasing the instability of an antigen through targeting for efficient degradation within the proteasomal pathway will provide a highly effective vaccine strategy for the induction of enhanced antigen-specific CTL responses *in vivo*.

For priming of naive CD8+ T-cells, pAPCs need to present specific peptides bound to self-MHC class I molecules [134, 169]. There are, however, two different pathways by which pAPCs can present the antigen to antiviral T-lymphocytes. On one side, pAPCs can

present peptides derived from degraded, endogenously synthesized proteins. On the other side, pAPCs do also have the ability to present exogenous antigens on MHC I molecules in a process termed cross-presentation *(see section 1.2)*. Bevan M. J. et al. injected MHC-mismatched cells expressing minor H antigens into mice and discovered that they were able to prime self-MHC-restricted CTLs specific for the immunizing minor H antigens [16]. He termed this process cross-priming. To which extent these two different pathways contribute to T-cell priming during viral infections *in vivo*, however, remains controversial.

There is strong evidence that priming of antiviral CTLs after infection with MVA mainly occurs via cross-priming [44]. As for MVA, which in general has the ability to infect non-APC as well as pAPCs [72], it has been found that it can induce CD8+ T-cells recognizing late viral antigens that are not synthesized within infected DCs due to an early block in viral life cycle in these DCs [32, 35]. Furthermore, a recombinant MVA expressing rapidly degraded protein enhanced direct presentation *in vitro* and was able to stimulate CTL *ex vivo* but failed to improve T-cell priming *in vivo*, whereas a long-lived antigen efficiently induced a robust CD8+ T-cell response [44]. Other experiments using infected TAP-deficient or MHC class I-mismatched non-pAPC donor cells evoked similar CD8+ T-cell responses regarding CTL frequencies and the immunodominance hierarchy when MVA was given as a live vaccine. These results together with the finding that downregulation of the cross-presentation capacity of DCs by *in vivo* maturation with CpG almost completely abrogated MVA-specific priming of CD8+ T-cells rather let to the assumption that during primary infection with MVA cross-presentation is the leading pathway for the stimulation of specific CTLs and that furthermore, long-lived antigen is the favored substrate for cross-priming *in vivo* [44]. Of note, these results were not dependent on the route of vaccination and apply to different model antigens tested in different mouse strains [44].

In vivo experiments performed in this study confirmed the presence of SIINFEKL-specific CTL responses after immunization with all recombinant vectors as measured by IFNγ-production upon *in vitro* stimulation with SIINFEKL peptide and subsequent FACS-analysis. Primary immune responses upon immunization with MVA-ova reached in average 1.9% SIINFEKL-specific CD8+ T-cells. In congruence with expectations, amounts of SIINFEKL-specific CD8+ T cells after immunization with MVA-ubiOVA and MVA-TO were lower compared to those obtained with MVA-ova immunization, even though not significantly. The lack of significant differences in CTL responses might be attributed to the remaining stability of fusion-proteins which probably can still be cross-presented. The

CTL responses in mice immunized with MVA-TOT, however, were slightly higher than those of MVA-ova- immunized mice. Yet this effect might also be attributed to the exclusion of one mouse in the MVA-ova- immunized group which failed to develop any immune response. Results of experiments would probably be more significant when an increased amount of mice (=n) would be immunized in both tested groups.

It has been demonstrated that both, direct and cross-presentation, can contribute to priming of naive T-cells after infection with vaccinia virus [103, 13] and that the contribution of one pathway might vary depending on the route of virus application [133]. Explanations that could account for the dominating role of cross-presentation in MVA priming in contrast to that seen after infection with vaccinia virus could be its loss of replication competence resulting in a sinlge round of antigen expression, its loss of multiple genes including at least two viral proteins with proposed anti-apoptotic functions [6, 8, 33]. It has been demonstrated that DCs undergo apoptosis earlier with MVA infection than with vaccinia viral infection and that MVA infection leads to an accelerated shutdown of host cell protein synthesis in DCs [44]. In addition, MVA has been reported to impair the capacity of DCs to migrate and to adequately respond to chemokines [66, 44]. So far, exclusive cross-presentation has only been postulated for viruses that do not infect DCs [134, 139] or that considerably interfere with DC antigen presentation [166]. Hence, MVA is the first virus for which cross-presentation has been shown to be of key relevance even though it can efficiently infect DCs and allows strong antigen presentation in these cells [44].

There is increasing evidence that cross-presentation is rather based on the transfer of whole proteins than on peptides generated during protein formation or proteasomal degradation [131, 155, 102]. These findings would be underlined by results of experiments performed in this study. Primary immunization with MVA expressing rapidly degradable ovalbumin with an efficient presentation of antigenic peptides *(Fig. 4.16, Fig. 4.27)* elicited a reduced CD8+ T-cell response to the ovalbumin-specific peptide SIINFEKL compared to MVA expressing stable ovalbumin that accumulate to higher steady-state levels *(Fig. 4.18, Fig. 4.30, Fig. 4.31)*.

Serna et al. developed an *in vitro* model in which ovalbumin is expressed by vaccinia-T7 in antigen donor cells and cross-presented by mouse macrophages [128]. They could show that treatment of antigen-donor cells with 2 μM lactacystine almost fully blocked cross-presentation of ovalbumin and that overexpression of the two cytosolic peptidases known

to degrade proteasome products, leucine aminopeptidase as well as thimet oligopeptidase, inhibited cross-presentation. They concluded that proteolytic intermediates of the proteasome and not full-length proteins constitute most of the antigen cross-presented by APCs when acquired from donor cells recently infected with vaccinia virus [128, 113].
By contrast, there is increasing evidence that the dominant form of ovalbumin cross-presented *in vivo* is the full-length protein [131, 102, 19]. Norbury et al. (2004) developed an *in vivo* model based on the injection of apoptotic vaccinia-infected cells expressing different forms of ovalbumin peptide. Neither pre-processed ovalbumin peptide nor an ovalbumin targeted for rapid proteasomal degradation in antigen donor cells were efficiently cross-presented [102]. The discrepancy between the *in vitro* results obtained by Serna et al. (2003) and the *in vivo* study performed by Norbury et al. (2004) might either be explained with the varying conditions *in vivo* or might be attributed to the different type of antigen-presenting cells used in these two studies.
Another crucial factor for the process of cross-presentation was addressed by Shen & Rock (2004). They investigated three ovalbumin constructs expressed by stably transfected DAP cells and targeted for different subcellular compartments for their capacity to elicit specific CTL responses by cross-presentation in H-2^{bxk} F1 mice. They showed that a membrane bound ovalbumin construct generated stronger CTL activity than the full-length form [131]. These results led to the suggestion that targeting antigens to the plasma membrane or endosomes is advantageous to increase specific CD8+ T-cell responses and that the localization of an antigen constitutes another important and relevant factor in cross-presentation.
In this study, rMVA expressing TOT, a protein that is targeted to cellular membranes by the transmembrane domain of tyrosinase, could elicit a higher ovalbumin-specific CTL response in priming when compared to MVA-ova expressing stable ovalbumin *(Fig. 4.31)*. This was, however, attributed to the low efficacy of MVA-ova immunization in this individual experiment. When compared to the average of CTL responses after MVA-ova immunizations, ovalbumin-specific CTL responses after MVA-TOT immunization were rather low and thus interpreted as result of a decreased efficacy of cross-presentation in priming. Hence these results are hard to interpret and might give an explanation why MVA-TO is advantageous to MVA-TOT in boosting *(Fig. 4.33, 4.34)* missing the transmembrane domain which might render a protein as subject for cross-presentation rather than direct presentation.

One major goal of T-cell vaccines is to generate long-lived memory CD8+ T-cells which

are capable of recognizing antigen and which can rapidly expand upon secondary antigen encounter to combat an infection. During CD8+ T-cell responses to infections there are three characteristic phases: a period of initial activation and expansion after antigen encounter, a following contraction phase in which the CD8+ T-cell population decreases to approximately 5-10% of their original quantity and the final establishment and maintenance of a memory T-cell pool [123]. The memory T-cell pool can persist over long periods of time and has an increased proliferation potential in response to either antigen or homeostatic signals [154]. To further enhance memory CD8+ T-cell populations, prime/boost vaccination strategies have proven to be advantageous. As explicitly described in *chapter 1* primary immune response after immunization with MVA can be rapidly initiated and is suggested to occur via cross-priming *in vivo* favoring stable mature protein as the substrate for cross-presentation [44]. In contrast, recent observations rather indicate a role for direct activation during secondary immunization with MVA. As it could be demonstrated that the expansion of virus-specific CD8+ T-cells was regulated by T-cell cross-competition favoring T-cells that are able to rapidly detect infected cells. With the outcome of this competition being influenced by the timing of antigen expression. T-cells recognizing epitopes derived from early viral proteins conferred better protection against infection and had an advantage to T-cell responses against late viral epitopes [73]. These results indicate an advantage of rapidly presented antigenic peptides after secondary immunization with MVA, leading to the hypothesis that direct presentation is the dominating pathway of T-cell activation during boost immunization with MVA.

With regard to *in vitro* results of this study, a rapidly degraded antigen like the TO-fusion protein expressed by MVA-TO, which could establish an improved SIINFEKL/MHC class I presentation on B16 cells, would prove to be a better boosting agent than MVA-ova expressing stable ovalbumin. In congruence with expectations, MVA-TO could elicit a remarkably stronger SIINFEKL-specific CD8+ T-cell response in C57BL/6 mice thirty days after immunization with MVA-ova when compared to a homologous prime-boost immunization with MVA-ova *(Fig. 4.33)*. As expected, boosting with MVA-TO was more effective than a second immunization with MVA-TOT after MVA-ova prime *(Fig. 4.34)*.

It can be stated that both, MVA-TO as well as MVA-TOT, were considerably better boosting agents reaching up to 10.2% SIINFEKL-specific CD8+ T-cells after MVA-TO and 9.45% after MVA-TOT boosting when compared to MVA-ova, which reached up to 7.78% SIINFEKL-specific CD8+ T-cells. As expected from *in vitro* results, MVA-ubiOVA boosting following MVA-ova priming was only sparsely more efficient than secondary im-

munization with MVA-ova, reaching a mean of 5.82% SIINFEKL-specific CD8+ T-cells compared to 5.52% after MVA-ova boosting.

Homologous MVA immunizations have already been used in phase I and phase II clinical trials of cancer immunotherapy with rather disappointing results, e.g. showing either no specific T-cell or antibody responses in any of the MVA-hTyr vaccinated stage II melanoma patients after three times of vaccination at four-week intervals [94] or only marginal response in patients with different solid tumors repeatedly immunized with MVA expressing human MUC1 [118]. Heterologous prime-boost regimens, however, can be advantageous to homologous MVA applications and have already been investigated in several studies [162, 91, 64, 108, 37, 57]. Heterologous prime-boost protocols do probably limit the effects of T-cell competition by reducing the amount of T-cells specific for other, maybe immunodominant epitopes expressed by MVA which would limit CTL responses to target antigens. Furthermore, it was discussed that pre-existing MVA or VV immunity might, for example in the case of a previous chickenpox vaccination, interfere with subsequent immunizations with MVA [36]. It would be interesting to test MVA-TO as a boosting agent after a heterologous prime with DNA to further investigate the beforementioned issues. As McConkey et al. (2003) have demonstrated, DNA priming before MVA boosting has been established as a promising tool to improve specific CD8+ T-cell responses in humans to a pre-erythrocytic malaria antigen [91].

Another strategy to further enhance antigen-specific CD8+ T-cell responses conducted within this study and presented under *appendix-A*, is based on findings that after viral infection CD8+ T-cell responses are predominantly directed to only a few peptides, the immunodominant peptides [165]. During the infection with MVA, $B8R_{20}$ comprises one of the most immunodominant peptides. The immunodomination by CD8+ T-cells for specific peptides expressed by the vector has been shown to limit CTL responses to inserted recombinant antigens. Smith et al. (2005) evaluated a clinical trial in melanoma patients involving repeated injections of MVA encoding a string of HLA-A*0201-restricted melanoma tumor antigen epitopes [136]. They could demonstrate that the vaccine driven CTL hierarchy is dominated by pox-viral-specific responses with the high affinity melan-A_{26-35} analogue epitope being the only melanoma-specific epitope above detection level after MVA immunization. Even though SIINFEKL is considered an immunodominant peptide [165], $B8R_{20}$ elicited a considerably stronger CTL response after immunization with either of the constructs used in this study. One strategy to address this issue and thus cir-

cumvent the immunodomination of CTLs for other vector-specific peptides was suggested to be the elimination of immunodominant peptides by gene deletion [136].
As depicted under *appendix-A*, the deletion of $B8R_{20}$ in an MVA priming vector (MVA-ovaB8R$^{-/-}$) could ultimately enhance CTL responses to the antigen-specific peptide SIINFEKL after boost immunization with MVA-ova. Whereas the CD8+ T-cell response to $B8R_{20}$ remained at significantly lower levels. These results strongly imply that immunodominance provides an important issue for the development of candidate vaccines for the elicitation of specific CTL responses and that improved vector design could include the deletion of genes encoding for immunodominant vector-specific peptides in order to enhance target antigen-specific immune responses.
Aside from $B8R_{20}$ gene deletion in priming, a $B8R_{20}$ knock out in boosting would be of considerable interest. The absence of $B8R_{20}$ stimulation in boosting would most likely further increase target antigen-specific CTL responses when compared to MVA-ovaB8R$^{-/-}$ prime and MVA-ova boost, since there would be a perspicuous advantage for SIINFEKL-specific T-cells during cross-competition in boost immunization.

In summary, this study shows that upon expression of N-end rule targeted ubiquitinated ovalbumin in MVA-ubiOVA infected cells, ovalbumin was marginally degraded more rapidly when compared to native ovalbumin, but could slightly increase MHC class I peptide presentation of an ovalbumin-specific peptide. Two other constructs targeted for rapid proteasomal processing within the UFD-pathway expressed by MVA-TO and MVA-TOT, in contrast, showed an enhanced degradation of the antigen and after infection with MVA-TO a markedly increased ovalbumin-specific peptide presentation. Primary immunization with all three vector constructs compared to MVA-ova, revealed that an instable protein was rather disadvantegous in priming with MVA, as the highest SIINFEKL-specific CD8+ T-cell response was detected after MVA-ova immunization. In boosting experiments, however, rapidly degraded antigen was more effective, resulting in a markedly increased ovalbumin-specific T-cell response. Hence, evaluation of MVA vector constructs expressing modified ovalbumin as priming or boosting agents could further substantiate the hypothesis that enhanced instability of a target antigen is disadvantageous during primary immunizations with MVA but clearly represents a promising antigen formulation to be used for secondary immunizations with MVA.
Results obtained in this study will contribute to improved rational vaccine design giving further information about desirable antigen formulations contained in MVA vaccines to increase CTL responses in vaccination.

6 Conclusion and future perspectives

With regard to the aims and objectives of this thesis some conclusions can be drawn. The degradation of the N-end rule-targeted antigen ubiOVA could only be enhanced rather marginally when compared to stable ovalbumin as detected in Western blot analysis. In other experiments, e.g. immunoperoxidase staining and pulse-chase analysis, no significantly improved protein degradation could be demonstrated. However, in flow cytometric analysis of B16-F1 cells infected with MVA-ubiOVA an increased presentation of SIINFEKL could be detected. In addition, supported by results of Western blot analysis, peptide presentation was partially proteasome dependent. These results confirmed that N-end rule targeting of proteins by replacement of their N-terminal amino acid residue with a destablizing amino acid like arginine and linkage to ubiquitin renders the antigen instable, leading to its degradation within the proteasomal pathway. Furthermore, this instability enhanced the amount of antigen-specific peptides presented on MHC class I for the detection by CTLs.

The two other constructs tested within this work, MVA-TO and MVA-TOT, expressing modified ovalbumin protein targeted for degradation within the UFD-pathway, could enhance ovalbumin degradation even more. UFD-targeting of the antigen by stable linkage of ubiquitin to the N-terminus of the signal sequence of tyrosinase could significantly increase the instability of the model antigen ovalbumin as confirmed by immunoperoxidase staining. Western blot analysis showed that the antibody specific for ovalbumin was able to detect multiple fragments after infection of cells with MVA-TO as well as after infection with MVA-TOT, making those results hard to interpret. Antigens might be cleaved into noncontiguous fragments directly after synthesis or they might also be a source for so called defective ribosomal proteins (DRiPs). Only one fragment of the TO-construct could only be detected when proteasomes were inhibited with lactacystine, which would be in line with experiments of immunoperoxidase staining and FACS analysis where only a minimal effect of proteasome inhibitors could be detected. Other proteases might be responsible for the generation of antigenic peptides in this case.

Presentation of the ovalbumin-specific peptide SIINFEKL could be increased after infection of cells with MVA-TO and MVA-TOT. Especially the TO-construct could significantly

enhance antigenic peptide presentation on the single cell level.

Given that all modified ovalbumin expression constructs tested within this study showed at least a slightly decreased protein stability and an enhanced antigenic peptide presentation, *in vivo* experiments were conducted to evaluate which antigen formulation (rapidly degraded or stable) is optimal for immunization with MVA in priming or boosting.

After vaccination of C57BL/6 mice with MVA-ubiOVA, MVA-TO and MVA-TOT in comparison to vaccination with MVA-ova, it can be concluded that a stable antigen is advantageous for an efficient generation of antigen-specific CD8+ T-cells in primary immunization with MVA. Moreover, if cross-presentation is of critical relevance in priming with MVA, the type of antigen cross-presented in C57BL/6 mice would be stable whole protein.

In boosting experiments, modified ovalbumin expression constructs were advantageous to MVA-ova expressing stable ovalbumin. Especially the two UFD-targeted constructs, MVA-TO and MVA-TOT, were able to elicit a strong antigen-specific CTL response. Hence, the optimal form of antigen in secondary immunization with MVA in C75BL/6 mice is rapidly degraded antigen.

Results obtained in this study could demonstrate that N-end rule targeting as well as UFD-targeting of ovalbumin as a model antigen could enhance ovalbumin-specific peptide presentation and confirmed that the instability of an antigen constitutes an important tool to improve recombinant MVA vaccines in eliciting strong, long-lasting immune responses.

Outlook

As demonstrated within this study, the stability of an antigen is of critical relevance in immunization strategies with MVA. The rapid processing of the model antigen ovalbumin in rMVA expressing the TO fusion construct could markedly increase the amount of antigen-specific CD8+ T-cells after secondary immunization with MVA.

Thus, targeting antigens to rapid proteasomal degradation within the N-end rule system or the UFD-pathway certainly is a promising approach to enhance the efficacy of viral vector vaccines. However, even though the model protein ovalbumin could be submitted to enhanced degradation within these pathways, the single strategies to enhance a protein‘s turnover have to be evaluated for each individual antigen. Especially conjugation of an antigen with the ubiquitinated signal sequence of tyrosinase comprises a promising and interesting approach applicable to other antigens.

Nevertheless, MVA expressing stable or modified ovalbumin constructs is still weakly immunogenic reaching only up to 3.54% SIINFEKL-specific CD8+ T-cells after peptide stimulation of splenocytes. Other peptides, like $B8R_{20}$, are able to elicit more than 11.5% vector-specific CD8+ T-cells after peptide stimulation. These results show that there are other factors than antigen stability that must be evaluated for efficient MVA priming.

In *appendix A* another method to enhance antigen-specific CTL responses was investigated. Kastenmueller et al. showed that for the induction and strength of primary CD8+ T-cell responses during boost vaccination, T-cell cross-competition seems to be a major regulator of the expansion of virus-specific T-cells. Furthermore, during boost immunization they found a switch in the immunodominance hierarchy favouring the proliferation of T-cells recognizing epitopes derived from early gene products. By deletion of the immunodominant peptide $B8R_{20}$ (early gene) in MVA, CTL responses to ovalbumin-specific peptide SIINFEKL (OVA_{257}(early gene)) could markedly be increased even when MVA-ovaB8R$^{-/-}$ was used as priming agent. In these experiments more than 9,1% ova-specific CTLs were reached. Further experiments using MVA-ovaB8R$^{-/-}$ as boosting agent should be performed as T-cell cross competition seemed to play a key role in boosting experiments.

The employment of a heterologous prime-boost regimen would be a highly interesting subject to be used with MVA-TO as boosting agent, as it had been demonstrated that the combined use of DNA-prime and MVA-boost is highly suitable for the induction of a strong CTL response.

Taking notice of all discussed factors to enhance antigen-specific immune response, it would be possible to further optimize vaccination strategies with recombinant viral vector MVA which should finally be evaluated in an ovalbumin expressing mouse-tumor model to specifically assess the clinical relevance and protective capacity of different vaccination approaches.

Bibliography

[1] **Akira, S., Uematsu, S., Takeuchi, O.**
Pathogen recognition and innate immunity.
Cell. 124(4) (2006) 783-801 Review

[2] **Alkhatib, G., Briedis, D.J.**
High-level eucaryotic in vivo expression of biologically active measles virus hemagglutinin by using an adenovirus type 5 helper-free vector system.
J Virol. 62(8) (1988) 2718-27

[3] **Amato, R.J., Hawkins, R.E., Kaufman, H.L., Thompson, J.A., Tomczak, P., Szczylik, C., McDonald, M., Eastty, S., Shingler, W.H., de Belin, J., Goonewardena, M., Naylor, S., Harrop, R.**
Vaccination of metastatic renal cancer patients with MVA-5T4: a randomized, double-blind, placebo-controlled phase III study.
Clin Cancer Res. 16(22) (2010) 5539-47

[4] **Andersson, H.A., Barry, M.A.**
Maximizing antigen targeting to the proteasome for gene-based vaccines.
Mol Ther. 10(3) (2004) 432-46

[5] **Anderson, R.J., Hannan, C.M., Gilbert, S.C., Laidlaw, S.M., Sheu, E.G., Korten, S., Sinden, R., Butcher, G.A., Skinner, M.A., Hill, A.V.**
Enhanced CD8+ T cell immune responses and protection elicited against Plasmodium berghei malaria by prime boost immunization regimens using a novel attenuated fowlpox virus.
J Immunol. 172(5) (2004) 3094-100

[6] **Antoine, G., Scheiflinger, F., Dorner, F., Falkner, F.G.**
The complete genomic sequence of the modified vaccinia Ankara strain: comparison with other orthopoxviruses.
Virology 244 (1998) 365-396

[7] **Anton, L.C., Snyder, H.L., Bennink, J.R., Vinitsky, A., Orlowski, M., Porgador, A., Yewdell, J.W.**
Dissociation of proteasomal degradation of biosynthesized viral proteins from generation of MHC class I-associated antigenic peptides.
J Immunol. 160(10) (1998) 4859-68

[8] **Aoyagi, M., Zhai, D., Jin, C., Aleshin, A.E., Stec, B., Reed, J.C., Liddington, R.C.**
Vaccinia virus N1L protein resembles a B cell lymphoma-2 (Bcl-2) family protein.
Protein Sci. 16(1) (2007) 118-24

[9] **Arlen, P.M., Gulley, J.L., Parker, C., Skarupa, L., Pazdur, M., Panicali, D., Beetham, P., Tsang, K.Y., Grosenbach, D.W., Feldman, J., Steinberg, S.M., Jones, E., Chen, C., Marte, J., Schlom, J., Dahut, W.**
A randomized phase II study of concurrent docetaxel plus vaccine versus vaccine alone in metastatic androgen-independent prostate cancer.
Clin Cancer Res. 12(4) (2006) 1260-9

[10] **Bachmair, A., Finley, D., Varshavsky, A.**
In vivo half-life of a protein is a function of its amino-terminal residue.
Science. 234 (1986) 179-186

[11] **Bagai, R., Valujskikh, A., Canaday, D.H., Bailey, E., Lalli, P.N., Harding, C.V., Heeger, P.S.**
Mouse endothelial cells cross-present lymphocyte-derived antigen on class I MHC via a TAP1- and proteasome-dependent pathway.
J Immunol. 174(12) (2005) 7711-5

[12] **Baldwin, P.J., van der Burg, S.H., Boswell, C.M., Offringa, R., Hickling, J.K., Dobson, J., Roberts, J.S., Latimer, J.A., Moseley, R.P., Coleman, N., Stanley, M.A., Sterling, J.C.**
Vaccinia-expressed human papillomavirus 16 and 18 e6 and e7 as a therapeutic vaccination for vulval and vaginal intraepithelial neoplasia.
Clin Cancer Res. 9(14) (2003) 5205-13

[13] **Basta, S., Chen, W., Bennink, J.R., Yewdell, J.W.**
Inhibitory effects of cytomegalovirus proteins US2 and US11 point to contributions from direct priming and cross-priming in induction of vaccinia virus-specific CD8(+) T cells.
J Immunol. 168(11) (2002) 5403-8

[14] **Beninga, J., Rock, K.L., Goldberg, A.L.**
Interferon-gamma can stimulate post-proteasomal trimming of the N terminus of an antigenic peptide by inducing leucine aminopeptidase.
J Biol Chem. 273(30) (1998) 18734-42

[15] **Berthoud TK, Fletcher H, Porter D, Thompson F, Hill AV, Todryk SM.**
Comparing human T cell and NK cell responses in viral-based malaria vaccine trials.
Vaccine. 28(1) (2009) 21-7

[16] **Bevan, M.J.**
Cross-priming for a secondary cytotoxic response to minor H antigens with H-2 congenic cells which do not cross-react in the cytotoxic assay.
J Exp Med. 143(5) (1976) 1283-8

[17] **Bronte, V., Carroll, M.W., Goletz, T.J., Wang, M., Overwijk, W.W., Marincola, F., Rosenberg, S.A., Moss, B., Restifo, N.P.**
Antigen expression by dendritic cells correlates with the therapeutic effectiveness of a model recombinant poxvirus tumor vaccine.
Proc Natl Acad Sci U S A. 94(7) (1997) 3183-8

[18] **Butt, T.R., Khan, M.I., Marsh, J., Ecker, D.J., Crooke, S.T.**
Ubiquitin-metallothionein fusion protein expression in yeast. A genetic approach for analysis of ubiquitin functions.
J Biol Chem. 263(31) (1988) 16364-71

[19] **Carbone, F.R., Bevan, M.J.**
Class I-restricted processing and presentation of exogenous cell-associated antigen in vivo.
J Exp Med. 171(2) (1990) 377-87

[20] **Carroll, M.W., Overwijk, W.W., Chamberlain, R.S., Rosenberg, S.A., Moss, B., Restifo, N.P.**
Highly attenuated modified vaccinia virus Ankara (MVA) as an effective recombinant vector: a murine tumor model.
Vaccine. 15(4) (1997) 387-94

[21] **Cascio, P., Hilton, C., Kisselev, A.F., Rock, K.L., Goldberg, A.L.**
26S proteasomes and immunoproteasomes produce mainly N-extended versions of an antigenic peptide.
EMBO J. 20(10) (2001) 2357-66

[22] **Celluzzi, C.M., Mayordomo, J.I., Storkus, W.J., Lotze, M.T., Falo, L.D. Jr.**
Peptide-pulsed dendritic cells induce antigen-specific CTL-mediated protective tumor immunity.
J Exp Med. 183(1) (1996) 283-7

[23] **Cerundolo, V., Benham, A., Braud, V., Mukherjee, S., Gould, K., Macino, B., Neefjes, J., Townsend, A.**
The proteasome-specific inhibitor lactacystin blocks presentation of cytotoxic T lymphocyte epitopes in human and murine cells.
Eur J Immunol. 27(1) (1997) 336-41

[24] **Chahroudi, A., Garber, D.A., Reeves, P., Liu, L., Kalman, D., Feinberg, M.B.**
Differences and similarities in viral life cycle progression and host cell physiology after infection of human dendritic cells with modified vaccinia virus Ankara and vaccinia virus.
J Virol. 80(17) (2006) 8469-81

[25] **Chanda, P.K., Natuk, R.J., Dheer, S.K., Lubeck, M.D., Bhat, B.M., Mason, B.B., Greenberg, L., Mizutani, S., Davis, A.R., Hung, P.P.**
Helper independent recombinant adenovirus vectors: expression of HIV env or HBV surface antigen.
Int Rev Immunol. 7(1) (1990) 67-77 Review

[26] **Chen, W., Masterman, K.A., Basta, S., Haeryfar, S.M., Dimopoulos, N., Knowles, B., Bennink, J.R., Yewdell, J.W.**
Cross-priming of CD8+ T cells by viral and tumor antigens is a robust phenomenon.
Eur J Immunol. 34(1) (2004) 194-9

[27] **Coffino, P.**
Regulation of cellular polyamines by antizyme.
Nat. Rev. Mol. Cell Biol. 2 (2001) 188-194

[28] **Cosma, A., Nagaraj, R., Buhler, S., Hinkula, J., Busch, D.H., Sutter, G., Goebel, F.D., Erfle, V.**
Therapeutic vaccination with MVA-HIV-1 nef elicits Nef-specific T-helper cell responses in chronically HIV-1 infected individuals.
Vaccine. 22(1) (2003) 21-9.

[29] **Crews, C.M.**
Feeding the machine: mechanisms of proteasome-catalyzed degradation of ubiquitinated proteins.
Curr. Opin. Chem. Biol. 7 (2003) 534-539

[30] **Dermime, S., Armstrong, A., Hawkins, R.E., Stern, P.L.**
Cancer vaccines and immunotherapy.
Br Med Bull. 62 (2002) 149-62 Review

[31] **Dick, L.R., Aldrich, C., Jameson, S.C., Moomaw, C.R., Pramanik, B.C., Doyle, C.K., DeMartino, G.N., Bevan, M.J., Forman, J.M., Slaughter, C.A.**
Proteolytic processing of ovalbumin and beta-galactosidase by the proteasome to a yield antigenic peptides.
J Immunol. 152(8) (1994) 3884-94

[32] **Di Nicola, M., Carlo-Stella, C., Mortarini, R., Baldassari, P., Guidetti, A., Gallino, G.F., Del Vecchio, M., Ravagnani, F., Magni, M., Chaplin, P., Cascinelli, N., Parmiani, G., Gianni, A.M., Anichini, A.**
Boosting T cell-mediated immunity to tyrosinase by vaccinia virus-transduced, CD34(+)-derived dendritic cell vaccination: a phase I trial in metastatic melanoma.
Clin Cancer Res. 10(16) (2004) 5381-90

[33] **Dobbelstein, M., Shenk, T.**
Protection against apoptosis by the vaccinia virus SPI-2 (B13R) gene product.
J Virol. 70(9) (1996) 6479-85

[34] **Drexler, I.,Heller, K., Wahren, B., Erfle, V., Sutter, G.**
Highly attenuated modified vaccinia virus Ankara replicates in baby hamster kidney cells, a potential host for virus propagation, but not in various human transformed and primary cells.
J Gen Virol. 79 (1998) 347-52

[35] **Drexler, I., Staib, C., Kastenmuller, W., Stevanovic, S., Schmidt, B., Lemonnier, F.A., Rammensee, H.G., Busch, D.H., Bernhard, H., Erfle, V., Sutter, G.**
*Identification of vaccinia virus epitope-specific HLA-A*0201-restricted T cells and comparative analysis of smallpox vaccines.*
Proc Natl Acad Sci U S A. 100(1) (2003) 217-22

[36] **Drexler, I., Staib, C., Sutter, G.**
Modified vaccinia virus Ankara as antigen delivery system: how can we best use its potential?
Curr Opin Biotechnol. 15(6) (2004) 506-12 Review

[37] **Dunachie, S.J., Walther, M., Vuola, J.M., Webster, D.P., Keating, S.M., Berthoud, T., Andrews, L., Bejon, P., Poulton, I., Butcher, G., Watkins, K., Sinden, R.E., Leach, A., Moris, P., Tornieporth, N., Schneider, J., Dubovsky, F., Tierney, E., Williams, J., Heppner, D.G. Jr, Gilbert, S.C., Cohen, J., Hill, A.V.**
A clinical trial of prime-boost immunisation with the candidate malaria vaccines RTS,S/AS02A and MVA-CS.
Vaccine. 24(15) (2006) 2850-9

[38] **Durbin, A.P., Wyatt, L.S., Siew, J, Moss, B., Murphy, B.R.**
The immunogenicity and efficacy of intranasally or parenterally administered replication-deficient vaccinia-parainfluenza virus type 3 recombinants in rhesus monkeys.
Vaccine. 16(13) (1998) 1324-30

[39] **Earl, P.L., Wyatt, L.S., Montefiori, D.C., Bilska, M., Woodward, R., Markham, P.D., Malley, J.D., Vogel, T.U., Allen, T.M., Watkins, D.I., Miller, N., Moss, B.**
Comparison of vaccine strategies using recombinant env-gag-pol MVA with or without an oligomeric Env protein boost in the SHIV rhesus macaque model.
Virology. 294(2) (2002) 270-81

[40] **Evans, D.T., Chen, L.M., Gillis, J., Lin, K.C., Harty, B., Mazzara, G.P., Donis, R.O., Mansfield, K.G., Lifson, J.D., Desrosiers, R.C., Galan, J.E., Johnson, R.P.**
Mucosal priming of simian immunodeficiency virus-specific cytotoxic T-lymphocyte responses in rhesus macaques by the Salmonella type III secretion antigen delivery system.
J Virol. 77(4) (2003) 2400-9

[41] **Falk, K., Rötzschke, O., Faath, S., Goth, S., Graef, I., Shastri, N., Rammensee, H.G.**
Both human and mouse cells expressing H-2Kb and ovalbumin process the same peptide, SIINFEKL.
Cell Immunol. 150(2) (1993) 447-52.

[42] **Fenner, F., Henderson, D.A., Arita, I., Jezek, Z., Ladnyi, I.D.**
Smallpox and its eradication.
WHO Geneva, (1988) 539- 592

[43] **Gallimore, A., Cranage, M., Cook, N., Almond, N., Bootman, J., Rud, E., Silvera, P., Dennis, M., Corcoran, T., Stott, J. et al.**
Early suppression of SIV replication by CD8+ nef-specific cytotoxic T cells in vaccinated macaques.
Nat Med. 1(11) (1995) 1167-73

[44] **Gasteiger, G., Kastenmuller, W., Ljapoci, R., Sutter, G., Drexler, I.**
Exclusive cross-priming of cytotoxic T-cells dictates antigen requisites for MVA vector vaccines.
J Virol. 81 (2007) 11925-36

[45] **Geier, E., Pfeifer, G., Wilm, M., Lucchiari-Hartz, M., Baumeister, W., Eichmann, K., Niedermann, G.**
A giant protease with potential to substitute for some functions of the proteasome.
Science. 283(5404) (1999) 978-81

[46] **Gherardi, M.M., Najera, J.L., Perez-Jimenez, E., Guerra, S., Garcia-Sastre, A., Esteban, M.**
Prime-boost immunization schedules based on influenza virus and vaccinia virus vectors potentiate cellular immune responses against human immunodeficiency virus Env protein systemically and in the genitorectal draining lymph nodes.
J Virol. 77(12) (2003) 7048-57

[47] **Gil-Torregrosa, B.C., Raul Castano, A., Del Val, M.**
Major histocompatibility complex class I viral antigen processing in the secretory pathway defined by the trans-Golgi network protease furin.
J Exp Med. 188(6) (1998) 1105-16

[48] **Girard, M.P., Osmanov, S.K., Kieny, M.P.**
A review of vaccine research and development: the human immunodeficiency virus (HIV).
Vaccine. 24(19) (2006) 4062-81

[49] **Glas, R., Bogyo, M., McMaster, J.S., Gaczynska, M., Ploegh, H.L.**
A proteolytic system that compensates for loss of proteasome function.
Nature. 392(6676) (1998) 618-22

[50] **Goedert, J.J.**
The epidemiology of acquired immunodeficiency syndrome malignancies.
Semin Oncol. 27(4) (2000) 390-401 Review

[51] **Goepfert, P.A., Elizaga, M.L., Sato, A., Qin, L., Cardinali, M., Hay, C.M., Hural, J., DeRosa, S.C., DeFawe, O.D., Tomaras, G.D., Montefiori, D.C., Xu, Y., Lai, L., Kalams, S.A., Baden, L.R., Frey, S.E., Blattner, W.A., Wyatt, L.S., Moss, B., Robinson, H.L.**
Phase 1 safety and immunogenicity testing of DNA and recombinant modified vaccinia Ankara vaccines expressing HIV-1 virus-like particles.
J Infect Dis. 203(5) (2011) 610-9

[52] **Goldberg, A.L., Cascio. P., Saric, T., Rock, K.L.**
The importance of the proteasome and subsequent proteolytic steps in the generation of antigenic peptides.
Mol. Immunology 39 (2002)147-164

[53] **Gonciarz-Swiatek, M., Rechsteiner, M.**
Proteasomes and antigen presentation: evidence that a KEKE motif does not promote presentation of the class I epitope SIINFEKL.
Mol. Immunology 43(12) (2006) 1993-2001

[54] **Grant, E.P., Michalek, M.T., Goldberg, A.L., Rock, K.L.**
Rate of Antigen Degradation by the Ubiquitin-Proteasome Pathway Influences MHC I Presentation.
J Immunol. (1995) 3750-8

[55] **Hanke, T., Barnfield, C., Wee, E.G., Agren, L., Samuel, R.V., Larke, N., Liljestrom, P.**
Construction and immunogenicity in a prime-boost regimen of a Semliki Forest virus-vectored experimental HIV clade A vaccine.
J Gen Virol. 84(Pt 2) (2003) 361-8.

[56] **Harpur, A.G., Zimiecki, A., Wilks, A.F., Falk, K., Rotzschke, O., Rammensee, H.G.**
A prominent natural H-2 Kd ligand is derived from protein tyrosine kinase JAK1.
Immunol Lett. 35(3) (1993) 235-7

[57] **Harrop, R., Connolly, N., Redchenko, I., Valle, J., Saunders, M., Ryan, M.G., Myers, K.A., Drury, N., Kingsman, S.M., Hawkins, R.E., Carroll, M.W.**
Vaccination of colorectal cancer patients with modified vaccinia Ankara delivering the tumor antigen 5T4 (TroVax) induces immune responses which correlate with disease control: a phase I/II trial.
Clin Cancer Res. 12 (2006) 3416-24

[58] **Heessen, S., Dantuma, N.P., Tessarz, P., Jellne, M., Masucci, M.G.**
Inhibition of ubiquitin/proteasome-dependent proteolysis in Saccharomyces cerevisiae by a Gly-Ala repeat.
FEBS Lett. 555(2) (2003) 397-404

[59] **Heit, A., Huster, K.M., Schmitz, F., Schiemann, M., Busch, D.H., Wagner, H.**
CpG-DNA aided cross-priming by cross-presenting B cells.
J Immunol. 172(3) (2004) 1501-7

[60] **Hershko, A., Chiechanover, A.**
THE UBIQUITIN SYSTEM
Annu. Rev. Biochem. 67 (1998) 425-79

[61] **Hickman-Miller, H.D., Yewdell, J.W.**
Youth has its privileges: maturation inhibits DC cross-priming.
Nat. Immunol. 7 (2006) 125-126

[62] **Hirsch, V.M., Fuerst, T.R., Sutter, G., Carroll, M.W., Yang, L.C., Goldstein S., Piatak, M. Jr, Elkins, W.R., Alvord, W.G., Montefiori, D.C., Moss, B., Lifson, J.D.**
Patterns of viral replication correlate with outcome in simian immunodeficiency virus (SIV)-infected macaques: effect of prior immunization with a trivalent SIV vaccine in modified vaccinia virus Ankara.
J Virol. 70(6) (1996) 3741-52

[63] **Hodge, J.W., Poole, D.J., Aarts, W.M., Gomez Yafal, A., Gritz, L., Schlom, J.**
Modified vaccinia virus ankara recombinants are as potent as vaccinia recombinants in diversified prime and boost vaccine regimens to elicit therapeutic antitumor responses.
Cancer Res. 63(22) (2003) 7942-9

[64] **Horton, H., Vogel, T.U., Carter, D.K., Vielhuber, K., Fuller, D.H., Shipley, T., Fuller, J.T., Kunstman, K.J., Sutter, G., Montefiori, D.C., Erfle, V., Desrosiers, R.C., Wilson, N., Picker, L.J., Wolinsky, S.M., Wang, C., Allison, D.B., Watkins, D.I.**
Immunization of rhesus macaques with a DNA prime/modified vaccinia virus Ankara boost regimen induces broad simian immunodeficiency virus (SIV)-specific T-cell responses and reduces initial viral replication but does not prevent disease progression following challenge with pathogenic SIVmac239.
J Virol. 76(14) (2002) 7187-202

[65] **Hoyt, M.A., Coffino, P.**
Ubiquitin-free routes into the proteasome.
Cell Mol Life Sci. 61(13) (2004) 1596-600 Review

[66] **Humrich, J.Y., Thumann, P., Greiner, S., Humrich, J.H., Averbeck, M., Schwank, C., Kämpgen, E., Schuler, G., Jenne, L.**
Vaccinia virus impairs directional migration and chemokine receptor switch of human dendritic cells.
Eur J Immunol. 37(4) (2007) 954-65

[67] **Hunt, L.T., Dayhoff, M.O.**
A surprising new protein superfamily containing Ovalbumin, Antithrombin-III, and Alpha1-proteinase inhibitor.
Biochem Biophys Res Commun. 95(2) (1980) 864-71

[68] **Huntington, J.A.,Stein, P.E.**
Structure and properties of Ovalbumin.
J Chromatogr B Biomed Sci Appl. 756(1-2) (2001) 189-98.

[69] **Janeway, C.A.Jr., Travers, P., Walport, M., Shlomchik, M.J.**
Immunobiology, the immune system in health and disease.
Garland Science Publishing, New York (USA)- Abingdon (UK), 2005, 6th edition, 1-823

[70] **Johnson, E.S., Ma, P.C., Ota, I.M., Varshavsky, A.**
A proteolytic pathway that recognizes ubiquitin as a degradation signal.
J Biol Chem. 270(29) (1995) 17442-56

[71] **Kahana, C., Asher, G., Shaul, Y.**
Mechanisms of protein degradation: an odyssey with ODC.
Cell Cycle. 4(11) (2005) 1461-4 Review

[72] **Kastenmuller, W., Drexler, I., Ludwig, H., Erfle, V., Peschel, C., Bernhard, H., Sutter, G.**
Infection of human dendritic cells with recombinant vaccinia virus MVA reveals general persistence of viral early transcription but distinct maturation-dependent cytopathogenicity.
Virology. 350(2) (2006) 276-88

[73] **Kastenmuller, W., Gasteiger, G., Gronau, J.H., Baier, R., Ljapoci, R., Busch, D.H., Drexler, I.**
Cross-competition of CD8+ T cells shapes the immunodominance hierarchy during boost vaccination.
J Exp Med. 204(9) (2007) 2187-98

[74] **Kaufman, H.L., Cohen, S., Cheung, K., DeRaffele, G., Mitcham, J., Moroziewicz, D., Schlom, J., Hesdorffer, C.**
Local delivery of vaccinia virus expressing multiple costimulatory molecules for the treatment of established tumors.
Hum Gene Ther. 17(2) (2006) 239-44

[75] **Kisselev, A.F., Akopian, T.N., Woo, K.M., Goldberg, A.L.**
The Sizes of Peptides Generated from Protein by Mammalian 26 and 20 S Proteasomes.
J Biol Chem. 273(4) (1998) 1982-9

[76] **Kloetzel, P.M.**
Anitgen processing by the proteasome.
Nat Rev Mol Cell Biol. 2(3) (2001) 179-87

[77] **Kloetzel, P.M.**
The proteasome and MHC class I antigen processing.
Biochim Biophys Acta. 1695(1-3) (2004) 225-33

[78] **Koup, R.A., Safrit, J.T., Cao, Y., Andrews, C.A., McLeod, G., Borkowsky, W., Farthing, C., Ho, D.D.**
Temporal association of cellular immune responses with the initial control of viremia in primary human immunodeficiency virus type 1 syndrome.
J Virol. 68(7) (1994) 4650-5

[79] **Kurowski, R., Renz-Polster, H.**
Grundbegriffe und -probleme
In: Basislehrbuch Innere Medizin
Renz-Polster, H., Krautzig, S., Braun, J. Elsevier GmbH, Urban & Fischer Verlag
München, 2004, 3.Auflage, 1058- 1061

[80] **Li, X., Coffino, P.**
Degradation of ornithine decarboxylase: exposure of the C-terminal target by a polyamine-inducible inhibitory protein.
Mol Cell Biol. 13(4) (1993) 2377-83

[81] **Li, X., Zhao, X., Fang, Y., Jiang, X., Duong, T., Fan, C., Huang, C.C., Kain, S.R.**
Generation of destabilized green fluorescent protein as a transcription reporter.
J Biol Chem. 273(52) (1998) 34970-5

[82] **Lowe, D.B., Shearer, M.H., Kennedy, R.C.**
DNA vaccines: successes and limitations in cancer and infectious disease.
J Cell Biochem. 98(2) (2006) 235-42 Review

[83] **Lu, X., Xu, L., Meissner, G.**
Activation of the skeletal muscle calcium release channel by a cytoplasmic loop of the dihydropyridine receptor.
J. Biol Chem. 269(9)(1994) 6511-6

[84] **Luckey, C.J., King, G.M., Marto. J.A., Venketeswaran, S., Maier, B.F., Crotzer, V.L., Colella, T.A., Shabanowitz, J., Hunt, D.F., Engelhard, V.H.**
Proteasomes can either generate or destroy MHC class I epitopes: evidence for nonproteasomal epitope generation in the cytosol.
J Immunol. 161(1) (1998) 112-21

[85] **Marshall, J.L., Gulley, J.L., Arlen, P.M., Beetham, P.K., Tsang, K.Y., Slack, R., Hodge, J.W., Doren, S., Grosenbach, D.W., Hwang, J., Fox, E., Odogwu, L., Park, S., Panicali, D., Schlom, J.**
Phase I study of sequential vaccinations with fowlpox-CEA(6D)-TRICOM alone and sequentially with vaccinia-CEA(6D)-TRICOM, with and without granulocyte-macrophage colony-stimulating factor, in patients with carcinoembryonic antigen-expressing carcinomas.
J Clin Oncol. 23(4) (2005) 720-31

[86] **Matsuzawa, S., Cuddy, M., Fukushima, T., Reed, J.C.**
Method for targeting protein destruction by using a ubiquitin-independent, proteasome-mediated degradation pathway.
Proc Natl Acad Sci U S A. 102(42) (2005) 14982-7

[87] **Mayordomo, J.I., Zorina, T., Storkus, W.J., Zitvogel, L., Celluzzi, C., Falo, L.D., Melief, C.J., Ildstad, S.T., Kast, W.M., Deleo, A.B.**
Bone marrow-derived dendritic cells pulsed with synthetic tumour peptides elicit protective and therapeutic antitumour immunity.
Nat Med. 1(12) (1995) 1297-302

[88] **Mayr, A., Bachmann, P. A.**
Zellkulturen. Virologische Arbeitsmethoden.
G.Wittmann.Stuttgart, Gustav Fischer Verlag. (1974) Band 1

[89] **Mayr, A., Hochstein-Mintzel, V., Stickl, H.**
Abstammung, Eigenschaften und Verwendung des attenuierten Vaccinia-Stammes MVA.
Infection 3 (1975) 6-14

[90] **McDermott, M.R., Graham, F.L., Hanke, T., Johnson, D.C.**
Protection of mice against lethal challenge with herpes simplex virus by vaccination with an adenovirus vector expressing HSV glycoprotein B.
Virology 169(1) (1989) 244-7

[91] **McConkey, S.J., Reece, W.H., Moorthy, V.S., Webster, D., Dunachie, S., Butcher, G., Vuola, J.M., Blanchard, T.J., Gothard, P., Watkins, K., Hannan, C.M., Everaere, S., Brown, K., Kester, K.E., Cummings, J., Williams, J., Heppner, D.G., Pathan, A., Flanagan, K., Arulanantham, N., Roberts, M.T., Roy, M., Smith, G.L., Schneider, J., Peto, T., Sinden, R.E., Gilbert, S.C., Hill, A.V.**
Enhanced T-cell immunogenicity of plasmid DNA vaccines boosted by recombinant modified vaccinia virus Ankara in humans.
Nat Med. 9(6) 2003 729-35

[92] **McReynolds, L., O'Malley,B.W.,Nisbet, A.D., Fothergill, J.E., Givol, D., Fields, S., Robertson, M., Brownlee, G.G.**
Sequence of chicken ovalbumin mRNA.
Nature 273 (1978) 723-8

[93] **Melief, C.J.**
Tumor eradication by adoptive transfer of cytotoxic T lymphocytes.
Adv Cancer Res. 58 (1992) 143-75 Review

[94] **Meyer, R.G., Britten, C.M., Siepmann, U., Petzold, B., Sagban, T.A., Lehr, H.A., Weigle, B., Schmitz, M., Mateo, L., Schmidt, B., Bernhard, H., Jakob, T., Hein, R., Schuler, G., Schuler-Thurner, B., Wagner, S.N., Drexler, I., Sutter, G., Arndtz, N., Chaplin, P., Metz, J., Enk, A., Huber, C., Wolfel, T.**
A phase I vaccination study with tyrosinase in patients with stage II melanoma using recombinant modified vaccinia virus Ankara (MVA-hTyr).
Cancer Immunol Immunother. 54(5) (2005) 453-67

[95] **Miller, J., Gordon, C.**
The regulation of proteasome degradation by multi-ubiquitin chain binding proteins.
FEBS Lett. 579 (2005) 3224-3230

[96] **Milligan, G.N., Morrison, L.A., Gorka, J., Braciale, V.L., Braciale, T.J.**
The recognition of a viral antigenic moiety by class I MHC-restricted cytolytic T lymphocytes is limited by the availability of the endogenously processed antigen.
J Immunol. 145(10) (1990) 3188-93

[97] **Moss, B.**
Genetically engineered poxviruses for recombinant gene expression, vaccination, and safety.
Proc. Natl. Acad. Sci. U. S. A (1996) 11341-11348

[98] **Moss, B.**
Poxviridae: The Viruses and Their Replication
In: Fields Virology
Fields, B.N., Knipe, D.M., Howley, P.M. , Lippincott- Raven Publishers,
Philidelphia, 1996, 3.Auflage, 2637-2671

[99] **Moutaftsi, M., Peters, B., Pasquetto, V., Tscharke, D.C., Sidney, J., Bui, H.H., Grey, H., Sette, A.**
A consensus epitope prediction approach identifies the breadth of murine T(CD8+)-cell responses to vaccinia virus.
Nat Biotechnol. 24(7) (2006) 817-9

[100] **Nisbet, A.D., Saundry, R.H., Moir, A.J., Fothergill, L.A., Fothergill, J.E.**
The complete amino-acid sequence of hen ovalbumin.
Eur J Biochem. 115(2) (1981) 335-45

[101] **Noble, M., Lewis, S.A., Cowan, N.J.**
The microtubule binding domain of microtubule-associated protein MAP1B contains a repeated sequence motif unrelated to that of MAP2 and tau.
J Cell Biol. 109(6 Pt 2) (1989) 3367-76

[102] **Norbury, C.C., Basta, S., Donohue, K.B., Tscharke, D.C., Princiotta, M.F., Berglund, P., Gibbs, J., Bennink, J.R., Yewdell, J.W.**
CD8+ T cell cross-priming via transfer of proteasome substrates.
Science. 304(5675) (2004) 1318-21

[103] **Norbury, C.C., Malide, D., Gibbs, J.S., Bennink, J.R., Yewdell, J.W.**
Visualizing priming of virus-specific CD8+ T cells by infected dendritic cells in vivo.
Nat Immunol. 3(3) (2002) 265-71

[104] **Overwijk, W.W., Surman, D.R., Tsung, K., Restifo, N.P.**
Identification of a Kb-restricted CTL epitope of beta-galactosidase: potential use in development of immunization protocols for "self" antigens.
Methods. Jun;12(2) (1997) 117-23.

[105] **Pantuck, A.J., van Ophoven, A., Gitlitz, B.J., Tso, C.L., Acres, B., Squiban, P., Ross, M.E., Belldegrun, A.S., Figlin, R.A.**
Phase I trial of antigen-specific gene therapy using a recombinant vaccinia virus encoding MUC-1 and IL-2 in MUC-1-positive patients with advanced prostate cancer.
J Immunother. 27(3) (2004) 240-53

[106] **Parmiani, G., Castelli, C., Dalerba, P., Mortarini, R., Rivoltini, L., Marincola, F.M., Anichini, A.**
Cancer immunotherapy with peptide-based vaccines: what have we achieved? Where are we going?
J Natl Cancer Inst. 94(11) (2002) 805-18 Review

[107] **Pegg, A.E.**
Regulation of ornithine decarboxylase.
J Biol Chem. 281(21) (2006) 14529-32 Review

[108] **Perez-Jimenez, E., Kochan, G., Gherardi, M.M., Esteban, M.**
MVA-LACK as a safe and efficient vector for vaccination against leishmaniasis.
Microbes Infect. 8(3) (2006) 810-22

[109] **Plotkin, S.A.**
Vaccines: past, present and future.
Nat Med. 11(4 Suppl) (2005) 5-11

[110] **Porgador, A., Yewdell, J.W., Deng, Y., Bennink, J.R., Germain, R.N.**
Localization, quantitation, and in situ detection of specific peptide-MHC class I complexes using a monoclonal antibody.
Immunity. 6(6) (1997) 715-26

[111] **Potter, N.S., Harding, C.V.**
Neutrophils process exogenous bacteria via an alternate class I MHC processing pathway for presentation of peptides to T lymphocytes.
J Immunol. 167(5) (2001) 2538-46

[112] **Princiotta, M.F., Finzi, D., Qian, S.B., Gibbs, J., Schuchmann, S., Buttgereit, F., Bennink, J.R., Yewdell, J.W.**
Quantitating protein synthesis, degradation, and endogenous antigen processing.
Immunity. 18(3) (2003) 343-54

[113] **Ramirez, M.C., Sigal, L.J.**
Macrophages and dendritic cells use the cytosolic pathway to rapidly cross-present antigen from live, vaccinia-infected cells.
J Immunol. 169(12) (2002) 6733-42

[114] **Ramsburg, E., Rose, N.F., Marx, P.A., Mefford, M., Nixon, D.F., Moretto, W.J., Montefiori, D., Earl, P., Moss, B., Rose, J.K.**
Highly effective control of an AIDS virus challenge in macaques by using vesicular stomatitis virus and modified vaccinia virus Ankara vaccine vectors in a single-boost protocol.
J Virol. 78(8) (2004) 3930-40

[115] **Realini, C., Rogers, S.W., Rechsteiner, M.**
KEKE motifs. Proposed roles in protein-protein association and presentation of peptides by MHC Class I receptors.
FEBS Letters 348 (1994) 109-113

[116] **Robinson, H.L., Amara, R.R.**
T cell vaccines for microbial infections.
Nat Med. 11(4Suppl) (2005) 25-32 Review

[117] **Rocha, C.D., Caetano, B.C., Machado, A.V., Bruna-Romero, O.**
Recombinant viruses as tools to induce protective cellular immunity against infectious diseases.
Int Microbiol. 7(2) (2004) 83-94

[118] **Rochlitz, C., Figlin, R., Squiban, P., Salzberg, M., Pless, M., Herrmann, R., Tartour, E.,Zhao, Y., Bizouarne, N., Baudin, M., Acres, B.**
Phase I immunotherapy with a modified vaccinia virus (MVA) expressing human MUC1 as antigen-specific immunotherapy in patients with MUC1-positive advanced cancer.
J Gene Med. 5(8) (2003) 690-9

[119] **Rodrigues, E.G., Zavala, F., Eichinger, D., Wilson, J.M., Tsuji, M.**
Single immunizing dose of recombinant adenovirus efficiently induces CD8+ T cell-mediated protective immunity against malaria.
J Immunol. 158(3) (1997) 1268-74

[120] **Rosenberg, S.A.**
A new era of cancer immunotherapy: converting theory to performance.
CA Cancer J Clin. 49(2) (1999) 70-3, 65

[121] **Rotzschke, O., Falk, K., Stevanovic, S., Jung, G., Walden, P., Rammensee, H.G.**
Exact prediction of a natural T cell epitope.
Eur J Immunol. 21(11) (1991) 2891-4

[122] **Saito, Z., Martin, W.G.**
Ovalbumin and other water-soluble proteins in avian yolk during embryogenesis.
Can J Biochem. 44(3) (1966) 293-301

[123] **Schepers, K., Arens, R., Schumacher, T.N.**
Dissection of cytotoxic and helper T cell responses.
Cell Mol Life Sci. 62(23) (2005) 2695-710

[124] **Schmitz, J.E., Kuroda, M.J., Santra, S., Sasseville, V.G., Simon, M.A., Lifton, M.A., Racz, P., Tenner-Racz, K., Dalesandro, M., Scallon, B.J., Ghrayeb, J., Forman, M.A., Montefiori, D.C., Rieber, E.P., Letvin, N.L., Reimann, K.A.**
Control of viremia in simian immunodeficiency virus infection by CD8+ lymphocytes.
Science 283(5403) (1999) 857-60

[125] **Schneider, J., Gilbert, S.C., Blanchard, T.J., Hanke, T., Robson, K.J., Hannan, C.M., Becker, M., Sinden, R., Smith, G.L., Hill, A.V.**
Enhanced immunogenicity for CD8+ T cell induction and complete protective efficacy of malaria DNA vaccination by boosting with modified vaccinia virus Ankara.
Nat Med. 4(4) (1998) 397-402

[126] **Schulz, M., Zinkernagel, R.M., Hengartner, H.**
Peptide-induced antiviral protection by cytotoxic T cells.
Proc Natl Acad Sci U S A. 88(3) (1991) 991-3

[127] **Schwarz, K., de Giuli, R., Schmidtke, G., Kostka, S., van den Broek, M., Kim, K.B., Crews, C.M., Kraft, R., Groettrup, M.**
The selective proteasome inhibitors lactacystin and epoxomicin can be used to either up- or down-regulate antigen presentation at nontoxic doses.
J Immunol. 164(12) (2000) 6147-57

[128] **Serna, A., Ramirez, M.C., Soukhanova, A., Sigal, L.J.**
Cutting edge: efficient MHC class I cross-presentation during early vaccinia infection requires the transfer of proteasomal intermediates between antigen donor and presenting cells.
J Immunol. 171(11) (2003) 5668-72

[129] **Shankaran, V., Ikeda, H., Bruce, A.T., White, J.M., Swanson, P.E., Old, L.J., Schreiber, R.D.**
IFNgamma and lymphocytes prevent primary tumour development and shape tumour immunogenicity.
Nature. 410(6832) (2001) 1107-11

[130] **Sheares, B.T., Robbins, P.W.**
Free in PMC Glycosylation of ovalbumin in a heterologous cell: analysis of oligosaccharide chains of the cloned glycoprotein in mouse L cells.
Proc Natl Acad Sci U S A. 83(7) (1986) 1993-7

[131] **Shen, L., Rock, K.L.**
Cellular protein is the source of cross-priming antigen in vivo.
Proc Natl Acad Sci U S A. 101(9) (2004) 3035-40

[132] **Shen, L., Rock, K.L.**
Priming of T cells by exogenous antigen cross-presented on MHC class I molecules.
Curr Opin Immunol. 18(1) (2006) 85-91 Review

[133] **Shen, X., Wong, S.B., Buck, C.B., Zhang, J., Siliciano, R.F.**
Direct priming and cross-priming contribute differentially to the induction of CD8+ CTL following exposure to vaccinia virus via different routes.
J Immunol. 169(8) (2002) 4222-9

[134] **Sigal, L.J., Crotty, S., Andino, R., Rock, K.L.**
Cytotoxic T-cell immunity to virus-infected non-haematopoietic cells requires presentation of exogenous antigen.
Nature. 398(6722) (1999) 77-80

[135] **Silva, C.L., Portaro, F.C., Bonato, V.L., de Camargo, A.C., Ferro, E.S.**
Thimet oligopeptidase (EC 3.4.24.15), a novel protein on the route of MHC class I antigen presentation.
Biochem Biophys Res Commun. 255(3) (1999) 591-5

[136] **Smith, C.L., Mirza, F., Pasquetto, V., Tscharke, D.C., Palmowski, M.J., Dunbar, P.R., Sette, A., Harris, A.L., Cerundolo, V.**
Immunodominance of poxviral-specific CTL in a human trial of recombinant-modified vaccinia Ankara.
J Immunol. 2005 175(12) 8431-7

[137] **Staib, C., Drexler, I., Sutter, G.**
Construction and Isolation of Recombinant MVA.
Methods in Molecular Biology, Vaccinia Virus and Poxvirology:Methods and Protocols, 269 (2004) 77-99

[138] **Staib, C., Drexler, I., Ohlmann, M., Wintersperger, S., Erfle, V., Sutter, G.**
Transient Host Range Selection for Genetic Engineering of Modified Vaccinia Virus Ankara.
Biotechniques 28 (2000) 1137-1148

[139] **Subklewe, M., Paludan, C., Tsang, M.L., Mahnke, K., Steinman, R.M., Münz, C.**
Dendritic cells cross-present latency gene products from Epstein-Barr virus-transformed B cells and expand tumor-reactive CD8(+) killer T cells.
J Exp Med. 193(3) (2001) 405-11

[140] **Sutter, G., Moss, B.**
Nonreplicating vaccinia vector efficiently expresses recombinant genes.
Proc Natl Acad Sci U S A. 89(22) (1992) 10847-51

[141] **Sutter, G., Wyatt, L.S., Foley, P.L., Bennink J.R., Moss, B.**
A recombinant vector derived from the host range-restricted and highly attenuated MVA strain of vaccinia virus stimulates protective immunity in mice to influenza virus.
Vaccine. 12(11) (1994) 1032-40

[142] **Tabe, L., Krieg, P., Strachan, R., Jackson, D., Wallis, E., Colman, A.**
Segregation of mutant ovalbumins and ovalbumin-globin fusion proteins in Xenopus oocytes. Identification of an ovalbumin signal sequence.
J Mol Biol. 180(3) (1984) 645-66

[143] **Taborsky, G.**
Phosphoproteins
Adv Protein Chem. 28 (1974) 1-210

[144] **Tobery, T.W., Siliciano, R.F.**
Targeting of HIV-1 antigens for rapid intracellular degradation enhances cytotoxic T lymphocyte (CTL) recognition and the induction of de novo CTL responses in vivo after immunization.
J Exp Med. 185(5) (1997) 909-20

[145] **Tobian, A.A., Harding, C.V., Canaday, D.H.**
Mycobacterium tuberculosis heat shock fusion protein enhances class I MHC cross-processing and -presentation by B lymphocytes.
J Immunol. 174(9) (2005) 5209-14

[146] **Tomkinson, B.**
Tripeptidyl peptidases: enzymes that count.
Trends Biochem Sci. 24(9) (1999) 355-9 Review

[147] **Townsend, A., Bastin, J., Gould, K., Brownlee, G., Andrew, M., Coupar, B., Boyle, D., Chan, S., Smith, G.**
Defective presentation to class I-restricted cytotoxic T lymphocytes in vaccinia-infected cells is overcome by enhanced degradation of antigen.
J Exp Med. 168(4) (1988) 1211-24

[148] **Tscharke, D.C., Karupiah, G., Zhou, J., Palmore, T., Irvine, K.R., Haeryfar, S.M., Williams, S., Sidney, J., Sette, A., Bennink, J.R., Yewdell, J.W.**
Identification of poxvirus CD8+ T cell determinants to enable rational design and characterization of smallpox vaccines.
J Exp Med. 201(1) (2005) 95-104

[149] **Tvinnereim, A.R., Hamilton, S.E., Harty, J.T.**
Neutrophil involvement in cross-priming CD8+ T cell responses to bacterial antigens.
J Immunol. 173(3) (2004) 1994-2002

[150] **Varshavsky, A.**
Regulated protein degradation.
Trends Biochem Sci. 30(6) (2005) 283-6 Review

[151] **Varshavsky, A.**
The N-end rule.
Cell. 69 (1992) 725-735

[152] **Vinitsky, A., Anton, L.C., Snyder, H.L., Orlowski, M., Bennink, J.R., Yewdell, J.W.**
The generation of MHC class I-associated peptides is only partially inhibited by proteasome inhibitors: involvement of nonproteasomal cytosolic proteases in antigen processing?
J Immunol. 159(2) (1997) 554-64

[153] **Wang, E.W., Kessler, B.M., Borodovsky, A., Cravatt, B.F., Bogyo, M., Ploegh, H.L., Glas, R.**
Integration of the ubiquitin-proteasome pathway with a cytosolic oligopeptidase activity.
Proc Natl Acad Sci U S A. 97(18) (2000) 9990-5

[154] **Wherry, E.J., Ahmed, R.**
Memory CD8 T-cell differentiation during viral infection.
J Virol. 78(11) (2004) 5535-45 Review

[155] **Wolkers, M.C., Brouwenstijn, N., Bakker, A.H., Toebes, M., Schumacher, T.N.**
Antigen bias in T cell cross-priming.
Science. 304 (2004) 1314-7

[156] **Woo, S.L., Beattie, W.G., Catterall, J.F., Dugaiczyk, A., Staden, R., Brownlee, G.G., O'Malley, B.W.**
Complete nucleotide sequence of the chicken chromosomal ovalbumin gene and its biological significance.
Biochemistry. 20(22) (1981) 6437-46

[157] **World Health Organisation, WHO**
http://www.who.int/malaria/world_malaria_report_2010/malaria2010_summary_keypoints_en.pdf

[158] **World Health Organisation, WHO**
http://www.who.int/mediacentre/factsheets/fs288/en/index.html

[159] **World Health Organisation, WHO**
http://www.who.int/vaccine_research/diseases/hiv/en/index.html

[160] **World Health Organisation, WHO**
http://www.who.int/whosis/whostat/EN_WHS10_Part2.pdf

[161] **World Health Organisation, WHO**
http://www.who.int/whr/2004/annex/topic/en/annex_2_en.pdf

[162] **Yang, Z.Y., Wyatt, L.S., Kong, W.P., Moodie, Z., Moss, B., Nabel, G.J.**
Overcoming immunity to a viral vaccine by DNA priming before vector boosting.
J Virol. 77(1) (2003) 799-803

[163] **Yewdell, J.W.**
The seven dirty little secrets of major histocompatibility complex class I antigen processing.
Immunol Rev. 207 (2005) 8-18 Review

[164] **Yewdell, J.W., Anton, L.C., Bennink, J.R.**
Defective ribosomal products (DRiPs): a major source of antigenic peptides for MHC class I molecules?
J Immunol. 157(5) (1996) 1823-6 Review

[165] **Yewdell, J.W., Bennink, J.R.**
Immunodominance in major histocompatibility complex class I-restricted T lymphocyte responses.
Annu Rev Immunol. 17 (1999) 51-88 Review

[166] **Yewdell, J.W., Hill, A.B.**
Viral interference with antigen presentation.
Nat Immunol. 3(11) (2002) 1019-25 Review

[167] **Zhang, M., MacDonald, A.I., Hoyt, M.A., Coffino, P.**
Proteasomes begin ornithine decarboxylase digestion at the C terminus.
J Biol Chem. 279(20) (2004) 20959-65

[168] **Zhang, M., Pickart, C.M., Coffino, P.**
Determinants of proteasome recognition of ornithine decarboxylase, a ubiquitin-independent substrate.
EMBO J. 22(7) (2003) 1488-96

[169] **Zinkernagel, R.M.**
On cross-priming of MHC class I-specific CTL: rule or exception?
Eur J Immunol. 32(9) (2002) 2385-92 Review

A A strategy to enhance CTL response based on vector modification

Another strategy to enhance antigen-specific CD8+ T-cell responses conducted within this study is based on findings that after viral infection CD8+ T-cell responses against different epitopes can be arranged in an immunodominance hierarchy. T-cell competition between T-cells of the same specificity has clearly been demonstrated. Nevertheless, competition of T-cells of different specificities is still controversial. Kastenmuller et al. could demonstrate that immunodominance hierarchies dramatically change between primary and secondary immune responses [73]. They showed that the induction and strength of primary CD8+ T-cell responses against various VV-specific epitopes in a naive host is largely independent from simultaneous priming of T-cells specific for other antigenic determinants delivered by the virus. However, during boost vaccinations, T-cell cross-competition seems to be a major regulator of the expansion of virus-specific T-cells. In their experiments neither the amount of presented peptide/MHC-I complexes nor the time after infection at which viral antigen expression occurs determined the outcome of T-cell responses during priming. Furthermore, during boost immunization they found a switch in the immunodominance hierarchy favouring the proliferation of T-cells recognizing epitopes derived from early gene products. In a homologous boost the expansion of $K3L_6$- and $A8R_{189}$-specific (both early genes) T-cells was successively suppressed by gradual appearance of cross-competing $B8R_{20}$- and OVA_{257}-specific (both early genes) T-cells, whereas $A3L_{270}$-specific (late gene) T-cells remained fully suppressed. Furthermore, only secondary immunization with MVA K1L OVA expressing OVA driven by a promoter with exclusive early activity could induce OVA_{257}-specific T-cells, whereas MVA P11 OVA (promoter with exclusive late activity) failed to expand OVA_{257}-specific T-cells.

Those results are supported by results obtained in this study. When C57BL/6 mice were primed with MVA-ova the cellular immune response was highly dominated by $B8R_{20}$-specific T-cells recognizing a determinant derived from an early gene product, however, was followed by $A3L_{270}$-specific T-cells (late gene product). Whereas $K3L_6$-specific (early gene product) T-cell response was rather close to detection limit. In boosting experiments early gene product $B8R_{20}$-specific T-cells expanded vigorously whereas T-cells recognizing the epitope from a late gene product ($A3L_{270}$) did not expand.

Suggesting that T-cells specific for early viral proteins might be able to suppress the expan-

sion of other early virus-specific T-cells [73], primary as well as secondary immunization excluding the dominating epitope would increase target antigen-specific T-cell responses. After the infection of C57BL/6 mice with recombinant MVA, $B8R_{20}$-specific T-cell response dominates both the primary and secondary response. Even though SIINFEKL is considered an immunodominant peptide [165], $B8R_{20}$ elicited a considerably stronger CTL response in priming and boosting with either of the constructs used in this study.
One way to address this issue and thus circumvent the immunodomination of CD8+ T-cells by other vector-specific peptides, was suggested to be the elimination of immunodominant peptides by genetic deletion [136]. To further investigate the above mentioned issues, a recombinant MVA $B8R_{20}$ knock out expressing ovalbumin was constructed (MVA-ovaB8R$^{-/-}$).

As depicted in *Fig. A.1*, after infection of DC2.4 cells presentation of the ovalbumin-specific peptide SIINFEKL did not differ between the two ovalbumin expression constructs MVA-ova and MVA-ovaB8R$^{-/-}$ justifying the suggestion that results of *in vivo* immunizations should not depend on differences in SIINFEKL presentation but can be attributed to deletion of the $B8R_{20}$ gene.

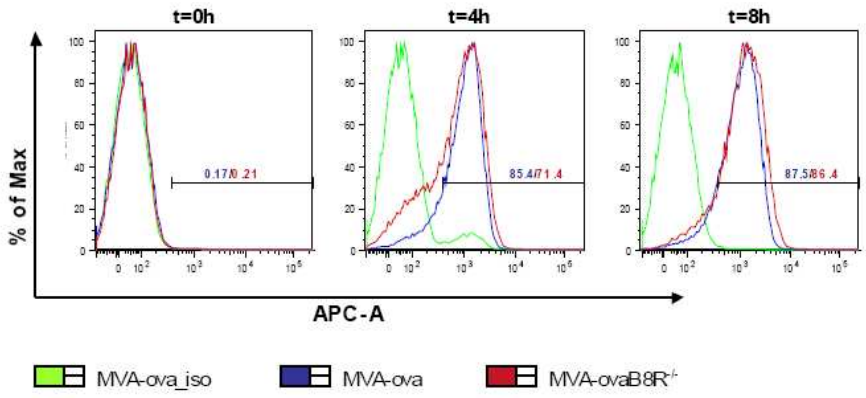

Figure A.1: *Kinetic analysis of SIINFEKL/H2-K^b expression in DC2.4 cells after infection with MVA-ova or MVA-ovaB8R$^{-/-}$.* Levels of SIINFEKL/H2-K^b complexes were determined by flow cytometry with the 25D1.16 mAb at indicated time points (t=0,4,8 h). Isotype stained cells are shown as negative control.

As described in section *3.6.1* eight C57BL/6 mice were immunized with 1×10^8 IU MVA-ovaB8R$^{-/-}$ i.p. (n=8) and boosted with 1×10^8 IU i.p. of MVA-TO (n=4) or MVA-ova (n=4) on day 30 post prime. Specific CD8+ T-cell responses were analyzed on day 6 post boost by ICS *(Fig. A2)*.

Those results were compared to results obtained earlier *(Fig. 4.20 A I)* in a homologous prime-boost setting with MVA-ova to further assess the relevance of $B8R_{20}$ gene deletion. As depicted in *(Fig. B.I)*, homologous boosting of C57BL/6 mice with MVA-ova still supports recall expansion of $B8R_{20}$-specific T-cells with $B8R_{20}$ dominating the T-cell response. $K3L_6$-specific (early gene product) as well as $A3L_{270}$-specific (late gene product) T-cell responses were marginal and at similar detection levels, indicating that $K3L_6$-specific T-cells might be suppressed by other immunodominant T-cells. When mice were primed with MVA-ova$B8R^{-/-}$, $K3L_6$-specific T-cells expanded during secondary immunization *(Fig. B.I)*. OVA_{257}-specific T-cell responses after priming with MVA-ova$B8R^{-/-}$ were explicitly higher as compared to priming with MVA-ova.

After boost immunization with MVA-TO up to 15% OVA_{257}-specific T-cells were detected after stimulation of splenocytes with SIINFEKL peptide *(Fig. A.II)*. Since cross-competition is suggested to be a major regulator of the expansion of virus-specific T-cells during boost vaccinations [73] it can be anticipated that ovalbumin-specific immune responses were even more vigorous when a MVA $B8R_{20}$ knock out would be used as boosting vaccine. One of the most dominant epitopes derived from an early gene product, $B8R_{20}$, would not stimulate T-cells for proliferation and allow for an enhanced expansion of SIINFEKL-specific T-cells. Nevertheless, in a homologous prime-boost immunization with MVA-ova$B8R^{-/-}$ Kastenmuller et al. could only detect an OVA_{257}-specific T-cell response of less than 6%. Yet, OVA_{257}-specific T-cell responses were still increased when compared to a homologous prime-boost with MVA-ova.

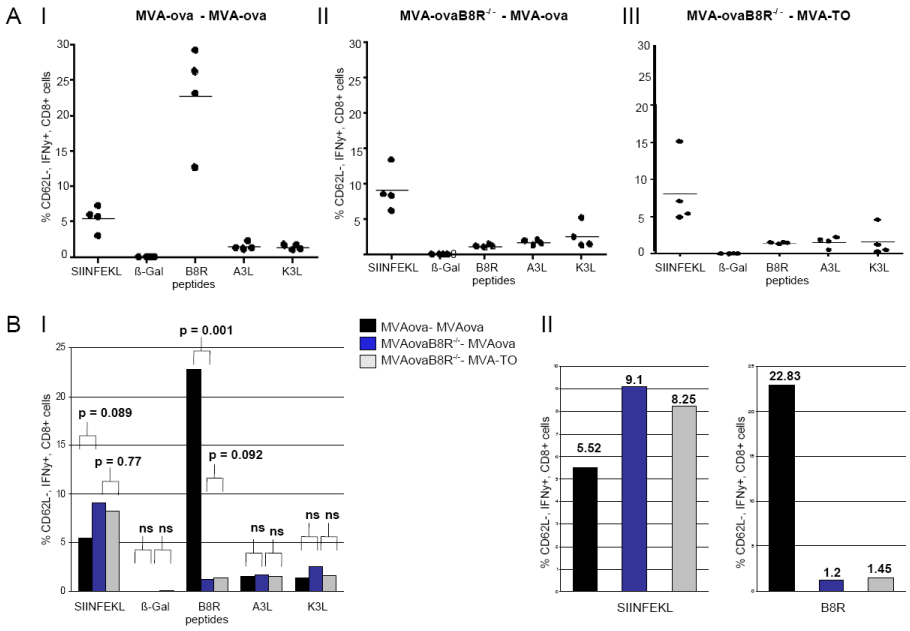

Figure A.2: *Antigen-specific CD8+ T-cells of C57BL/6 mice isolated on day six post boost.* Frequencies of IFNγ-producing CD62L-, CD8+ T-cells specific for the ovalbumin epitope SIINFEKL and MVA epitopes $B8R_{20}$, $A3L_{270}$ and $K3L_6$ are shown. Samples stimulated with ß-Gal_{96} peptide served as negative control. (A I) Specific CD8+ T-cell responses of a homologous prime/boost setting with MVA-ova were compared to a heterologous setting with MVA-ovaB8R$^{-/-}$ prime and MVA-ova (A II) or MVA-TO (A III) boost. (B I) Mean frequency of CD62L-, IFNγ+, CD8+ T-cells compared for all (AI,II,III) experimental settings. The significance for different responses to SIINFEKL-stimulation was evaluated as p=0.089 for MVA-ova prime- MVA-ova boost versus MVA-ovaB8R$^{-/-}$ prime- MVA-ova boost and p=0.77 for MVA-ovaB8R$^{-/-}$ prime- MVA-ova boost versus MVA-ovaB8R$^{-/-}$ prime- MVA-TO boost. (B II) Mean frequency of IFNγ-producing CD62L-, CD8+ T-cells specific for the ovalbumin epitope SIINFEKL compared for all experimental settings (AI,II,III) and for the vector-specific epitope $B8R_{20}$ (right panel).